



UNIL | Université de Lausanne

Unicentre

CH-1015 Lausanne

<http://serval.unil.ch>

---

Year : 2016

## IN-SITU SPECIATION MEASUREMENTS AND BIOAVAILABILITY DETERMINATION OF PLUTONIUM IN NATURAL WATERS OF A KARST SYSTEM USING DIFFUSION IN THIN FILMS (DGT) TECHNIQUES

CUSNIR Ruslan

CUSNIR Ruslan, 2016, IN-SITU SPECIATION MEASUREMENTS AND BIOAVAILABILITY  
DETERMINATION OF PLUTONIUM IN NATURAL WATERS OF A KARST SYSTEM USING  
DIFFUSION IN THIN FILMS (DGT) TECHNIQUES

Originally published at : Thesis, University of Lausanne

Posted at the University of Lausanne Open Archive <http://serval.unil.ch>

Document URN : urn:nbn:ch:serval-BIB\_7E9D808F3BA46

### **Droits d'auteur**

L'Université de Lausanne attire expressément l'attention des utilisateurs sur le fait que tous les documents publiés dans l'Archive SERVAL sont protégés par le droit d'auteur, conformément à la loi fédérale sur le droit d'auteur et les droits voisins (LDA). A ce titre, il est indispensable d'obtenir le consentement préalable de l'auteur et/ou de l'éditeur avant toute utilisation d'une oeuvre ou d'une partie d'une oeuvre ne relevant pas d'une utilisation à des fins personnelles au sens de la LDA (art. 19, al. 1 lettre a). A défaut, tout contrevenant s'expose aux sanctions prévues par cette loi. Nous déclinons toute responsabilité en la matière.

### **Copyright**

The University of Lausanne expressly draws the attention of users to the fact that all documents published in the SERVAL Archive are protected by copyright in accordance with federal law on copyright and similar rights (LDA). Accordingly it is indispensable to obtain prior consent from the author and/or publisher before any use of a work or part of a work for purposes other than personal use within the meaning of LDA (art. 19, para. 1 letter a). Failure to do so will expose offenders to the sanctions laid down by this law. We accept no liability in this respect.



**UNIL** | Université de Lausanne

Faculté de biologie  
et de médecine

**Institut de Radiophysique**

**IN-SITU SPECIATION MEASUREMENTS AND BIOAVAILABILITY  
DETERMINATION OF PLUTONIUM IN NATURAL WATERS OF A KARST SYSTEM  
USING DIFFUSION IN THIN FILMS (DGT) TECHNIQUES**

**Thèse de doctorat ès sciences de la vie (PhD)**

présentée à la

Faculté de biologie et de médecine  
de l'Université de Lausanne

par

**Ruslan CUSNIR**

Master, chimiste diplômé EPF Lausanne

**Jury**

Prof. Luisa Bonafé, Présidente  
Prof. François Bochud, Directeur de thèse  
Dr. Pascal Froidevaux, Co-directeur  
Prof. Laura Sigg, experte  
Prof. Rizlan Bernier-Latmani, experte

Lausanne 2016



UNIL | Université de Lausanne

Faculté de biologie  
et de médecine

**Ecole Doctorale**

Doctorat ès sciences de la vie

# Imprimatur

Vu le rapport présenté par le jury d'examen, composé de

<b>Président · e</b>	Madame Prof. Luisa <b>Bonafé</b>
<b>Directeur · rice de thèse</b>	Monsieur Prof. François <b>Bochud</b>
<b>Co-directeur · rice</b>	Monsieur Dr Pascal <b>Froidevaux</b>
<b>Experts · es</b>	Madame Prof. Rizlan <b>Bernier-Latmani</b>
	Madame Prof. Laura <b>Sigg</b>

le Conseil de Faculté autorise l'impression de la thèse de

**Monsieur Ruslan Cusnir**

master en chimie de l'Ecole Polytechnique Fédérale de Lausanne

intitulée

**IN-SITU SPECIATION MEASUREMENTS AND BIOAVAILABILITY DETERMINATION  
OF PLUTONIUM IN NATURAL WATERS OF A KARST SYSTEM USING DIFFUSION  
IN THIN FILMS (DGT) TECHNIQUES**

Lausanne, le 9 février 2016

pour le Doyen  
de la Faculté de biologie et de médecine

Prof. Luisa Bonafé

## **Acknowledgements**

I am so grateful to many people who kindly shared their ideas, experience and gave their support to the «Pu-DGT» project. My supervisor, Dr. Pascal Froidevaux, entrusted me with the doctoral position in his laboratory, where I discovered the magic of experimental work with infinitely small amounts of matter. Without his permanent presence, active involvement, openness to discuss and to revise the findings this work wouldn't be possible.

Dr. Maud Jaccard and Dr. Claude Bailat made a huge contribution by accepting to get entangled in a thorny deal of mathematical modeling. Their effort proved that an interdisciplinary collaboration is not just blowing hot air. Claude Bailat's proofreading and priceless advice on scientific editing made our papers lively and comprehensive. I am totally indebted to Dr. Marcus Christl from ETH Zurich for measurements of Pu in environmental samples and to Dr. Philipp Steinmann from OFSP Bern, who took part in field campaign and contributed to geochemical modeling of our experimental findings. Prof. François Bochud was my thesis director, so patiently and kindly providing support in advancing and getting organized throughout my doctorate. I'd like to thank my thesis experts, Prof. Laura Sigg from EAWAG and Prof. Rizlan Bernier-Latmani from EPFL, for their critical eye on this project. As ever, this work was brought to life through the direct financial support of the SNSF (grant 200021-140230) and OFSP, enormous thanks for that.

The amazing team of the IRA surrounded me during the three years of my work with their affection, enthusiasm and good humor. Thank you so much for giving me the chance to work with you - it's been such a great experience!



## Table of contents

Acknowledgements.....	2
Lay public summary.....	8
Résumé grand public.....	10
Summary .....	11
Résumé.....	14
General Introduction.....	18
1. The bioavailability of radionuclides .....	19
2. DGT technique for bioavailability measurements of radionuclides .....	20
3. Plutonium in the environment.....	24
Thesis framework.....	26
1. Scope of the thesis .....	27
2. Structure of the thesis.....	28
References.....	31
Chapter 1: A DGT technique for plutonium bioavailability measurements.....	33
1.1 Abstract .....	34
1.2 Introduction.....	34
1.3 Experimental .....	37
1.3.1 Materials and methods .....	37
1.3.2 Diffusion experiments .....	38
1.3.3 Deployment of DGT in laboratory conditions .....	40
1.4 Results and discussion.....	41
1.4.1 Determination of D for plutonium .....	41
1.4.2 Deployment of DGT in laboratory conditions .....	49
1.5. Supporting information.....	52
1.6 Acknowledgements.....	52
1.7 References.....	53
Chapter 2: Speciation and bioavailability measurements of environmental plutonium using diffusion in thin films.....	55
2.1 Abstract .....	56
2.2 Introduction.....	56
2.3 Protocol .....	61
2.3 Representative results.....	76

2.3.1 Diffusion experiments .....	76
2.3.2 Studies on Pu bioavailability in natural freshwaters.....	78
2.4 Discussion .....	80
2.4.1 Laboratory diffusion experiments.....	80
2.4.2 Studies of Pu bioavailability in natural freshwaters.....	81
2.5 Disclosures.....	84
2.6 Acknowledgements .....	84
2.7 References.....	85
Chapter 3: Probing the kinetic parameters of Pu-NOM interactions in freshwaters using the DGT technique.....	87
3.1 Abstract .....	88
3.2 Introduction.....	88
3.3 Experimental .....	90
3.3.1 Materials and methods .....	90
3.3.2 Diffusion experiments .....	92
3.3.3 Deployment of DGTs with different gel thickness .....	93
3.3.4 ADBL and PAM models to determine the dissociation constant $k_{dis}$ and the lability criteria $\xi$ .....	94
3.3.5 Dynamic numerical model .....	97
3.3.6 Deployment of DGTs in field conditions .....	98
3.4 Results and discussion.....	100
3.4.1 Diffusion coefficients of Pu (V) in the PAM gel.....	100
3.4.2 Deployment of DGTs with different gel thicknesses and calculation of the dissociation constant ( $k_{dis}$ ) and of the lability degree ( $\xi$ ).....	101
3.4.3 Dynamic numerical model .....	105
3.4.4 Deployment of DGTs in field conditions .....	109
3.5 Supporting information.....	110
3.6 Acknowledgements .....	110
3.7 References.....	111
Chapter 4: Plutonium is bioavailable in karstic freshwater environments.....	113
4.1 Abstract .....	114
4.2 Introduction.....	114
4.3 Study area.....	117
4.3.1 The karst freshwater system.....	117
4.4 Materials and methods .....	119
4.4.1 Sample preparation.....	119

4.4.1.1 Water samples .....	119
4.4.1.2 Aquatic plants samples .....	121
4.4.2 DGTs .....	122
4.4.3 Pu measurements by AMS .....	123
4.5 Results .....	124
4.5.1 Pu concentrations in bulk water .....	124
4.5.2 Pu speciation in natural waters.....	125
4.5.3 Pu concentrations in ultrafiltered fractions.....	125
4.5.4 DGT measurements of free and labile Pu species .....	127
4.5.5 Distribution of Pu in different compartments of aquatic mosses and plants .....	127
4.6 Discussion.....	130
4.7 Conclusion .....	132
4.8 Acknowledgements.....	134
4.9 Contributions.....	134
4.10 References.....	135
Conclusions and prospects.....	138
Appendix.....	143
Appendix 1: Supporting information for Chapter 1 .....	144
Appendix 2: Supporting information for Chapter 2 .....	154
Appendix 3: Supporting information for Chapter 3 .....	156
Appendix 4: Supporting information for Chapter 4 .....	168
Appendix 5 : Curriculum vitae .....	175
Appendix 6 : List of publications resulted from the thesis .....	176





## **Lay public summary**

Nuclear activities of 1945-1975 have released in the environment significant amounts of radioactive elements. Three main sources contributed to contamination with plutonium: nuclear weapon tests, discharges from nuclear facilities and nuclear accidents. Global atmospheric fallout has marked pristine environments with trace amounts of  $^{239}\text{Pu}$  and  $^{240}\text{Pu}$ . Plutonium is an alpha-particle emitter with long half life and it is dangerous when incorporated in the organism. The amount of Pu which can be assimilated by living organisms depends on its chemical form and on local physico-chemical characteristics of the environment. To study the bioavailability of plutonium in aquatic environments, we developed a technique of diffusive gradients in thin films (DGT), which allows measuring free and labile Pu species only, diffusing through a thin layer of a polymer gel. DGT devices exposed in freshwaters in the mineral Venoge spring and organic-rich Noiraigue Bied brook have demonstrated that the major fraction of Pu in these waters is fully available for biouptake. Similarly, the ultrafiltration technique has shown that in both mineral and organic-rich water the major fraction of Pu is found in the dissolved phase. Laboratory experiments using the DGT technique revealed a relatively high dissociation rate constant for Pu complexes with natural organic matter, suggesting that such complexes in natural environment can contribute to biouptake of Pu by aquatic organisms. Sequential elution of Pu from different compartments of aquatic mosses (Venoge) and plants (Noiraigue) indicated that the major fraction of Pu was co-precipitated with calcite on their extracellular parts. The development and testing of the DGT technique for Pu measurements in the frame of this project paves the way for further applications of DGTs to study the bioavailability and speciation of Pu in contaminated and marine environments.



## Résumé grand public

Les activités nucléaires des années 1945-1975 ont relâché dans l'environnement d'importantes quantités d'éléments radioactifs. Trois sources principales ont contribué à la contamination par le plutonium: les essais d'armes nucléaires, les rejets des installations nucléaires et les accidents nucléaires. Les retombées atmosphériques globales ont marqué l'environnement avec des traces de  $^{239}\text{Pu}$  et  $^{240}\text{Pu}$ . Le plutonium est un émetteur de particules alpha de longue période et il est dangereux lorsqu'il est incorporé dans l'organisme. La quantité de Pu pouvant être assimilée par les organismes vivants dépend de sa forme chimique et des caractéristiques physico-chimiques locales de l'environnement en question. Pour étudier la biodisponibilité du plutonium dans les milieux aquatiques, nous avons développé une technique du gradient de diffusion en couche mince (DGT), qui permet de mesurer seules les espèces libres de Pu, capables de diffuser à travers une mince couche d'un gel polymère. Les dispositifs DGT exposés dans les eaux douces de la source de la Venoge et du Bied de Noiraigue, riche en matière organique, ont démontré que la majeure fraction de Pu dans ces eaux est entièrement disponible pour l'assimilation biologique. De même, la technique d'ultrafiltration a démontré que dans l'eau minérale et dans l'eau riche en matière organique, le Pu se trouve principalement dans la phase dissoute. Des expériences de laboratoire utilisant la technique DGT ont révélé une constante de dissociation relativement élevée pour des complexes de Pu avec la matière organique naturelle, ce qui suggère que ces complexes en milieu naturel peuvent contribuer à l'accumulation de Pu par les organismes aquatiques. L'éluotion séquentielle de Pu de différents compartiments de mousses aquatiques (Venoge) et de plantes (Noiraigue) a montré que la majeure partie du Pu a été co-précipité avec la calcite sur leurs parties extracellulaires. Le développement et l'application de la technique DGT pour les mesures de Pu dans le cadre de ce projet ouvre la voie à de nouvelles applications de DGTs pour étudier la biodisponibilité et la spéciation du Pu dans des environnements marins contaminés.

## Summary

The speciation and the bioavailability of trace elements in the aquatic environments are the key limiting factors defining the toxic effects to the aquatic biota. Radioactive elements found in the environment arouse particular interest since they can exert radiotoxic effects at low concentrations, yet insufficient to show any chemotoxic effects. Plutonium (Pu) is a heavy artificial radionuclide of particular concern due to its long half-life and alpha-particle emission. Assessing the speciation and the bioavailability of Pu in natural waters is essential in order to predict its environmental risks.

The overall goal of this research work was to develop the technique of the diffusive gradients in thin films (DGT) for *in-situ* bioavailability measurements of Pu. We first aimed to determine the diffusion coefficients (D) of Pu in the diffusive polyacrylamide (PAM) gel. Afterwards, we intended to test in laboratory experiments the feasibility of the DGT technique for Pu measurements, using Chelex resin as a binding phase. The positive outcome of the initial experiments with Pu allowed us to expand the application of the DGT technique to further studies on the molecular interactions of Pu with natural organic matter (NOM) and on the mobility of Pu in +IV and +V oxidation states. To measure the bioavailable fraction of Pu in natural waters, DGT samplers with large surface area were fabricated and deployed in two, chemically distinct, karstic freshwater environments. The results of DGT measurements were complemented with ultrafiltration technique, providing the distribution of Pu between colloid-bound and truly dissolved fractions. Finally, the determination of Pu in different compartments of aquatic mosses and plants enabled us to integrate all the results into a model of Pu speciation in karstic freshwater environments.

The determination of diffusion coefficients of Pu in solutions of different chemical composition demonstrated that the mobility of Pu species in natural waters depends on the

content of natural colloids and natural organic matter. Diffusion experiments yielded higher diffusion coefficients for Pu in the simple buffered solutions, compared to solutions containing Pu in the presence of fulvic or humic substances. Similarly, the diffusion of Pu was less restrained in water from a mineral spring, compared to the Pu diffusion in organic-rich water. Enriching natural waters with colloids by ultrafiltration also reduced the diffusion coefficients of Pu. The effects of the redox speciation of Pu were also quantified using the DGT technique. As demonstrated, Pu (V) was more mobile compared to Pu (IV) in both raw buffered solutions and in the presence of humic substances.

The interaction of Pu with natural organic matter results in the formation of soluble complexes, altering its speciation in natural waters. The rate of dissociation of these complexes determines the fraction of free Pu, available for biouptake. Multiple DGT devices with different diffusive layer thicknesses were used to estimate the dissociation constant,  $k_{dis}$ , of Pu-NOM complexes and the extent of their contribution to the biouptake of Pu. Using a mathematical dynamic model, we found a relatively high  $k_{dis}$  for Pu-NOM complexes ( $k_{dis} = 7.5 \times 10^{-3} \text{ s}^{-1}$ ), suggesting that in the organic-rich natural waters Pu is fully available for biouptake.

The findings obtained in laboratory experiments were thereafter confirmed in the field studies. DGT samplers deployed in the mineral water of the Venoge spring (NOM < 1 mg L<sup>-1</sup>) measured the major fraction of Pu as bioavailable. In the organic-rich water (NOM = 15 mg L<sup>-1</sup>) of the Noiraigue Bied brook the fraction of free Pu was lower compared to the Venoge spring. However, the DGT devices with thicker diffusive gel layer accumulated twice as much Pu, as expected from the theory for labile complexes. This indicated that the dissociation of soluble Pu-NOM complexes in this water contributed to the uptake of Pu.

The distribution of Pu eluted from different compartments of the aquatic mosses and plants demonstrated that the major fraction of Pu is co-precipitated with calcite on the leaves surfaces. Pu concentrations determined in the mosses (*Fontinalis antipyretica*) from the Venoge spring suggest that Pu is possibly found in a chemical form similar to a soluble uranyl-carbonate complex in water; this complex can further co-precipitate with calcite when CO<sub>2</sub> is degassing from the water. Aquatic plants (*Phragmites australis*) in the Noiraigue Bied brook contained even a greater fraction of Pu within the calcite. However, the presence of organic matter at high concentration can complex Pu and contribute to a higher biouptake of Pu in this water since the diffusion and dissociation of the Pu-NOM complexes will create additional flux to the plant.

## Résumé

La spéciation et la biodisponibilité des éléments de concentration en traces dans les milieux aquatiques sont les principaux facteurs limitant qui définissent les effets toxiques sur les organismes aquatiques. Les éléments radioactifs présents dans l'environnement suscitent un intérêt particulier car ils peuvent exercer des effets radiotoxiques à de faibles concentrations, encore insuffisantes pour montrer les effets chimiotoxiques. L'élément plutonium (Pu) est un radionucléide artificiel lourd particulièrement préoccupant en raison de sa longue période de désintégration et de son émission de particules alpha. Évaluer la spéciation et la biodisponibilité du Pu dans les eaux naturelles est essentiel pour prédire ses risques environnementaux.

L'objectif global de ce projet de recherche était de développer la technique du gradient de diffusion en couche mince (DGT) pour les mesures de la biodisponibilité du Pu *in-situ*. Tout d'abord, nous avons eu pour but de déterminer les coefficients de diffusion (D) de Pu dans le gel de diffusion de polyacrylamide (PAM) et de tester en laboratoire la faisabilité de la technique DGT pour les mesures Pu, en utilisant une résine Chelex en tant que phase captante. L'issue positive des premières expériences avec Pu nous a permis d'étendre l'application de la technique DGT à de nouvelles études sur les interactions moléculaires de Pu avec la matière organique naturelle (NOM) et sur la mobilité des espèces Pu dans leurs états d'oxydation +IV et +V. Pour mesurer la fraction biodisponible de Pu dans les eaux naturelles, des dispositifs DGT de grande surface ont été fabriqués et déployés dans deux milieux aquatiques karstiques de compositions chimiques distinctes. Les résultats des mesures DGT ont été complétés par la technique d'ultrafiltration, qui permet de déterminer la distribution de fractions de Pu lié aux colloïdes ainsi que la fraction véritablement dissoute. Enfin, la détermination de Pu dans différents compartiments de mousses et de



plantes aquatiques nous a permis d'intégrer tous les résultats dans un modèle de spéciation de Pu dans des environnements aquatiques karstiques.

La détermination des coefficients de diffusion de Pu dans des solutions de composition chimique différente a démontré que la mobilité des espèces de Pu dans les eaux naturelles dépend de la teneur en colloïdes naturels et en matière organique dissoute. Les expériences de diffusion ont donné des coefficients de diffusion plus élevés pour le Pu dans les solutions tamponnées simples, par rapport aux solutions contenant le Pu en présence de substances humiques ou fulviques. De même, la diffusion de Pu était plus importante dans l'eau provenant d'une source minérale, par rapport à la diffusion de Pu dans l'eau de source riche en matière organique. Enrichir les eaux naturelles avec des colloïdes par ultrafiltration réduit également les coefficients de diffusion de Pu. Les effets de la spéciation redox de Pu ont également été quantifiés en utilisant la technique DGT. Nous avons démontré que Pu (V) est plus mobile que Pu (IV) tant dans les solutions brutes tamponnées qu'en présence de substances humiques.

L'interaction du Pu avec la matière organique naturelle se traduit par la formation de complexes solubles, ce qui modifie la spéciation du Pu dans les eaux naturelles. Le taux de dissociation de ces complexes détermine la fraction du Pu libre, disponible pour l'assimilation biologique. Plusieurs sondes DGT avec des gels de diffusion d'épaisseurs différentes ont été utilisées afin d'estimer la constante de dissociation,  $k_{dis}$ , des complexes Pu-NOM, ainsi que l'ampleur de leur contribution à l'assimilation de Pu. En utilisant un modèle mathématique dynamique, nous avons trouvé une valeur relativement élevée de  $k_{dis}$  pour les complexes Pu-NOM ( $k_{dis} 7.5 \times 10^{-3} \text{ s}^{-1}$ ), ce qui suggère que dans les eaux naturelles riches en matières organiques, le Pu est entièrement disponible pour l'assimilation biologique.

Les résultats obtenus dans les expériences de laboratoire ont ensuite été confirmés dans des études de terrain. Les sondes DGT déployées dans l'eau de la source de la Venoge (NOM < 1 mg L<sup>-1</sup>) ont mesuré la majeure partie de Pu comme biodisponible. Dans l'eau riche en matière organique (NOM = 15 mg L<sup>-1</sup>) du Bied de la Noiraigue, la fraction du Pu libre a été inférieure à celle de la source de la Venoge. Cependant, les dispositifs DGT avec le gel de diffusion le plus épais ont accumulé deux fois plus de Pu, par rapport à ce qui est attendu selon la théorie pour des complexes non labiles. Ceci indique que la dissociation de complexes Pu-NOM solubles dans cette eau a contribué à l'absorption de Pu.

La distribution de Pu dans différents compartiments des mousses et des plantes aquatiques obtenue par élution sélective a montré que la majeure fraction du Pu est co-précipitée avec la calcite sur la surface des feuilles. Les concentrations de Pu déterminées dans les mousses (*Fontinalis antipyretica*) de la source de la Venoge suggèrent que Pu est probablement présent dans une forme chimique similaire à un complexe soluble de carbonate de plutonyle; ce complexe peut en outre co-précipiter avec la calcite lorsque le CO<sub>2</sub> est dégazé de l'eau. Les plantes aquatiques (*Phragmites australis*) dans le Bied de la Noiraigue contenaient une fraction encore plus élevée de Pu dans la fraction calcite. Cependant, la présence de la matière organique à des concentrations élevées peut conduire à la formation de complexes de Pu et contribuer à une assimilation plus importante dans cette eau, étant donné que la diffusion et la dissociation des complexes Pu-NOM créeront un flux supplémentaire à la plante.



## **General Introduction**

## 1. The bioavailability of radionuclides

Once released into natural environment, artificial radioactive elements can be incorporated by living organisms with water and food, thus spreading through all the levels of the food chain. Aquatic environments, being the largest reserve of living forms and of primary producers in particular, represent an extremely sensitive environmental compartment with respect to pollution and radioactive contamination. Although some elements remain radioactive for many thousands of years, their toxic effects and radiological risks to the aquatic biota depend to a large extent on the local physico-chemical processes.<sup>1</sup> The total concentration of a radionuclide in the aquatic environment is not a reliable indicator for the prediction of its radiological risks. Basic biogeochemical processes, such as biotic and abiotic oxidation and reduction, sorption and desorption, precipitation and dissolution affect the distribution and the partitioning of the radionuclides between dissolved and immobile phases. Thus, the effective exposure levels are determined by the fraction of a radionuclide which can potentially be taken up by living organisms. The bioavailability of a radionuclide in water defines the amount of radionuclide able to interact with living organisms and available for biological uptake.

Currently, the assessment of the potential of a radionuclide to be taken up by living organisms relies mainly on the understanding and knowledge of its fundamental chemical properties and molecular interactions with abiotic and biotic components of the ecosystem. Additionally, the evaluation of radionuclide uptake by living organisms is often based on *concentration ratios* (CR) approach.<sup>2</sup> A CR is experimentally defined as the ratio of radionuclide concentrations in the organism to that in the living medium of the organism. In spite of the large number of experimental datasets available from different studies in contaminated environments, the CRs suffer from an impressive variability.<sup>3,4</sup> This variability

supports the idea that the bioavailability of a radionuclide in water is strongly influenced by site-specific physico-chemical parameters of a particular ecosystem. To assess the bioavailability of a radionuclide and to predict its radiological risks to biota, a reliable *in-situ* approach is needed.

## **2. DGT technique for bioavailability measurements of radionuclides**

Conventional techniques for water sampling and analysis of radionuclides applied in field studies are time- and labour consuming, requiring large volumes of water and highly sensitive detection methods. Moreover, analytical data retrieved with such techniques are restricted only to a few point samples, while the speciation and the bioavailability of radionuclides are dynamic phenomena, dependent on a number of *in-situ* parameters. Handling and storage of water samples alter the natural speciation of trace elements and disturb their dynamic interactions with NOM, natural colloids and soluble components, thus introducing more uncertainty for predicting their availability to aquatic biota. The assessment of radiological risks of radionuclides in natural waters requires a continuous *in-situ* monitoring approach, providing quantitative integrated record of radionuclide species, available for biological uptake.

Diffusive gradients in thin films (DGT) technique is a passive sampling technique, based on diffusion of free and labile radionuclide species from the sampled water medium through a thin film of PAM gel.<sup>5-7</sup> The diffusing species are captured and accumulated within a binding phase, *e.g.* Chelex resin. After a known deployment time, the radionuclide is measured in the binding phase and its time-averaged mean concentration in water can be calculated. Since a DGT sampler continuously removes the radionuclide from water, taking

into account flow rate variations and any other change of *in-situ* physico-chemical parameters just like aquatic organisms, it is considered as a good chemical proxy to the measure of bioavailability.<sup>8</sup> Additionally, the DGT technique provides a powerful tool for dynamic radionuclide speciation in aquatic ecosystems, making possible to quantify their interactions with NOM and other soluble components.<sup>9,10</sup>

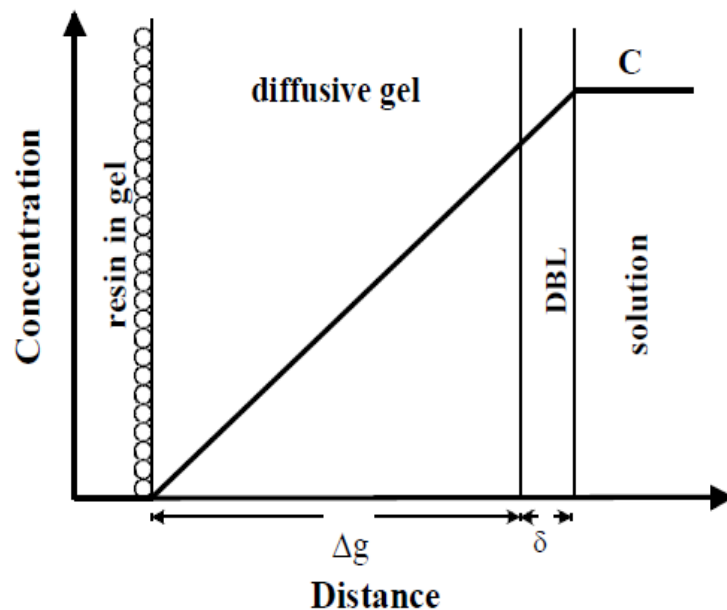


**Figure 1.** Schematic representation of the DGT technique principle.

Figure 1 demonstrates the principle behind the functioning of the DGT technique. The PAM diffusive gel layer is composed on 15 % of polymer and 85 % of water, thus providing a surrogate to simple aquatic organisms which are characterized by passive uptake of dissolved contaminants from water. When a DGT device is deployed in a solution, a gradient of concentration of the diffusing species is established within the gel: between the gel-solution interface where the concentration of any given species is assumed constant and the binding resin-gel interface, where the concentration of the diffusing species is equal to zero since they are captured by the resin and removed from the diffusive gel layer. The

diffusive gel enables to control the mass transport of metal ion species from the solution to the binding phase. Since the mass transport within the PAM gel is diffusion controlled, it can be well defined by Fick's law of diffusion. The flux  $F$  of metal is then given by equation 1:

$$F = \frac{D \times C_b}{\Delta g} \quad (1)$$

where  $D$  is the effective diffusion coefficient of metal species,  $C_b$  the concentration of metal species in the bulk solution and  $\Delta g$  the thickness of the diffusive layer. Additionally, the flux of metal species can be given as the mass ( $M$ ) per unit area ( $S$ ) per unit of time ( $t$ ):

$$F = \frac{M}{S \times t} \quad (2)$$

Combining eq. 1 and eq. 2 gives the eq. 3 for calculating the concentration  $C_{DGT}$  of labile (bioavailable) species in water:

$$C_{DGT} = \frac{M \times \Delta g}{D \times S \times t} \quad (3)$$

In practice, the  $M$  of metal species accumulated within the binding phase during the time of deployment  $t$  of the DGT device is determined with mass spectrometry, or any other suitable analytical method. The  $C_{DGT}$  of any measured species is usually a fraction of the total concentration measured in the bulk water and indicates the proportion of dissolved and/or labile species available for biouptake.

One of the sensible parameters in the eq. 3 is the thickness of the diffusive layer  $\Delta g$ . In fact, the diffusive path of any species measured with the DGT consists of the PAM diffusive gel of a known thickness  $\Delta g$  plus thickness of the diffusive boundary layer, DBL ( $\delta$  in the figure 1). DBL represents a physical layer on the solid-liquid interface where the mass transport is only diffusion-controlled. The thickness of the DBL is strongly dependent on the flow rate at the surface and is negligibly small in well stirred solutions. However, when complexing molecules (*e.g.* EDTA and citrate ligands, fulvic and humic substances) are



present in the solution, as it is often in the case of natural freshwaters, the supply of free metal to the DGT device can be reduced in function of dissociation kinetics of metal-ligand complexes. Thus, the  $\Delta g$  coming out of the eq. 3 will appear greater as expected even in a well stirred solution. This apparent thickness is called the “apparent diffusive boundary layer” (ADBL) and is indicative of the kinetics of metal-ligand interactions in solution. The DGT technique combined with special mathematical treatment provides a tool for probing the dynamic interactions of metals with organic ligands in solution by measuring the ADBL.

The DGT technique has been extensively applied during the last 20 years by environmental scientists to study the bioavailability of trace elements in water and soils. Data on DGT applications for radionuclide measurements are scarce in the scientific literature, however, some applications for radionuclide measurements have also been reported. DGTs deployed for one month in the lake Llyn Trawsfynydd (Wales, Great Britain), receiving authorized liquid radioactive discharges, provided credible values for radiocesium ( $^{134}\text{Cs}$  and  $^{137}\text{Cs}$ ) concentrations, compared to average bulked grab samples.<sup>11</sup> DGTs revealed that the highest mobility of  $^{226}\text{Ra}$  in the sediment from a sedimentation pond, receiving discharges from a phosphate plant, correlated with high fluxes of Fe, as well as As and Co, explained by the reductive mobilization of these elements within the sediment.<sup>12</sup> Somewhat controversial data are available on uranium measurements with the DGT technique. Vandenhove *et al.* reported in several publications that DGTs did not provide significant advantages for predicting U bioavailability to plants, compared simply to dissolved  $\text{UO}_2^{2+}$  concentration.<sup>13,14</sup> Hutchins *et al.* found that DGTs with Chelex resin as a binding phase were not satisfactorily accurate in both synthetic and natural freshwaters and unable to measure U in seawater.<sup>15</sup> The authors also emphasized the pH sensitivity of U diffusion coefficients in the gel, crucial for proper interpretation of DGT measurements. A commercially available

affinity membrane with amino binding functional groups (DE 81) was used in the DGTs by Li *et al.* to measure U in natural water in the St. Lawrence River (Canada), suggesting that dissociation of  $\text{UO}_2(\text{CO}_3)_2^{2-}$  complexes created the main input of U.<sup>16,17</sup> To our knowledge, there is no data on DGT applications to measure the bioavailability of transuranium elements, such as Pu.

### 3. Plutonium in the environment

Plutonium (Pu) is a heavy artificial radionuclide, produced by interaction of the naturally-occurring  $^{238}\text{U}$  with neutrons. Civil and military nuclear activities have generated up today a global stockpile of about  $495 \pm 10$  tons of separated Pu, while nuclear energy production continuously generates Pu as a byproduct of nuclear fission within spent fuel.<sup>18,19</sup> Although the main source of environmental Pu nowadays is the global fallout after atmospheric nuclear weapon tests (NWT) of the 1960s and several nuclear accidents, Pu is one of the primordial radionuclides and was present on the Earth earlier. Infinitely small amounts of  $^{244}\text{Pu}$  with half-life of 80 million years can still be detected in the Earth's crust, however this isotope has decayed since long time and does not represent any danger to the environment.<sup>20</sup> The isotopes of interest – fallout  $^{238}\text{Pu}$  (half-life 87.7 years),  $^{239}\text{Pu}$  (half-life 24100 years),  $^{240}\text{Pu}$  (half-life 6563 years) – make up the global inventory of environmental Pu, in both pristine environments and in areas contaminated due to nuclear activities. The estimation of the above-ground NWTs is three tons of  $^{239+240}\text{Pu}$  released in the atmosphere, with nearly 80 % in the northern hemisphere.

Pu is an alpha-particle emitter and its potential source of uptake is incorporation with water and food. In the human organism, Pu resembles the pathway of Fe and is being deposited nearly equally in the skeleton and liver.<sup>21,22</sup> The complex behavior of Pu in the

environment makes the task of predicting accurately its radiological risks to biota challenging. Once considered as strongly sorbing and immobile species due to its low solubility,<sup>23</sup> Pu is being re-evaluated in view of new findings on its interactions with natural colloids and NOM. Colloid-facilitated migration of Pu over large distances has been documented in contaminated areas at the Nevada Test Site (USA) and near the Mayak nuclear site (Russia).<sup>24-26</sup> In natural waters, Pu can be found in both reduced (+III, +IV) and oxidized (+V, +VI) forms, exhibiting converse chemical properties.<sup>27,28</sup> Plutonium in +III and +IV oxidation states exists predominately in solid phase and has increased capacity to sorb to inorganic colloids and naturally occurring organic matter (NOM) molecules. Plutonium in +III and +IV oxidation states is considered to be less mobile. More soluble oxidized forms of plutonium (+V and +VI, +V being most likely) can potentially contribute to a higher biological transfer to aquatic organisms due to higher mobility. Moreover, the oxidation and reduction of Pu can take place at environmentally relevant conditions, with profound implications to its biogeochemical cycling.<sup>29-31</sup> Finally, various molecular interactions of Pu with dissolved NOM and mineral components of water are of particular interest to environmental scientists, attempting to describe the biological uptake of Pu in natural aquatic ecosystems.

## **Thesis framework**

## 1. Scope of the thesis

The aim of this doctoral thesis was to develop a DGT technique for the bioavailability measurements of Pu and to apply this technique *in-situ* in order to measure the free and labile Pu fraction in natural freshwaters of the karst system of the Swiss Jura Mountains. Previous studies revealed an enhanced mobility of  $^{239+240}\text{Pu}$  compared to  $^{137}\text{Cs}$  and  $^{241}\text{Am}$  in the mineral, calcium-rich Venoge spring.<sup>32</sup> Since the DGT technique allows for measurement of free and labile Pu species, available for biouptake, it provides a good surrogate for the determination of the bioavailability of this radionuclide in the pristine environment with low concentrations of Pu of fallout origin.

The calibration of the DGT technique for Pu measurements was the first step to begin with, since there were no studies on Pu with DGTs, to our knowledge. To determine the diffusion coefficients of Pu, a two-compartment diffusion cell was fabricated at the in-house workshop. We conducted a series of laboratory experiments and determined the diffusion coefficient of Pu in the PAM gel, in solutions simulating different chemical environments. Additionally, these experiments allowed us to establish new protocols for studies of molecular interactions of Pu with NOM and natural colloids. Finally, to demonstrate the applicability of the DGT technique for Pu measurements we tested commercially available DGT devices with Chelex resin as binding phase in laboratory solutions, containing Pu. In addition, laboratory experiments with commercially available DGTs equipped with diffusive gels of different thicknesses made it possible to expand laboratory studies with Pu and to reveal fundamental data on molecular interactions of Pu with NOM. Dissociation kinetics of soluble Pu-NOM complexes studied in these experiments was integrated into a dynamic numerical model to estimate the dissociation rate constant,  $k_{dis}$ , of Pu-NOM complexes. This model sheds new light on the role of NOM in the biouptake of Pu.

To measure the bioavailability of Pu in natural freshwaters using the DGT technique, we fabricated DGT devices of large surface area (105 cm<sup>2</sup>) which were deployed in field conditions. We choose for field studies two chemically distinct karstic freshwater environments in the Swiss Jura Mountains – the mineral Venoge spring and the organic-rich Noiraigue Bied brook. To reveal a broad context of Pu speciation in these waters, DGT measurements were complemented with additional techniques. Cross-flow ultrafiltration (CFUF) provided data on truly dissolved and colloid-bound fraction of Pu, while sequential elution (SE) from aquatic mosses and plants yielded the distribution of Pu in different compartments of these organisms, permanently immersed in water. Finally, the hypothetical  $[\text{Pu}^{\text{V}}\text{O}_2^+(\text{CO}_3)_n]^{m-}$  species in carbonate-rich oxic Venoge waters was evidenced using selective precipitation with silica gel. An extensive collaboration with the Laboratory of Ion Beam Physics at the ETH Zurich made it possible to measure environmental Pu with sufficient accuracy, using accelerator mass spectrometry (AMS). Data obtained in the field studies with DGTs, as well as the findings of laboratory experiments on Pu-NOM interactions resulted in a geochemical model of Pu speciation in karstic freshwater environments.

## **2. Structure of the thesis**

This thesis includes four main chapters. In the first chapter we determined the diffusion coefficients of Pu in the PAM gel, using a diffusion cell. We used to work with Pu (IV) to optimize data interpretation for Pu (IV) species only. D of Pu was previously not available in the scientific literature and it is necessary for the interpretation of the data retrieved with DGT measurements. Cell diffusion experiments yielded a series of D for Pu in solutions of different chemical compositions, providing us with a tool to compare the mobility of Pu species in chemically distinct environments. The calibration of the DGT

technique and  $D$  of Pu were described in an original article in *Environmental Science and Technology*.<sup>33</sup>

The second chapter of this thesis includes further cell diffusion experiments, expanded to Pu (V) species. Pu (V) is considered as a more mobile species, and more labile in presence of complexing organic molecules. In this chapter we demonstrate that  $D$  of Pu (V) is higher compared to Pu (IV), in both raw solution and in presence of humic acid (HA). Results of the first application of large-surface DGT samplers in the mineral Venoge spring show that most of Pu in this water is available for biouptake. The detailed protocol of cell diffusion experiments and fabrication of large-surface DGT sampler for Pu measurements made the subject of an instructive article in the *Journal of Visualized Experiments*.<sup>34</sup>

In the third chapter we used DGT samplers of several diffusive layer thicknesses and a dynamic numerical model to provide new insights into the dissociation kinetics of soluble Pu-NOM complexes. The dissociation rate of Pu-NOM complexes determines the amount of free Pu, available for biological uptake by aquatic organisms. We applied a dynamic numerical model to estimate the dissociation constant ( $k_{dis} > 10^3 \text{ s}^{-1}$ ) of Pu complexes with NOM, extracted from organic-rich water of the Noiraigue Bied brook. Additionally, more accurate experiments with Pu (V) and Pu (V) – HA interactions are described in this chapter, which made the core of another original article, submitted to *Environmental Science and Technology*.<sup>35</sup>

The concluding, fourth chapter, describes the geochemical model of Pu speciation in karstic freshwater environments, resulting from broad field studies. DGTs deployed in the mineral Venoge spring and organic-rich Noiraigue Bied brook revealed that Pu is fully available for biological uptake, while CFUF showed low proportion of colloid-bound Pu. We also found that the co-precipitation with calcite was the major input of plutonium to the

aquatic plants and mosses biomass. These results are in good correlation with our previous findings from laboratory experiments. The geochemical model of Pu speciation in karstic freshwaters is intended for publication in an original article submitted to *Nature Geoscience*.<sup>36</sup>



## References

- 1 Eriksen, D. O. *et al.* Radionuclides in produced water from Norwegian oil and gas installations – concentrations and bioavailability. *Czechoslovak Journal of Physics* **56**, D43-D48 (2006).
- 2 Tamponnet, C. *et al.* An overview of BORIS: Bioavailability of Radionuclides in Soils. *Journal of Environmental Radioactivity* **99**, 820-830, doi:10.1016/j.jenvrad.2007.10.011 (2008).
- 3 Lembrechts, J. A review of literature on the effectiveness of chemical amendments in reducing the soil-to-plant transfer of radiostrontium and radiocesium. *Science of the Total Environment* **137**, 81-98, doi:10.1016/0048-9697(93)90379-k (1993).
- 4 Van Bergeijk, K. E., Noordijk, H., Lembrechts, J. & Frissel, M. J. Influence of pH soil type and soil organic matter content on soil-to-plant transfer of radiocesium and strontium as analyzed by a nonparametric method. *Journal of Environmental Radioactivity* **15**, 265-276 (1992).
- 5 Zhang, H. & Davison, W. Diffusional characteristics of hydrogels used in DGT and DET techniques. *Analytica Chimica Acta* **398**, 329-340, doi:10.1016/s0003-2670(99)00458-4 (1999).
- 6 Davison, W. & Zhang, H. In-situ speciation measurements of trace components in natural-waters using thin-film gels. *Nature* **367**, 546-548 (1994).
- 7 Davison, W. & Zhang, H. Progress in understanding the use of diffusive gradients in thin films (DGT) - back to basics. *Environmental Chemistry* **9**, 1-13, doi:10.1071/en11084 (2012).
- 8 Zhang, H. & Davison, W. Direct in situ measurements of labile inorganic and organically bound metal species in synthetic solutions and natural waters using diffusive gradients in thin films. *Analytical Chemistry* **72**, doi:10.1021/ac0004097 (2000).
- 9 van Leeuwen, H. P. *et al.* Dynamic speciation analysis and bioavailability of metals in aquatic systems. *Environmental Science & Technology* **39**, 8545-8556, doi:10.1021/es050404x (2005).
- 10 Warnken, K. W., Davison, W., Zhang, H., Galceran, J. & Puy, J. In situ measurements of metal complex exchange kinetics in freshwater. *Environmental Science & Technology* **41**, 3179-3185, doi:10.1021/es062474p (2007).
- 11 Murdock, C., Kelly, M., Chang, L. Y., Davison, W. & Zhang, H. DGT as an in situ tool for measuring radiocesium in natural waters. *Environmental Science & Technology* **35**, 4530-4535, doi:10.1021/es0100874 (2001).
- 12 Gao, Y., Baeyens, W., De Galan, S., Poffijn, A. & Leermakers, M. Mobility of radium and trace metals in sediments of the Winterbeek: Application of sequential extraction and DGT techniques. *Environmental Pollution* **158**, 2439-2445, doi:10.1016/j.envpol.2010.03.022 (2010).
- 13 Duquene, L., Vandenhove, H., Tack, F., Van Hees, M. & Wannijn, J. Diffusive gradient in thin FILMS (DGT) compared with soil solution and labile uranium fraction for predicting uranium bioavailability to ryegrass. *Journal of Environmental Radioactivity* **101**, 140-147, doi:10.1016/j.jenvrad.2009.09.007 (2010).
- 14 Vandenhove, H., Antunes, K., Wannijn, J., Duquene, L. & Van Hees, M. Method of diffusive gradients in thin films (DGT) compared with other soil testing methods to predict uranium phytoavailability. *Science of the Total Environment* **373**, 542-555, doi:10.1016/j.scitotenv.2006.12.023 (2007).
- 15 Hutchins, C. M. *et al.* Evaluation of a titanium dioxide-based DGT technique for measuring inorganic uranium species in fresh and marine waters. *Talanta* **97**, 550-556, doi:10.1016/j.talanta.2012.05.012 (2012).
- 16 Li, W., Zhao, J., Li, C., Kiser, S. & Cornett, R. J. Speciation measurements of uranium in alkaline waters using diffusive gradients in thin films technique. *Analytica Chimica Acta* **575**, 274-280, doi:10.1016/j.aca.2006.05.092 (2006).
- 17 Li, W., Li, C., Zhao, J. & Cornett, R. J. Diffusive gradients in thin films technique for uranium measurements in river water. *Analytica Chimica Acta* **592**, 106-113, doi:10.1016/j.aca.2007.04.012 (2007).
- 18 Materials, I. P. o. F. Global Fissile Material Report 2013: Increasing Transparency of Nuclear Warhead and Fissile Material Stocks as a Step toward Disarmament. (2013).
- 19 Feiveson, H., Glaser, A., Mian, Z. & von Hippel, F. in *Unmaking the Bomb: a Fissile Material Approach to Nuclear Disarmament and Nonproliferation* 69-+ (Mit Press, 2014).
- 20 Taylor, D. M. Environmental plutonium - Creation of the universe to twenty-first century mankind. *Plutonium in the Environment* **1**, 1-14 (2001).
- 21 Froidevaux, P., Bochud, F. & Haldimann, M. Retention half times in the skeleton of plutonium and Sr-90 from above-ground nuclear tests: A retrospective study of the Swiss population. *Chemosphere* **80**, 519-524, doi:10.1016/j.chemosphere.2010.04.049 (2010).

- 22 Froidevaux, P. & Haldimann, M. Plutonium from Above-Ground Nuclear Tests in Milk Teeth: Investigation of Placental Transfer in Children Born between 1951 and 1995 in Switzerland. *Environmental Health Perspectives* **116**, 1731-1734, doi:10.1289/ehp.11358 (2008).
- 23 Bunzl, K., Kracke, W., Shimmack, W. & Auerswald, K. Migration of fallout Pu-239+240, Am-241 and Cs-137 in various horizons of a forest soil under pine. *Journal of Environmental Radioactivity* **28**, 17-34, doi:10.1016/0265-931x(94)00066-6 (1995).
- 24 Kersting, A. B. *et al.* Migration of plutonium in ground water at the Nevada Test Site. *Nature* **397**, 56-59, doi:10.1038/16231 (1999).
- 25 Novikov, A. P. *et al.* Colloid transport of plutonium in the far-field of the Mayak Production Association, Russia. *Science* **314**, 638-641, doi:10.1126/science.1131307 (2006).
- 26 Xu, C. *et al.* Colloidal Cutin-Like Substances Cross-Linked to Siderophore Decomposition Products Mobilizing Plutonium from Contaminated Soils. *Environmental Science & Technology* **42**, 8211-8217, doi:10.1021/es801348t (2008).
- 27 Choppin, G. R., Bond, A. H. & Hromadka, P. M. Redox speciation of plutonium. *Journal of Radioanalytical and Nuclear Chemistry* **219**, 203-210, doi:10.1007/bf02038501 (1997).
- 28 Kersting, A. B. Plutonium Transport in the Environment. *Inorganic Chemistry* **52**, 3533-3546, doi:10.1021/ic3018908 (2013).
- 29 Xu, C. *et al.* Plutonium Immobilization and Remobilization by Soil Mineral and Organic Matter in the Far-Field of the Savannah River Site, US. *Environmental Science & Technology* **48**, 3186-3195, doi:10.1021/es404951y (2014).
- 30 Kaplan, D. I. *et al.* Eleven-year field study of Pu migration from Pulli, IV, and VI sources. *Environmental Science & Technology* **40**, 443-448, doi:10.1021/es050073o (2006).
- 31 Kaplan, D. I. *et al.* Influence of oxidation states on plutonium mobility during long-term transport through an unsaturated subsurface environment. *Environmental Science & Technology* **38**, 5053-5058, doi:10.1021/es049406s (2004).
- 32 Froidevaux, P., Steinmann, P. & Pourcelot, L. Long-Term and Long-Range Migration of Radioactive Fallout in a Karst System. *Environmental Science & Technology* **44**, 8479-8484, doi:10.1021/es100954h (2010).
- 33 Cusnir, R., Steinmann, P., Bochud, F. & Froidevaux, P. A DGT Technique for Plutonium Bioavailability Measurements. *Environmental Science & Technology* **48**, 10829-10834, doi:10.1021/es501149v (2014).
- 34 Cusnir, R., Steinmann, P., Christl, M., Bochud, F. & Froidevaux, P. Speciation and bioavailability measurements of environmental plutonium using diffusion in thin films. *Journal of Visualized Experiments*, e53188, doi:10.3791/53188 (2015).
- 35 Cusnir, R. *et al.* Probing the kinetic parameters of Pu-NOM interactions in freshwaters using the DGT technique. *Environmental Science and Technology* Submitted (2015).
- 36 Cusnir, R., Christl, M., Steinmann, P., Bochud, F. & Froidevaux, P. Plutonium is bioavailable in karstic freshwater environments. *Nature Geoscience* Submitted (2015).

## **Chapter 1: A DGT technique for plutonium bioavailability measurements**

With Philipp Steinmann, François Bochud and Pascal Froidevaux

Article published in:

*Environmental Science and Technology* (2014), volume 18, issue 48, pp. 10829-10834

DOI: 10.1021/es501149v

## **1.1 Abstract**

The toxicity of heavy metals in natural waters is strongly dependant on the local chemical environment. Assessing the bioavailability of radionuclides predicts the toxic effects to aquatic biota. The technique of diffusive gradients in thin films (DGT) is largely exploited for bioavailability measurements of trace metals in waters. However, it has not been applied for plutonium speciation measurements yet. This study investigates the use of DGT technique for plutonium bioavailability measurements in chemically different environments. We used a diffusion cell to determine the diffusion coefficients (D) of plutonium in polyacrylamide (PAM) gel and found D in the range of  $2.06 - 2.29 \times 10^{-6} \text{ cm}^2 \text{ s}^{-1}$ . It ranged between  $1.10$  and  $2.03 \times 10^{-6} \text{ cm}^2 \text{ s}^{-1}$  in the presence of fulvic acid and in natural waters with low DOM. In the presence of 20 ppm of humic acid of an organic-rich soil, plutonium diffusion was hindered by a factor of 5, with a diffusion coefficient of  $0.50 \times 10^{-6} \text{ cm}^2 \text{ s}^{-1}$ . We also tested commercially available DGT devices with Chelex resin for plutonium bioavailability measurements in laboratory conditions and the diffusion coefficients agreed with those from the diffusion cell experiments. These findings show that the DGT methodology can be used to investigate the bioaccumulation of the labile plutonium fraction in aquatic biota.

## **1.2 Introduction**

The release of artificial radionuclides into the environment as a result of nuclear accidents, nuclear weapon tests (NWT) and nuclear waste disposal contributes to the radioactive contamination of the environment and provides an additional exposure risk factor via ingestion through water and food. Plutonium is of particular concern since it is an alpha-particle emitter with a long half-life and its stockpile is continuously increasing as a by-product of nuclear power production.<sup>1</sup> Although most of current environmental plutonium

originates from the global fallout of the NWT<sup>2</sup>, specific areas were significantly affected by accidental releases of plutonium.<sup>3</sup> The presence of residual plutonium contamination in Palomares soils has been confirmed more than 30 years later following the 1966 plane crash involving two nuclear bombs, even though considerable remediation efforts towards contamination removal were undertaken.<sup>4</sup> More recently, a continuous series of major radioactive water leaks from the damaged Fukushima Daiichi nuclear plant<sup>5</sup> arouse concern regarding the potential radioactive contamination of the ocean and ground waters and set a necessity for a reliable risk assessment tool in case of accidental radioactive discharge.

Plutonium, as a low-soluble, strongly sorbing contaminant, is considered a highly immobile species. However, recent laboratory and field studies have demonstrated that colloid-facilitated plutonium transport over significant distances occurs in subsurface environments and groundwater systems.<sup>6,7</sup> An enhanced mobility of fallout plutonium and its excess compared to <sup>241</sup>Am and <sup>137</sup>Cs have been demonstrated in the waters and mosses from the Venoge spring of the karst system in the Swiss Jura Mountains, evoking the possible role of colloidal transport and enhanced bioavailability.<sup>8</sup> Naturally-occurring colloids in these environments include humic acids, mineral colloids and particles, as well as heterogeneous aggregates of humic acid-coated iron hydroxide particles and organic nuclei coated by a Fe-Ca rich layer.<sup>9</sup> The association of plutonium with colloid species can increase its mobility, but will potentially reduce the bioavailability of the radionuclide.

The technique of diffusive gradients in thin films (DGT) is widely used for passive sampling of trace metals. It allows the determination of time-weighted average concentrations of bioavailable contaminant species.<sup>10,11</sup> A DGT sampler device consists of a diffusive gel layer, permeable for labile contaminant species, providing a surrogate of aquatic organisms, and a binding gel layer containing the binding agent, with both layers

embedded into a plastic housing. The DGT technique has been successfully applied for determining radioelements such as U,  $^{226}\text{Ra}$ ,  $^{137}\text{Cs}$  and  $^{134}\text{Cs}$  in natural waters.<sup>12,13,14, 15</sup> To our knowledge, DGT has not yet been applied for plutonium speciation measurements and the diffusion coefficient for plutonium in polyacrylamide (PAM) gels is unknown.

The aim of this work was to develop the DGT technique for plutonium bioavailability measurements in freshwaters environment. We determined the diffusion coefficients of  $^{239}\text{Pu}$  in the PAM gel in different laboratory conditions by performing a series of experiments in a diffusion cell at picomolar concentrations. Additionally, we carried out further cell diffusion experiments with fulvic and humic acids of soil organic matter as binding ligands for  $^{239}\text{Pu}$ . Natural waters sampled at a mineral spring and an organic-rich brook of the Swiss Jura Mountains were enriched in natural colloids by ultrafiltration and used in the experiments in order to support the hypothesis of colloidal binding of  $^{239}\text{Pu}$ . To demonstrate the binding capacity of Chelex resin and the applicability of the DGT technique for in-situ plutonium measurements, we exposed commercially available DGT samplers with Chelex resin as the binding phase in standardized solutions and compared the results obtained with experiments carried out in a diffusion cell.

## 1.3 Experimental

### 1.3.1 Materials and methods

All reagents used were of analytical grade from Merck or Fluka or Sigma-Aldrich.

Experiments on plutonium diffusion were performed in a specially fabricated diffusion cell with a polyacrylamide gel diaphragm of 0.39 mm.<sup>16</sup> We constructed a Teflon<sup>®</sup> cell with two 100 mL compartments, interconnected by a 1.7 cm diameter window. Teflon<sup>®</sup> was chosen in order to avoid plutonium adsorption on the walls surface. A gel disc placed between the two compartments enabled the diffusion of plutonium species from compartment A, initially containing <sup>239</sup>Pu at a known concentration in the range of 100-140 mBq mL<sup>-1</sup> (SI-7), into compartment B, initially containing a solution of the same volume and same chemical composition as A, without <sup>239</sup>Pu. PAM gel sheets and DGT sampler units with Chelex resin as the binding layer were purchased from DGT Research Limited, Lancaster, UK. All solutions were prepared with deionised water (< 0.05 µS cm<sup>-1</sup>) and used at room temperature (21-25°C) in equilibrium with atmospheric CO<sub>2</sub>. The pH of the solutions was maintained with 2-amino-2-hydroxymethyl-1,3-propanediol (Tris) or 3-(N-morpholino)propanesulfonic acid (MOPS) buffers at 10 mM concentration and adjusted with 0.1 M HCl and/or 0.1 M NaOH. The ionic strength was fixed at 10-20 mM with Na<sub>2</sub>SO<sub>4</sub>. Fulvic (FA, ≈2000-3500 Da) and humic (HA, 5000-40'000 Da) acids were extracted from an organic soil of an Alpine valley, separated, desalted and characterized according to the procedure described in Supporting Information. Dissolved organic matter (DOM) concentrations were determined using absorbance at different wavelengths according to Carter *et al.*<sup>17</sup> <sup>239</sup>Pu standard solution at 10 Bq mL<sup>-1</sup> was provided by the metrology group of the Institute of Radiation Physics, Lausanne, Switzerland (source PU239-ELSC10 from CEA), and used at suitable concentrations by dilution. <sup>238</sup>Pu (source, PU238-ELSC10 from CEA) was also used in some experiments to

lower the concentration 300 times, due to a higher specific activity, thus avoiding the risk of PuO<sub>2</sub> precipitation. <sup>239</sup>Pu stock solution at the +V oxidation state was prepared according to Xu et al.<sup>18, 19</sup> Plutonium analyses were carried out on PIPS detector (450 mm<sup>2</sup>) in an Alpha Analyst spectrometer with Apex Alpha software (Canberra, France). Thorium (as <sup>232</sup>Th) was obtained from Sigma-Aldrich and analyzed using a Perkin-Elmer Optima 3300 DV ICP-OES spectrometer.

### **1.3.2 Diffusion experiments**

Diffusion coefficients of plutonium in different laboratory conditions were measured using a diffusion cell according to the previously described procedure by Zhang and Davison.<sup>16</sup> Since plutonium can be present in several different oxidation states (III to VI) in environmental conditions, we chose to adjust the oxidation state of plutonium to IV to simplify the interpretation of our experimental data to the diffusion of the <sup>239</sup>Pu (IV) species only. The oxidation state of plutonium was adjusted to IV by evaporation and calcination of a suitable aliquot of <sup>239</sup>Pu tracer solution with NaHSO<sub>4</sub> and H<sub>2</sub>SO<sub>4</sub> as recommended by Bajo *et al.*<sup>20</sup> The residue was dissolved in 75 mL of 10 mM MOPS, resulting in a solution of 10 mM Na<sub>2</sub>SO<sub>4</sub>, adjusted at pH 6.50-7.00 and left overnight exposed to the atmosphere for equilibration with CO<sub>2</sub> prior to the diffusion experiment.

Some experiments were designed to check for the oxidation state of plutonium during and after the diffusion experiment. In one experiment designed to control the +IV oxidation state of plutonium, all the solutions were degassed with N<sub>2</sub> until the oxygen probe (Cellox 325) read < 0.5 ppm, and the diffusion experiment was carried out in a glove box under N<sub>2</sub> flux. The presence of Pu (IV) was evidenced in some experiments by extraction of plutonium in compartment A with HDEHP (bis(2-ethylhexyl)phosphoric acid) in hexane, which extracts the +IV and +VI oxidation state but not the +III and +V oxidation states.<sup>21</sup> In



an experiment with a double spike of  $^{238}\text{Pu}$  at +IV and  $^{239}\text{Pu}$  at +V oxidation states, SPE (solid phase extraction) on TEVA resin was used to specifically extract Pu (IV) from the B compartment in nitric acid media. Pu (V) was not extracted in these conditions. In one experiment thorium was used as a proxy for plutonium. In natural environmental conditions, thorium is always present as Th (IV), thus avoiding the problem of the complex chemistry of plutonium. However, the solubility of thorium is very low in these conditions and Th (IV) was maintained in solution at concentration compatible with ICP-OES analysis only at pH below 4. Otherwise, the experimental conditions were similar to those with plutonium.

In the experiments with organic matter, 1.5 mg of freeze-dried FA or HA were dissolved together with plutonium tracer and equilibrated overnight. Each compartment was well stirred with a miniature electrical mixer throughout the experiment. 2.0 mL sample aliquots were taken from both compartments simultaneously at regular time intervals of 10 min. In the experiment with HA, aliquots were taken with intervals of several hours because of a very low diffusion rate. Aliquots from compartment B were evaporated and wet ashed with nitric and perchloric acid before electrodeposition and measurements by alpha-spectrometry. Gel discs were retrieved at the end of each experiment and analyzed for plutonium accumulation. A detailed description of the analytical procedure can be found in the SI. Activity of the diffused  $^{239}\text{Pu}$  (IV) (mBq) was plotted as a function of time and the slope  $\Delta A/\Delta t$  used for calculations of diffusion coefficients  $D$  ( $\text{cm}^2 \text{s}^{-1}$ ) according to equation (1):

$$D = \frac{\Delta g}{C \times S} \times \frac{\Delta A}{\Delta t} \quad (1),$$

where  $\Delta g$  is the diffusion gel thickness (cm),  $C$  the initial  $^{239}\text{Pu}$  (IV) concentration ( $\text{mBq mL}^{-1}$ ),  $S$  the diffusion area ( $\text{cm}^2$ ), and  $A$  the activity (mBq) of  $^{239}\text{Pu}$  (IV) species diffused in compartment B at the time  $t$  (s). Equation 1 is only valid when the concentration of diffusing

$^{239}\text{Pu}$  (IV) species in compartment B is negligibly low, compared to the concentration in compartment A, and when the diffusion of  $^{239}\text{Pu}$  (IV) species follows a linear function. In all experiments used for D calculation the concentration of  $^{239}\text{Pu}$  (IV) in compartment B throughout the duration of the experiment did not exceed 1-2 % of the initial concentration in compartment A. Uncertainties on D were calculated by a quadratic summation of relative uncertainty on the gel thickness, on the surface area, on the initial concentration and on the slope  $\Delta A/\Delta t$ . Uncertainty on the slope was obtained by calculating the linear regression on the experimental data using Igor<sup>®</sup> Pro software (WaveMetrics, USA). The coverage factor was  $k=1$ .

In order to simulate the bioavailability of plutonium in natural conditions, we carried out similar diffusion experiments as previously described, using natural waters sampled at two sites of the karst system in the Swiss Jura Mountains (Venoge spring and Noiraigue Bied brook, SI). Bulk waters were filtered through a 0.65  $\mu\text{m}$  filter, the pH adjusted to 7.00 with MOPS buffer and spiked with  $^{239}\text{Pu}$  (IV). The physico-chemical characterization of the waters is given in the SI.

To investigate the hypothesis of colloidal binding of the environmental plutonium in the Venoge spring and Noiraigue Bied brook, we subjected bulk waters to ultrafiltration through an 8 kDa Millipore Pellicon XL polyethersulphone membrane (surface area 50  $\text{cm}^2$ ) to reach the concentration factor ( $cf$ ) of 5. Retentate fractions were then spiked with  $^{239}\text{Pu}$  (IV) and used in diffusion experiments as described above.

### **1.3.3 Deployment of DGT in laboratory conditions**

To test the performance of Chelex resin as binding phase for plutonium species, we deployed DGT samplers with a diffusive gel thickness of 0.78 mm in a laboratory solution containing 0.43  $\text{mBq mL}^{-1}$  of  $^{239}\text{Pu}$  (IV), 10 mM  $\text{NaNO}_3$  and 10 mM MOPS buffered at pH 6.50.

We used a clean 5 L polypropylene beaker to expose three DGT units with 0.78 mm gel upon constant stirring at room temperature for 72 hours. To prevent the evaporation of the solution and any potential contamination, the beaker was sealed with Parafilm<sup>®</sup> throughout the experiment. One DGT unit was retrieved every 24 hours of deployment, rinsed with deionized water and the resin gel layer removed and analyzed for plutonium content according to the standard procedure (SI). Aliquots of the solution were collected and analyzed at regular time intervals to monitor the concentration of plutonium in the exposure solution and to check for any potential loss of plutonium due to adsorption on the beaker walls. Activities of <sup>239</sup>Pu (IV) accumulated in the Chelex resin were plotted as a function of deployment time and used for the calculation of the diffusion coefficients according to equation 1.

## **1.4 Results and discussion**

### **1.4.1 Determination of D for plutonium**

Laboratory solutions containing <sup>239</sup>Pu at picomolar concentrations are prone to modifications leading to the formation of intrinsic colloids, precipitation and adsorption of <sup>239</sup>Pu on labware walls and thus to the loss of the radionuclide species from the experimental system. To avoid these potential drawbacks, we provided controlled experimental conditions for diffusion coefficient determination. Tris and MOPS buffers were chosen to stabilize the pH of solutions in the range of environmental pH values of 6.50-7.25. To test the stability of the experimental system prior to diffusion coefficient measurements, we designed a long-term experiment in the diffusion cell containing <sup>239</sup>Pu (IV) in a Tris buffered solution at pH 5.50 in compartment A. Diffusion of <sup>239</sup>Pu (IV) through the PAM gel took place during 55 hours. Results show a clear trend of <sup>239</sup>Pu (IV) concentration increase in

compartment B throughout the experiment, yielding a typical diffusion function (Figure 2, SI). After 55 hours, 25 % of the initial  $^{239}\text{Pu}$  (IV) was found in compartment B. At this concentration, the back diffusion of  $^{239}\text{Pu}$  (IV) species from the B compartment to the A compartment becomes significant. The concentrations of  $^{239}\text{Pu}$  (IV) measured in compartment A at the end of the experiments make it possible to recalculate the total  $^{239}\text{Pu}$  (IV) balance in the diffusion system throughout the experiment. The apparent loss of  $^{239}\text{Pu}$  (IV) was less than 5 % compared to the initially introduced  $^{239}\text{Pu}$  (IV) activity into compartment A, lying in limits of the experimental error. Thus, plutonium was not lost by adsorption on the walls of compartment A. These results demonstrate the soundness of the experimental approach selected and proves that no adsorption of  $^{239}\text{Pu}$  (IV) species on the walls of the diffusion cell occurs during the timeframe of the experiment.

The diffusion coefficients of plutonium in the PAM hydrogel must be known prior to bioavailability field measurements using DGTs. The diffusion coefficients of  $^{239}\text{Pu}$  (IV) species in different laboratory conditions were measured using the two-compartment diffusion cell approach and are outlined in Table 1. A slightly lower diffusion coefficient is observed in the Tris ( $2.06 \times 10^{-6} \text{ cm}^2 \text{ s}^{-1}$ ) buffered solution compared to the MOPS ( $2.29 \times 10^{-6} \text{ cm}^2 \text{ s}^{-1}$ ) buffered solution due to a more pronounced complexation capacity of the Tris molecule. It could also be explained by a slight difference of pH in the two experiments (7.25 and 6.50 respectively). Nevertheless, we consider that it has no significant influence on  $^{239}\text{Pu}$  (IV) speciation in this pH range. Figure 1 displays a linear increase of  $^{239}\text{Pu}$  (IV) in compartment B of the diffusion cell throughout the experiment duration of up to 120 minutes. Regression coefficient,  $r^2$ , in all the experiments, is above 0.95. These data enable the calculation of the diffusion coefficient using the slope  $\Delta A/\Delta t$  with relatively low uncertainty (Table 1).

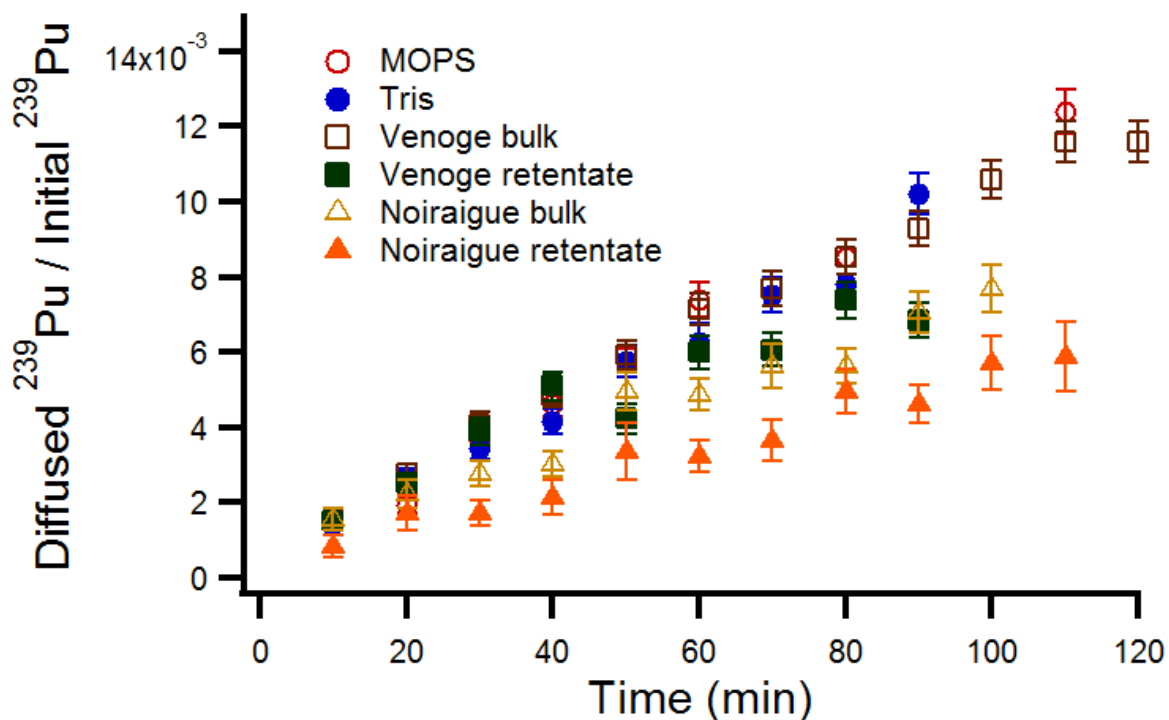


**Figure 1.** Normalized activities (mBq) of  $^{239}\text{Pu}$  (IV) accumulated in the initially zero concentration compartment B of the diffusion cell plotted as a function of time in solutions of different compositions. From top to bottom: MOPS (red open circle), Tris (blue full circle), bulk from Venoge spring (brown open square), retentate from Venoge spring (green full square), bulk from Noiraigue Bied brook (brown open triangle), retentate from Noiraigue Bied brook (orange full triangle).

By lowering the mass concentration 300 times using  $^{238}\text{Pu}$  (IV), which has a higher specific activity compared to  $^{239}\text{Pu}$ , similar diffusion coefficient was obtained ( $2.06 \pm 0.13 \times 10^{-6} \text{ cm}^2 \text{ s}^{-1}$ ). This demonstrates that the relatively high concentration used in compartment A during the diffusion experiment did not result in  $\text{PuO}_2$  precipitation.

Plutonium can be present in four different oxidation states in natural environmental conditions. We decided to work with the + IV oxidation state because higher oxidation states such as + V and + VI can be reduced in presence of organic matter. Experiment with degassed solution in a gloves box in absence of oxygen results also in similar diffusion coefficient as in presence of oxygen ( $2.02 \pm 0.15 \times 10^{-6} \text{ cm}^2 \text{ s}^{-1}$ ). This results demonstrates that oxidation of Pu (IV) to Pu (V) did not occur significantly during the timeframe of the experiments (two hour). In the end of one experiment with Pu (IV), plutonium in compartment A was extracted in HDEHP in hexane. Results show that the organic phase contained  $65 \pm 10\%$  of the plutonium compared to the initial concentration. As HDEHP extracts 80% of Pu (IV) and Pu (VI) in one extraction, this result also supports that the oxidation state (+IV) has not change significantly all along the experiment.

Additionally, Th (IV) can be used as a proxy for Pu (IV) since it does not change its oxidation state in environmental conditions. Nevertheless we were not able to maintain thorium in solution at the concentration necessary for ICP-OES measurements at a pH value above 4. Thus we carried out a diffusion experiment using Th (IV) at pH 4. Thorium behaved in the same way as plutonium in the diffusion experiment. The calculated diffusion coefficient was  $1.30 \pm 0.07 \times 10^{-6} \text{ cm}^2 \text{ s}^{-1}$ , a value significantly lower than for plutonium, but still in the same range (Figure 3). In this experiment, the concentration of Th (IV) used was much higher than that of Pu and the pH lower. Thus both diffusion coefficients cannot be directly compared. Nevertheless, thorium was present as Th (IV), without oxidation taken place. Thus the fact that both diffusion coefficients are in a similar range may also be an indirect indication that plutonium kept its +IV oxidation state in our diffusion experiments.

The flux of  $^{239}\text{Pu}$  through the diffusive gel depends on the size distribution and on the molecular weight of the diffusing  $^{239}\text{Pu}$  species. The experiment in presence of 20 ppm of FA

indicated that the diffusion of  $^{239}\text{Pu}$  (IV) is hindered compared to Tris/MOPS buffered raw solutions, but still remains in the same range with a diffusion coefficient of  $2.03 \times 10^{-6} \text{ cm}^2 \text{ s}^{-1}$ .<sup>1</sup> The ratio of  $^{239}\text{Pu}$  (IV) concentration measured in the PAM gel disc, retrieved at the end of the diffusion experiment with FA, to the initial  $^{239}\text{Pu}$  (IV) concentration in the A compartment was 0.4, showing no specific accumulation of FA-Pu species in the gel. A slight coloration of the B compartment by FA during the experiment shows that FA molecules have diffused through the gel. In addition, Levy et al. demonstrated that the dissociation of most metal-FA complexes (including Cu, Pb, Ni, Cd, Mn and Co) was sufficiently fast so that it does not limit DGT measurements.<sup>22</sup> Conversely, as shown in Figure 2, the diffusion of  $^{239}\text{Pu}$  (IV) in presence of 20 ppm of HA is reduced significantly, with a diffusion coefficient of  $0.50 \times 10^{-6} \text{ cm}^2 \text{ s}^{-1}$  (calculated with the first three points). The reason behind this dramatic drop in diffusion coefficient resides in the chemical nature of HA, which represents a complex mixture of large organic molecules with numerous coordination sites, available for binding trace metal ions. Large organic complexes will not diffuse as easily as FA through the PAM gel but can accumulate in the gel. Van der Veecken *et al.* reported a ten-fold accumulation of HA in the PAM gel.<sup>23</sup> The concentration of  $^{239}\text{Pu}$  (IV) in the PAM gel disc retrieved at the end of the experiment with HA was 3.5 times higher than the initial concentration of  $^{239}\text{Pu}$  (IV) in compartment A. This enrichment of the gel with  $^{239}\text{Pu}$  (IV) supports the idea of HA accumulation in the PAM gel, which was also observed visually by a coloration of the gel at the end of the experiment. It may explain the deviation from linearity of the HA plot on Figure 2 during the long timeframe of the experiment (100 hours). Coloration of the B compartment was not observed in the experiment with HA, thus to the opposite of FA, diffusion of HA through the gel is minimal. On the other hand, HA-Pu complexes can be labile, allowing some of the plutonium to diffuse through the gel. In this case, D will be

strongly dependant on the free plutonium concentration at the diffusive boundary layer (DBL). The observation that some of the plutonium has indeed diffused through the gel may show that the Pu-HA complexes are possibly partly labile.

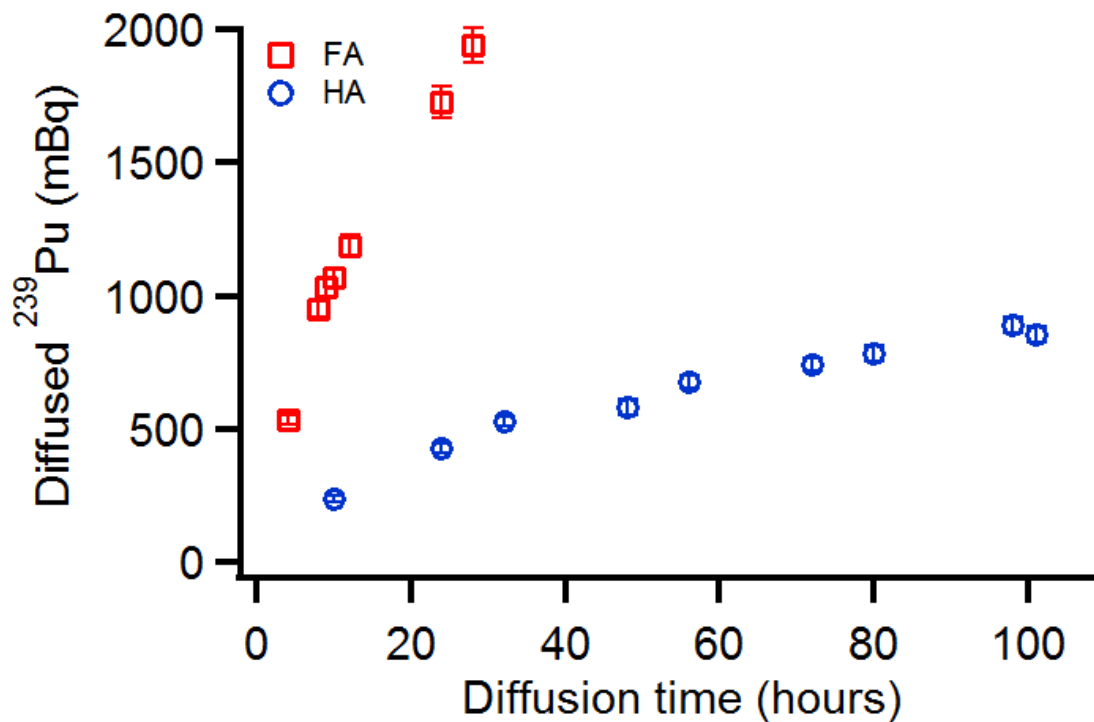


**Figure 2.** Accumulation of <sup>239</sup>Pu (IV) in the initially zero concentration compartment B of the diffusion cell in the presence of 20 ppm of fulvic (FA, red open square) or humic acid (HA, blue open circle). In case of HA, the first three points only (linear domain) were used to calculate the diffusion coefficient, because of HA and <sup>239</sup>Pu (IV) accumulation in the gel during the timeframe of the experiment.

Experiments carried out with natural waters, containing dissolved organic matter and rich in natural colloidal particles, as well as in retentate fractions enriched in natural colloids by ultrafiltration, indicate the reduced mobility of <sup>239</sup>Pu (IV) species. Diffusion coefficients of <sup>239</sup>Pu (IV) in bulk waters of the mineral, carbonate-rich Venoge spring ( $D = 1.89 \times 10^{-6} \text{ cm}^2 \text{ s}^{-1}$ ) and organic-rich Noiraigue Bied brook ( $D = 1.38 \times 10^{-6} \text{ cm}^2 \text{ s}^{-1}$ ) are 17% and 40 % lower



compared to the values obtained in the MOPS buffered laboratory solution. Noiraigue waters contained 13 ppm of DOM while Venoge waters contained only 1 ppm of DOM (SI). The larger decrease in  $D_{Pu}$  in the bulk water of Noiraigue compared to Venoge bulk water demonstrates the role of DOM as binding molecules for plutonium. Furthermore, diffusion coefficients of  $^{239}Pu$  (IV) measured in the retentate fractions are 15 % and 20 % lower compared to the bulk for mineral and organic-rich waters respectively, with values of  $1.60 \times 10^{-6}$  and  $1.10 \times 10^{-6} \text{ cm}^2 \text{ s}^{-1}$ . These results confirm that plutonium species will bind to natural colloids in natural environment, with consequences on mobility and bioavailability.

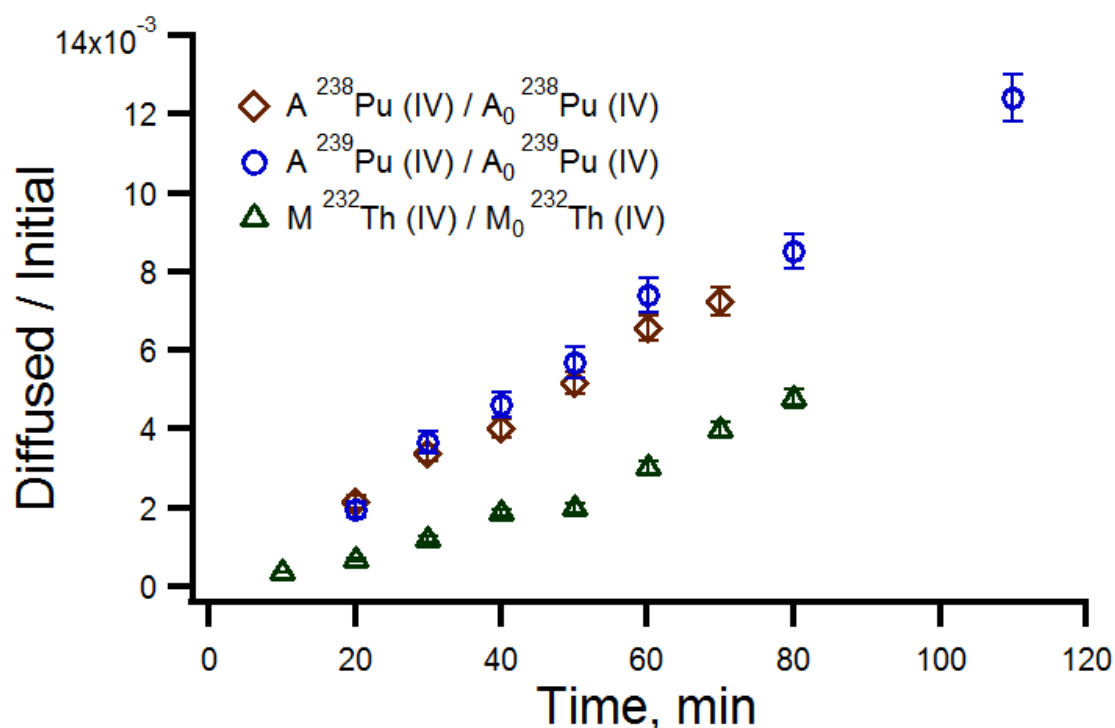


**Figure 3.** Activities (mBq) of  $^{239}Pu$  (IV) and  $^{238}Pu$  (IV) normalized to the initial activity in the compartment A and masses of  $^{232}Th$  (IV) accumulated in the initially zero concentration compartment B normalized to the initial mass in the compartment A of the diffusion cell, plotted as a function of time. Diffusion of thorium was performed at pH 4.

**Table 1.** Diffusion coefficients of  $^{239}\text{Pu}$  (IV) ( $\times 10^{-6} \text{ cm}^2 \text{ s}^{-1}$ ) in PAM gel. Experiments were carried out in the two-compartment diffusion cell with single gel thickness of 0.39 mm in solutions of different compositions at room temperature. DGT devices were deployed in 5 L standardized solutions containing  $0.43 \text{ mBq mL}^{-1}$  of  $^{239}\text{Pu}$  (IV).

Experimental conditions	pH	D
Tris buffer 10 mM / $\text{NaNO}_3$ 10 mM	7.25	$2.06 \pm 0.15$
MOPS buffer 10 mM / $\text{Na}_2\text{SO}_4$ 10 mM	6.50	$2.29 \pm 0.15$
MOPS buffer 10 mM / $\text{Na}_2\text{SO}_4$ 10 mM	6.50	$2.02 \pm 0.15^{\text{a)}$
MOPS buffer 10 mM / $\text{Na}_2\text{SO}_4$ 10 mM	6.50	$2.06 \pm 0.13^{\text{b)}$
Fulvic acid 20 ppm / MOPS 10 mM / $\text{Na}_2\text{SO}_4$ 20 mM	7.00	$2.03 \pm 0.19$
Humic acid 20 ppm / MOPS 10 mM / $\text{Na}_2\text{SO}_4$ 20 mM	6.80	$0.50 \pm 0.03^{\text{c)}$
Venoge spring bulk water / MOPS 10 mM / $\text{Na}_2\text{SO}_4$ 10 mM	7.00	$1.89 \pm 0.11$
Venoge spring retentate fraction / MOPS 10 mM / $\text{Na}_2\text{SO}_4$ 10 mM	7.00	$1.60 \pm 0.21$
Noiraigue Bied brook bulk water / MOPS 10 mM / $\text{Na}_2\text{SO}_4$ 10 mM	7.00	$1.38 \pm 0.12$
Noiraigue Bied brook retentate / MOPS 10 mM / $\text{Na}_2\text{SO}_4$ 10 mM	7.00	$1.10 \pm 0.10$
0.39 mm DGT / 5 L glass beaker / MOPS 10 mM / $\text{NaNO}_3$ 10 mM	7.00	$1.33 \pm 0.10$
0.78 mm DGT / 5 L plastic beaker / MOPS 10 mM / $\text{NaNO}_3$ 10 mM	6.50	$2.45 \pm 0.30$

a) experiment carried out in a glove box in nitrogen atmosphere

b) experiment carried out with  $247 \text{ mBq mL}^{-1}$  solution of  $^{238}\text{Pu}$  (IV)

c) calculated using the first three points of Figure 2.

Polyacrylamide diffusive gel discs retrieved from the diffusion cell after each experiment were systematically analyzed for  $^{239}\text{Pu}$  (IV) accumulation. The ratios of  $^{239}\text{Pu}$  (IV) concentration in the gel to  $^{239}\text{Pu}$  (IV) concentration in the A solution did not exceed 0.5-0.6, which is in a good agreement with the expected half concentration in the gel, when the diffusion gradient in the gel is established, according to the DGT theory<sup>10</sup>. These findings prove no significant interaction of  $^{239}\text{Pu}$  (IV) species with PAM gel.

#### **1.4.2 Deployment of DGT in laboratory conditions**

We tested the  $^{239}\text{Pu}$  (IV) uptake using commercial DGT devices. Linear uptake of  $^{239}\text{Pu}$  (IV) in the DGTs was observed, as displayed in Figure 3. Once again, we were able to calculate the diffusion coefficient in PAM gel, using this alternative experiment. Taking into account the uncertainty, the measured diffusion coefficient of  $2.45 \pm 0.30 \times 10^{-6} \text{ cm}^2 \text{ s}^{-1}$  is in a good agreement with the measured D in the diffusion cell ( $2.29 \pm 0.15 \times 10^{-6} \text{ cm}^2 \text{ s}^{-1}$ ). In a previous experiment in a 5 L glass beaker at pH 7.00 with three DGT devices with 0.39 mm gel, we observed a significant steady decrease of the bulk concentration of  $^{239}\text{Pu}$  (IV) in the solution, probably due to adsorption on the glass walls. While the results show a linear uptake of  $^{239}\text{Pu}$  (IV) (Figure 3, SI), the expected  $^{239}\text{Pu}$  (IV) accumulated in the Chelex resin was much lower. The calculated D was  $1.33 \times 10^{-6} \text{ cm}^2 \text{ s}^{-1}$ , much lower compared to similar diffusion experiments. This result confirms that glassware is not adequate to carry out experiments with plutonium at neutral pH, even in well buffered solutions.

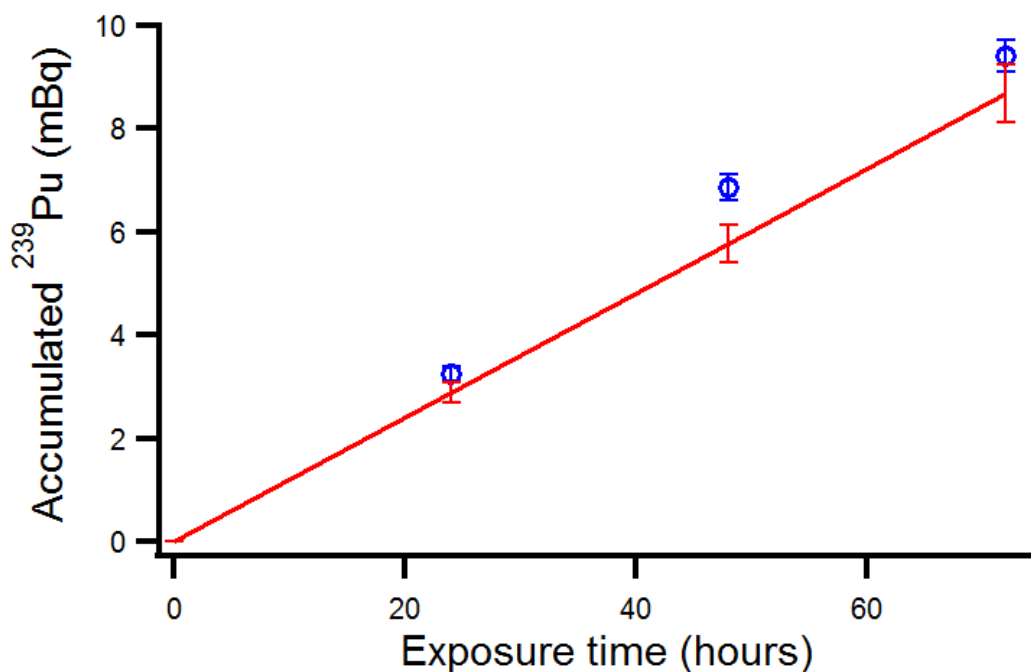


**Figure 4.** DGT uptake of  $^{239}\text{Pu}$  (IV) from a 5 L laboratory solution of  $0.43 \text{ mBq mL}^{-1}$  concentration. DGT samplers with 0.78 mm diffusive gel thickness and Chelex resin gel as binding phase were deployed (open blue circles). Straight red line represents the calculated flux (equation 1) in this system for a diffusion coefficient of  $2.29 \pm 0.15 \times 10^{-6} \text{ cm}^2 \text{ s}^{-1}$  as determined for the MOPS system in the diffusion cell.

Our findings demonstrate that the DGT technique can be applied for plutonium bioavailability measurements in freshwaters, with Chelex resin as a binding phase. The use of commercially available DGTs for plutonium measurements is conceivable for contaminated areas, however, detection limits and ultratrace concentrations of plutonium in the environment can present a challenge for in-situ DGT applications, taking into account the saturation of the Chelex binding layer by other, more abundant ions. Larger diffusion surfaces compared to conventional DGT devices might be necessary. Modeling the flux of plutonium with the diffusion coefficients measured in this work in chemically different environments (Figure 5) shows a clear trend of gradually decreasing flux of plutonium

species with enrichment of the waters with DOM or naturally occurring colloids. Our results show that plutonium species behave in a very similar way as other heavy metals when experimental conditions are adjusted to avoid hydrolysis. In this respect, the theory and experiments designed by others<sup>24,22,25,26</sup> to improve our knowledge of the bioavailability of metals and liability of metal-complexes using DGT can be applied to study the plutonium-DOM interaction in natural systems. In addition, the use of picomolar solutions in our work also demonstrates that DGT is applicable to environmental level of plutonium concentration. Part of this further work is now underway in our laboratory.

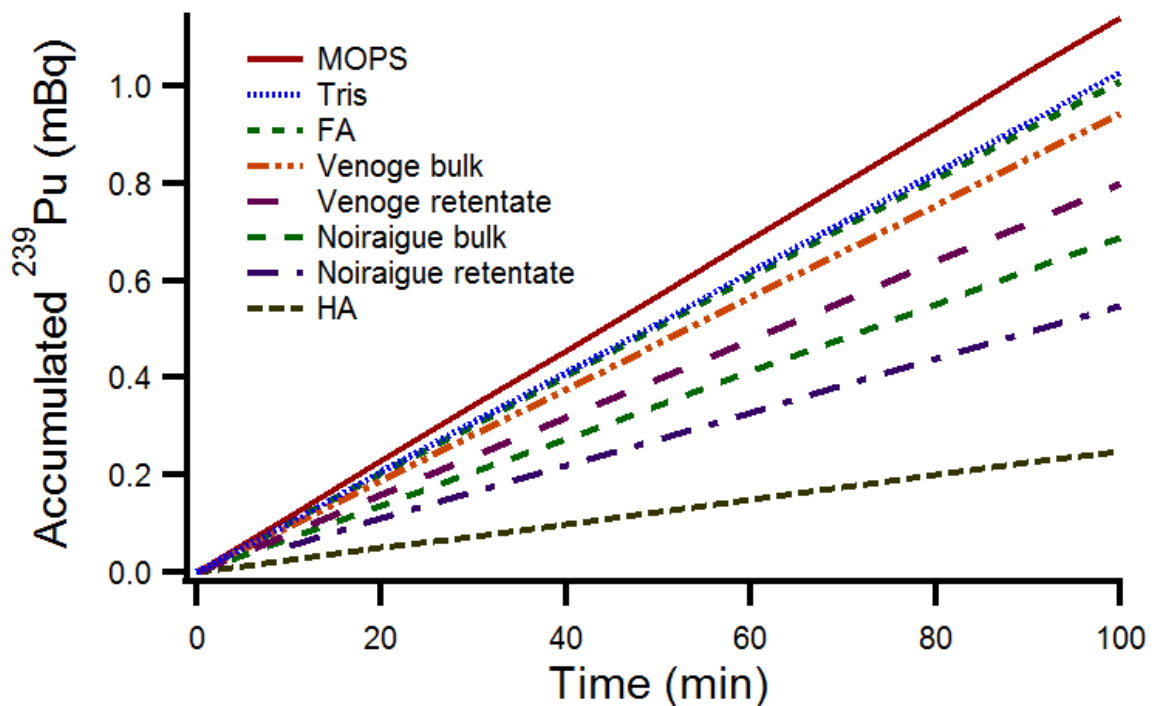


**Figure 5.** <sup>239</sup>Pu flux through PAM gel in chemically different environments theoretically calculated for D given in the Table 1, 0.39 mm diffusive gel thickness and  $C_0=100 \text{ mBq mL}^{-1}$ . From top to bottom: MOPS, Tris, FA, Venoge bulk, Venoge retentate, Noiraigue Bied bulk, Noiraigue Bied retentate, HA.

### **1.5. Supporting information**

Detailed description of the extraction, desalting and characterization of fulvic and humic acids from an organic soil of an Alpine valley, Switzerland. Detailed description of the plutonium determination. Description of water sampling, characterization and ultrafiltration. Figure showing the stability of the diffusing solution and figure of DGT measurement in a glass beaker. This material is available free of charge via the Internet at <http://pubs.acs.org>.

### **1.6 Acknowledgements**

This work was founded by the Swiss National Science Foundation (grant n° 200021-140230) and by the Swiss Federal Office of Public Health (PF and PS). One reviewer is thanked for suggesting additional experiments with lower concentration ( $^{238}\text{Pu}$ ) and with Th (IV) as a proxy for Pu (IV).

## 1.7 References

1. Kersting, A. B., Plutonium Transport in the Environment. *Inorganic Chemistry* **2013**, *52*, (7), 3533-3546.
2. Alvarado, J. A. C.; Steinmann, P.; Estier, S.; Bochud, F.; Haldimann, M.; Froidevaux, P., Anthropogenic radionuclides in atmospheric air over Switzerland during the last few decades. *Nature Communications* **2014**, *5*, 3030-3030.
3. Taylor, D. M., Environmental plutonium - Creation of the universe to twenty-first century mankind. *Plutonium in the Environment* **2001**, *1*, 1-14.
4. Jimenez-Ramos, M. C.; Garcia-Tenorio, R.; Vioque, I.; Manjon, G.; Garcia-Leon, A., Presence of plutonium contamination in soils from Palomares (Spain). *Environmental Pollution* **2006**, *142*, (3), 487-492.
5. Schneider, S.; Walther, C.; Bister, S.; Schauer, V.; Christl, M.; Synal, H. A.; Shozugawa, K.; Steinhauser, G., Plutonium release from Fukushima Daiichi fosters the need for more detailed investigations. *Scientific Reports* **2013**, *3*, 5.
6. Utsunomiya, S.; Ewing, R. C.; Novikov, A. P.; Kalmykov, S. N.; Horreard, F.; Merkulov, A.; Clark, S. B.; Myasoedov, B. F.; Tkachev, V. V., Colloid transport of plutonium in the far-field of the Mayak Production Association, Russia. *Abstracts of Papers of the American Chemical Society* **2007**, *233*.
7. Kersting, A. B.; Efurud, D. W.; Finnegan, D. L.; Rokop, D. J.; Smith, D. K.; Thompson, J. L., Migration of plutonium in ground water at the Nevada Test Site. *Nature* **1999**, *397*, (6714), 56-59.
8. Froidevaux, P.; Steinmann, P.; Pourcelot, L., Long-Term and Long-Range Migration of Radioactive Fallout in a Karst System. *Environ. Sci. Technol.* **2010**, *44*, (22), 8479-8484.
9. Mavrocordatos, D.; Mondy-Couture, C.; Atteia, O.; Leppard, G. G.; Perret, D., Formation of a distinct class of Fe-Ca(-C-org)-rich particles in a complex peat-karst system. *Journal of Hydrology* **2000**, *237*, (3-4), 234-247.
10. Davison, W.; Zhang, H., In-situ speciation measurements of trace components in natural-waters using thin-film gels. *Nature* **1994**, *367*, (6463), 546-548.
11. Zhang, H.; Davison, W., Direct in situ measurements of labile inorganic and organically bound metal species in synthetic solutions and natural waters using diffusive gradients in thin films. *Anal. Chem.* **2000**, *72*, (18).
12. Li, W.; Zhao, J.; Li, C.; Kiser, S.; Cornett, R. J., Speciation measurements of uranium in alkaline waters using diffusive gradients in thin films technique. *Anal. Chim. Acta* **2006**, *575*, (2), 274-280.
13. Li, W. J.; Li, C. S.; Zhao, J. J.; Cornett, R. J., Diffusive gradients in thin films technique for uranium measurements in river water. *Anal. Chim. Acta* **2007**, *592*, (1), 106-113.
14. Leermakers, M.; Gao, Y.; Navez, J.; Poffijn, A.; Croes, K.; Baeyens, W., Radium analysis by sector field ICP-MS in combination with the Diffusive Gradients in Thin Films (DGT) technique. *Journal of Analytical Atomic Spectrometry* **2009**, *24*, (8), 1115-1117.
15. Murdock, C.; Kelly, M.; Chang, L. Y.; Davison, W.; Zhang, H., DGT as an in situ tool for measuring radiocesium in natural waters. *Environ. Sci. Technol.* **2001**, *35*, (22), 4530-4535.
16. Zhang, H.; Davison, W., Diffusional characteristics of hydrogels used in DGT and DET techniques. *Anal. Chim. Acta* **1999**, *398*, (2-3), 329-340.
17. Carter, H. T.; Tipping, E.; Koprivnjak, J. F.; Miller, M. P.; Cookson, B.; Hamilton-Taylor, J., Freshwater DOM quantity and quality from a two-component model of UV absorbance. *Water Research* **2012**, *46*, (14), 4532-4542.
18. Xu, C.; Athon, M.; Ho, Y.-F.; Chang, H.-S.; Zhang, S.; Kaplan, D. I.; Schwehr, K. A.; DiDonato, N.; Hatcher, P. G.; Santschi, P. H., Plutonium Immobilization and Remobilization by Soil Mineral and Organic Matter in the Far-Field of the Savannah River Site, US. *Environ. Sci. Technol.* **2014**, *48*, (6), 3186-3195.
19. Saito, A.; Roberts, R. A.; Choppin, G. R., Preparation of solutions of tracer level Plutonium(V). *Anal. Chem.* **1985**, *57*, (1), 390-391.
20. Bajo, S.; Eikenberg, J., Preparation of a stable tracer solution of plutonium(IV). *Radiochim. Acta* **2003**, *91*, (9), 495-497.
21. Akatsu, J., Separation of plutonium-238 from fission-products by solvent-extraction using HDEHP. *Journal of Nuclear Science and Technology* **1973**, *10*, (11), 696-699.
22. Levy, J. L.; Zhang, H.; Davison, W.; Galceran, J.; Puy, J., Kinetic Signatures of Metals in the Presence of Suwannee River Fulvic Acid. *Environ. Sci. Technol.* **2012**, *46*, (6), 3335-3342.
23. Van der Veecken, P. L. R.; Chakraborty, P.; Van Leeuwen, H. P., Accumulation of Humic Acid in DET/DGT Gels. *Environ. Sci. Technol.* **2010**, *44*, (11), 4253-4257.
24. Arvajeh, M. R. S.; Lehto, N.; Garmo, O. A.; Zhang, H., Kinetic Studies of Ni Organic Complexes Using Diffusive Gradients in Thin Films (DGT) with Double Binding Layers and a Dynamic Numerical Model. *Environ. Sci. Technol.* **2013**, *47*, (1), 463-470.

25. Uribe, R.; Mongin, S.; Puy, J.; Cecilia, J.; Galceran, J.; Zhang, H.; Davison, W., Contribution of Partially Labile Complexes to the DGT Metal Flux. *Environ. Sci. Technol.* **2011**, *45*, (12), 5317-5322.
26. Warnken, K. W.; Davison, W.; Zhang, H.; Galceran, J.; Puy, J., In situ measurements of metal complex exchange kinetics in freshwater. *Environ. Sci. Technol.* **2007**, *41*, (9), 3179-3185.



## **Chapter 2: Speciation and bioavailability measurements of environmental plutonium using diffusion in thin films**

With Philipp Steinmann, Marcus Christl, François Bochud and Pascal Froidevaux

Article published in:

*Journal of Visualized Experiments* (2015), issue 105, DOI: 10.3791/53188

Video-article available in open-access at <http://www.jove.com/video/53188/speciation-bioavailability-measurements-environmental-plutonium-using>

## 2.1 Abstract

The biological uptake of plutonium (Pu) in aquatic ecosystems is of particular concern since it is an alpha-particle emitter with long half-life which can potentially contribute to the exposure of biota and humans. The diffusive gradients in thin films technique is introduced here for *in-situ* measurements of Pu bioavailability and speciation. A diffusion cell constructed for laboratory experiments with Pu and the newly developed protocol make it possible to simulate the environmental behavior of Pu in model solutions of various chemical compositions. Adjustment of the oxidation states to Pu (IV) and Pu (V) described in this protocol is essential in order to investigate the complex redox chemistry of plutonium in the environment. The calibration of this technique and the results obtained in the laboratory experiments enable to develop a specific DGT device for *in-situ* Pu measurements in freshwaters. Accelerator-based mass-spectrometry measurements of Pu accumulated by DGTs in a karst spring allowed determining the bioavailability of Pu in a mineral freshwater environment. Application of this protocol for Pu measurements using DGT devices has a large potential to improve our understanding of the speciation and the biological transfer of Pu in aquatic ecosystems.

## 2.2 Introduction

Plutonium is an artificial radionuclide present in the environment as a result of the global fallout following the nuclear bomb tests and nuclear accidents. The redox chemistry of plutonium has important implications for its migration and biogeochemical cycling in environmental aquatic systems<sup>1</sup>. Plutonium has a complex chemistry and can exist in four oxidation states (III, IV, V, VI) at the same time. Therefore, the distribution of redox species of plutonium in natural waters is extremely sensitive to local chemical environment<sup>2,3</sup>. The oxidation state of plutonium also depends on the origin of the source — this statement

being mostly relevant for contaminated environments and disposal sites. Reduced plutonium species (+III and +IV) are found predominately in anoxic environments and originate from global fallout and stocked waste effluents, while higher oxidation states (+V and +VI) can be found among decay products of other actinides and in oxic environments<sup>4</sup>.

The mobility and the environmental behavior of plutonium can be predicted to some extent from the redox speciation. Plutonium in +III and +IV oxidation states exists predominately in solid phase and has increased capacity to sorb to inorganic colloids and naturally occurring organic matter (NOM) molecules. Plutonium in +III and +IV oxidation states is considered to be less mobile. More soluble oxidized forms of plutonium (+V and +VI, +V being most likely)<sup>5</sup> can potentially contribute to a higher biological transfer to aquatic organisms due to higher mobility. Nevertheless, in presence of NOM, particularly of humic acid, Pu (V) is being reduced<sup>17</sup>, shifting the partitioning several orders of magnitude in favor of precipitation. Despite the fact that the reduction rate of Pu (V) to Pu (IV) is 4 to 5 orders of magnitude faster than the reverse reaction, remobilization of Pu (IV) under oxidizing conditions may also take place<sup>1</sup>. Recent experimental data on mineral sediments amended with Pu (IV) and subjected to natural oxidizing conditions have demonstrated that the concentration of soluble Pu in aqueous phase increased over time<sup>1,6</sup>. The authors explain it by oxidative desorption of Pu (IV) and formation of more soluble Pu (V) and Pu (VI) species. Oxidation of Pu (IV) may also occur due to naturally encountered manganese oxides<sup>7</sup>. These observations are important for bioavailability modeling and environmental risk assessment of waste disposal and contaminated sites.

Studies on bioavailability and speciation of plutonium is a challenging task in both laboratory and *in-situ* conditions. Low environmental concentrations, the variability of redox

species and the interactions with natural colloids make it difficult to simulate the biogeochemical behavior of plutonium. The technique of diffusive gradients in thin films (DGT) based on the diffusion of free and labile contaminant species through a polyacrylamide (PAM) gel is widely used for environmental measurements of trace elements<sup>8</sup>. A DGT sampler represents a three-layer device made of a binding phase (for the majority of trace metals it is Chelex resin contained in the PAM gel), diffusive gel layer (PAM gel of varying thickness) and a filter membrane protecting the gel and holding the assembly together. Thin films of polyacrylamide gel, consisting of 85% of water, enable free and labile complex species to diffuse more rapidly than plutonium bound to large NOM molecules or natural colloidal particles. A set-up designed to study plutonium diffusion in thin PAM gel films in laboratory conditions is called a diffusion cell<sup>9</sup>. A diffusion cell is a two-compartment vessel where two separate compartments are interconnected by an opening of a given surface. The opening, *i.e.*, the window between the two chambers contains a disc of diffusion gel of a given thickness. We constructed a Teflon cell with two 100 ml compartments and a circular diffusion window 1.7 cm in diameter. One compartment is removable, facilitating the assembly. A 0.5 cm wide groove carved around the diffusion window on the fixed compartment serves to place the diffusive gel disc. The groove depth should be similar to PAM gel thickness intended for use. We choose to work with a 0.39 mm PAM gel, thus the groove depth in our diffusion cell is 0.39 mm. A detailed picture of the diffusion cell is given in Figure 1.

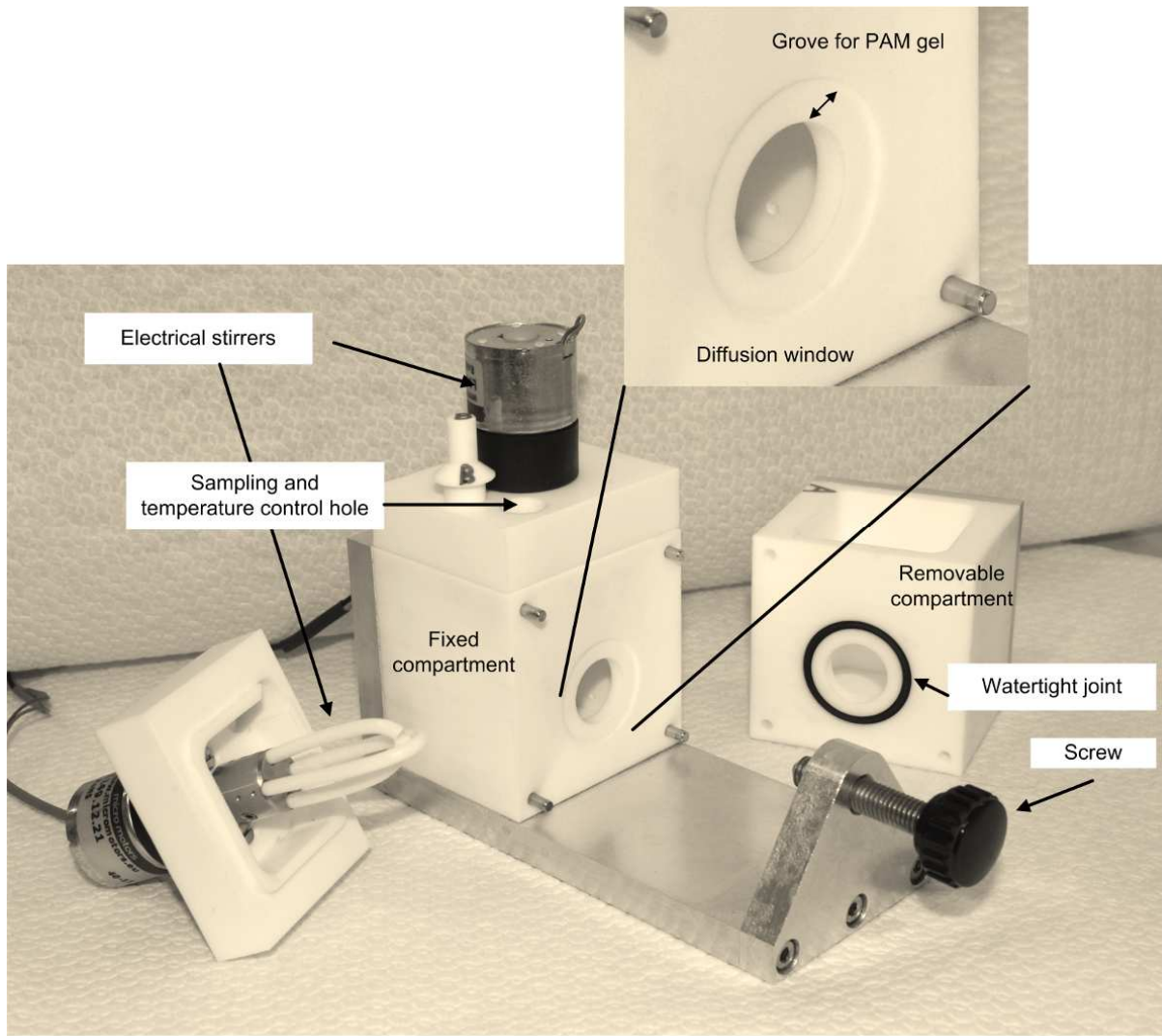


**Figure 1.** Diffusion cell used for experiments on Pu diffusion through the PAM gel. The groove thickness 0.5 cm, the groove depth 0.39 mm.

When a solution initially containing plutonium is placed into one compartment (A), diffusing Pu species will establish a concentration gradient in the gel and will start to accumulate in the second compartment (B), initially containing a solution of the same chemical composition without Pu. The initial concentration of Pu species in compartment A is defined such that it remains constant or changes very little (by 1%-2% at most) throughout the diffusion experiment. Plotting the amount of diffused Pu versus time provides a means to analyze the mobility of Pu species prevailing in the different simulated environmental conditions. Diffusion in thin films provides a valuable alternative for studies on Pu mobility and speciation and can be successfully applied in field conditions<sup>10</sup>. One can replace the diffusion cell by a passive sampler, manufactured with the PAM diffusive gel and Chelex resin as the binding phase, which serves to accumulate diffusing Pu species. Such a sampler can be exposed in field conditions — the amount of Pu accumulated in the resin will be indicative of the speciation and the bioavailability of Pu in the respective environment<sup>10</sup>.

In this work, we used a diffusion cell to investigate the mobility of Pu (IV) and Pu (V) species and their interactions with NOM in laboratory conditions. Furthermore, we applied large passive DGT samplers of a surface of 105 cm<sup>2</sup> to study the bioavailability of Pu in a karstic spring of the Swiss Jura Mountains (Venoge River) where a significant fraction of Pu was found in the intracellular parts of aquatic mosses in a previous work<sup>11</sup>. Because of the very low level of plutonium present in this pristine environment, accelerator-based mass spectrometry (AMS) techniques available at ETH Zurich were used to measure plutonium isotopes.

## 2.3 Protocol

### 1. Plutonium Tracer Preparation

#### 1. Pu (IV) tracer preparation

1. From the Pu stock solution transfer an appropriate aliquot containing the desired amount of Pu for the experiment into a 25 ml glass beaker. Work with 10 Bq of  $^{239}\text{Pu}$  at a time.
2. Add 1 ml concentrated  $\text{HNO}_3$ , 0.6 ml 1 M  $\text{NaHSO}_4$ , 0.4 ml concentrated  $\text{H}_2\text{SO}_4$ . Evaporate to dryness on a hot plate. Heat slowly at 200 °C at the beginning to avoid acid projection.
3. Once no liquid is left in the beaker, anneal the residue at 400 °C – 500 °C until no white fumes emanate. The residue is white when cooled and soluble in the buffer chosen for the experiment.

Note: Pu (IV) source prepared in this way can be stored dry up to several months<sup>12</sup>.

#### 2. Pu(V) tracer preparation<sup>13</sup>

##### 1. Pu oxidation

1. Transfer an aliquot from the Pu stock solution into a plastic 20 ml liquid-scintillation vial with a leakproof cap. Work with 10 Bq of  $^{239}\text{Pu}$  at a time. Add 0.01 ml of 0.01 M  $\text{KMnO}_4$  and leave the mixture in the dark for at least 6 hr.

##### 2. Pu(VI) extraction

1. Prior to extraction prepare a solution of 0.5 M thenoyltrifluoroacetone (TTA) in cyclohexane and protect it from light exposure. Always prepare this solution immediately prior to each experiment.

2. Add to the oxidized Pu solution 2 ml of 0.1 M CH<sub>3</sub>COONa at pH 4.7 and 2 ml of 0.5 M thenoyltrifluoroacetone (TTA) in cyclohexane. Wrap the bottle with aluminum foil to keep the reaction mixture in the dark, shake for 10 min. Separate the organic phase containing Pu(VI) with a pipette and transfer to a clean glass vial.
3. Pu (VI) to Pu (V) photoreduction
  1. Leave the glass vial containing Pu (VI)-TTA complex in cyclohexane at room light for 2 hr.
4. Pu (V) extraction
  1. Add to the light-exposed solution 1 ml of 0.1 M CH<sub>3</sub>COONa at pH 4.7 and shake for 5 min. Remove aqueous phase, containing Pu (V). Determine the concentration of this source by liquid scintillation counting taking a 100 μl aliquot.

Note: Prepare Pu (V) solutions immediately prior to each experiment since the long-term stability of Pu in +V oxidation state is being questioned.

## 2. Preparation of the Solutions Used in the Experiments

1. Prepare buffered solutions
  1. Make 10 mM solution of MOPS (3-(*N*-morpholino)propanesulfonic acid) buffer. Take 200 ml of this solution and adjust to the desired pH by drop wise addition of 0.1 M HCl (pH 6.5 for use with Pu(IV) and pH 5.5 for use with Pu(V)).
2. Prepare solutions for experiments with Pu (IV)
  1. Solution A



1. Dissolve Pu (IV) prepared at the step 1.1 in several milliliters of 10 mM MOPS buffered solution at pH 6.5. Thoroughly wash the beaker with the same solution.
  2. Bring the volume to 72 ml with 10 mM MOPS buffered solution at pH 6.5. Check the pH and re-adjust to 6.5 with 0.1 M NaOH. Transfer 72 ml of this solution into a clean beaker — this is the (A) solution to be introduced into compartment A of the diffusion cell.
2. Solution B
1. Take 72 ml of 10 mM MOPS buffered solution at pH 6.5; add 0.75 ml of 1 M Na<sub>2</sub>SO<sub>4</sub>. Check the pH, re-adjust to 6.5 if necessary. Transfer 72 ml of this solution into a clean beaker — this is the « B » solution to be introduced into « B » compartment of the diffusion cell.
3. Prepare solutions with NOM
1. Weigh 1.4 mg of freeze-dried fulvic or humic acid to a obtain concentration of 20 ppm and dissolve it in the « A » solution containing Pu (IV). Prepare this solution 24 hr prior to experiment and to allow for equilibration.
3. Prepare solutions for experiments with Pu (V)
1. Solution A
    1. Dissolve Pu (V) obtained at the step 1.2.4 in 72 ml of 10 mM MOPS buffered solution at pH 5.5; add 0.75 ml of 1 M NaNO<sub>3</sub>. Check the pH and adjust to 5.5 if necessary. Transfer 72 ml of this solution into a clean beaker. Prepare the solution with Pu (V) immediately prior to experiment.
  2. Solution B

1. Take 72 ml of 10 mM MOPS buffered solution at pH 5.5; add 0.75 ml of 1 M  $\text{NaNO}_3$ . Check the pH and adjust to 5.5 if necessary. Transfer 72 ml of this solution into a clean beaker.
3. Prepare solutions with NOM
  1. Weigh 1.4 mg of freeze-dried fulvic or humic acid to obtain a concentration of 20 ppm and dissolve in the A solution containing Pu (V). Leave the solution for 24 hr to reach the steady state between Pu (IV) and Pu (V) species. Prior to diffusion experiment perform a liquid phase extraction to determine the fraction of Pu (V) as described in the Section 3.4.2.

### **3. Laboratory Diffusion Experiments**

1. Prepare PAM gel
  1. Wet a plastic tray with several milliliters of electrolyte (*e.g.*, 10 mM  $\text{NaNO}_3$ ), place the PAM gel strip in and expand uniformly over the surface. Place cautiously a sharp punch of 2.7 cm in diameter on the gel surface. Avoid sliding the punch over the gel surface.
  2. Use local focused lighting if necessary, it may help to visualize the transparent PAM gel. Press the punch firmly against gel surface and release once it is cut.
2. Assembly of the diffusion cell
  1. Position the PAM gel disc with tweezers into the groove over the diffusion window in a smooth-faced manner. Turn the screw such that the two compartments of the diffusion cell hold together, interconnected via the PAM gel disc.
  2. Mark A and B diffusion cell's compartments. Assemble the diffusion cell with the gel disc immediately prior to each experiment; do not allow the gel to dry.

### 3. Launching a diffusion experiment

1. Slowly pour the A and B solutions into the corresponding compartments. Make sure that both solutions are poured at the same speed in order to provide equal volume in each compartment at any time, otherwise the diffusive gel can be damaged.
2. Launch the timer once the solutions are in the cell. Place the miniature electric mixers over the diffusion cell. At this time the diffusion experiment is considered started.

### 4. Taking samples throughout diffusion experiment

1. Take samples of equal volume within regular time intervals from the A and B compartments simultaneously in order to keep volumes constant throughout the experiment.

1. Take a 1.00 ml sample simultaneously in each compartment immediately at the beginning of the experiment to determine the initial Pu concentration in the A compartment.

2. Use a sampling time interval of 10 min in experiments without addition of NOM and 20 min to several h in experiments with humic acid. 2.00 ml aliquots are sufficient to provide good sensitivity for alpha-spectrometric measurements.

### 2. Liquid phase extraction of Pu (IV) and Pu (V)

1. At the end of the diffusion experiment take separately 4 ml samples from the A and the B compartments into plastic test-tubes with leakproof caps. Acidify samples with 1 ml 2 M HCl.

2. Add 5 ml of 0.5 M bis-(2-ethyl hexyl) phosphoric acid (HDEHP) solution in cyclohexane and agitate test-tubes vigorously for 5 min. Leave samples to allow for phase separation. Remove the water phase containing Pu (V).

### 3. Back-extraction of Pu (IV)

1. Back-extract Pu (IV) from the remaining organic phase with 5 ml of 5%  $(\text{NH}_4)_2\text{C}_2\text{O}_4$ .

### 4. Sample Treatment

#### 1. Spike samples with an internal standard

1. Spike samples to be analyzed with a yield tracer. Use a spike of 1.00 ml of  $^{242}\text{Pu}$  tracer of 25 mBq  $\text{ml}^{-1}$  activity concentration for alpha-spectrometric measurements.

#### 2. Oxidize samples' matrix

1. Evaporate samples to dryness on a hot plate with 2.00 ml of concentrated  $\text{HNO}_3$ .

### 5. Radiochemical Separation of Pu

#### 1. Adjust Pu oxidation state

1. Dissolve dry samples from point 4.2.1 in 5 ml 8 M  $\text{HNO}_3$ , add 20 mg  $\text{NaNO}_2$ , heat samples at 70 °C during 10 min. This step allows adjusting the oxidation state of Pu to +IV.

#### 2. Solid phase extraction of Pu

1. Wet a quaternary amine-based anion exchange resin column (such as TEVA) with 1.5 ml 8 M  $\text{HNO}_3$ . Use micro-columns made of 1 ml pipette tip with 100 mg of the resin conditioned with 1.5 ml 8 M  $\text{HNO}_3$ .
2. Pass the solution of point 5.1.1 through the resin column with flow rate of about 1  $\text{ml min}^{-1}$ . Rinse the sample beaker with 2 ml 8 M  $\text{HNO}_3$  three times and transfer washouts to resin columns.

#### 3. Elute Pu

1. Wash columns with 3 ml 9 M HCl. Elute Pu with 3 ml solution 9 M HCl/0.1 M HI. Evaporate eluates on the hot plate. Treat with 2 ml concentrated HNO<sub>3</sub>, evaporate to dryness. Repeat if necessary until the brown iodine color disappears.
2. Determine Pu concentration in the samples by any available method.
 

**Note.** For the concentrations range of <sup>239</sup>Pu used in this protocol alpha-spectrometry provides a good sensitivity. Prepare sources for alpha-spectrometric counting by electroplating on stainless steel discs<sup>14</sup>. Count sources on PIPS detector (450 mm<sup>2</sup>) in a spectrometer.

## 6. Analysis of the Data

1. Plot diffused Pu versus time
  1. Plot the activity of Pu (mBq) accumulated in the B compartment versus time (min). Correct for volume of the sample taken out during the diffusion experiment: activity of accumulated Pu (mBq) at time t is equal to the concentration (mBq ml<sup>-1</sup>) determined in the sample multiplied by the volume of the solution (ml) in the compartment B at the moment of sampling (see example of the spreadsheet — **Figure 2**).
  2. To plot on the same graph data from several experiments with different Pu concentrations, use concentrations normalized to the initial Pu concentration of compartment A.
2. Calculate diffusion coefficient
  1. Calculate diffusion coefficient D (cm<sup>2</sup> sec<sup>-1</sup>) of Pu species for each experiment<sup>10</sup>. Use equation (1):

$$D = \frac{\Delta g}{C \times S} \times \frac{\Delta A}{\Delta t} \quad (1)$$

where  $\Delta g$  is the diffusion gel thickness (cm),  $C$  the initial Pu concentration (mBq ml<sup>-1</sup>),  $S$  the diffusion area (cm<sup>2</sup>), and  $A$  the activity (mBq) of Pu species diffused in compartment B at the time  $t$  (sec).  $\Delta A/\Delta t$  is the slope of the linear plot of Pu diffused into the B compartment versus time.

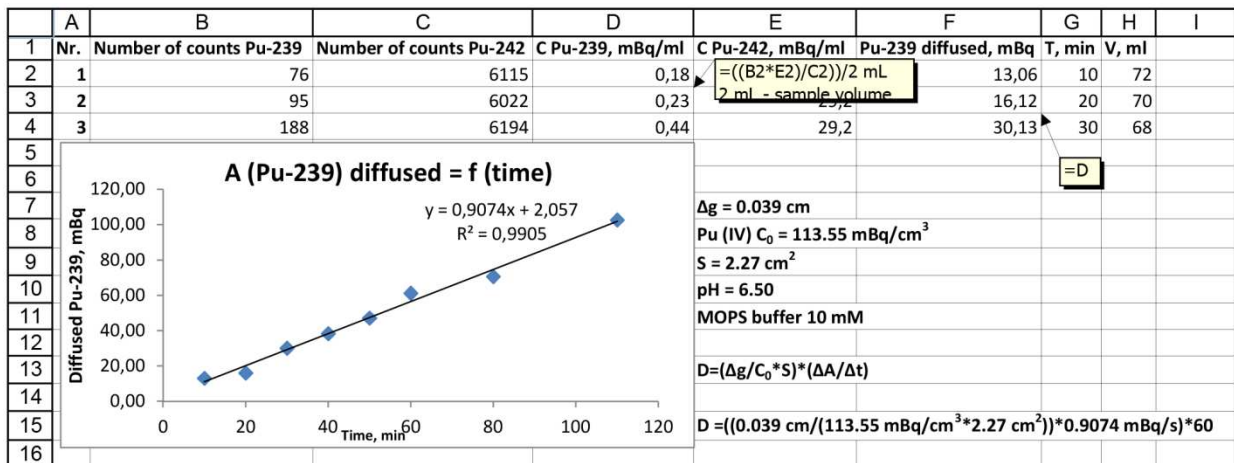


**Figure 2.** Snapshot of the Excel Worksheet used for calculations of the diffusion coefficient.

## 7. Bioavailability Studies of Pu in Natural Freshwaters

1. Prepare DGT samplers
  1. Wet a plastic tray with several milliliters of electrolyte (*e.g.*, 10 mM NaNO<sub>3</sub>), place the bottom plate (see **Figure 3**) of the DGT sampler. Use local lighting if necessary, it may help to visualize transparent gels.
  2. Position a 6 cm × 22 cm Chelex resin gel strip and expand uniformly over the plate's surface. Place on the top of the resin gel layer a 6 cm × 22 cm PAM diffusive gel strip and expand uniformly over the surface. Make sure that gels are not sliding and are positioned in a smooth-faced manner.
  3. Cover the diffusive gel layer with a 6 cm × 22 cm piece of a filter membrane. Place the cover frame of the DGT sampler (see **Figure 3**) over the filter membrane and close the assembly slightly pressing the frame on the edges.
  4. Cut the extending gel parts off with a sharp lancet, open and realign gel layers if necessary until a smooth plate surface is obtained. Fix the assembly with screws.
  5. Wet the DGT samplers with several milliliters of electrolyte (*e.g.*, 10 mM NaNO<sub>3</sub>). Store wet in a sealed plastic bag up to several weeks at 4-5 °C.
2. Deployment of DGTs in a natural body of water
  1. Take the DGT sampler out of the plastic bag. Fix DGT samplers in the holder as shown on the **Figure 4**.
  2. Deploy DGTs in the body of water either suspending them on a strong rope or installing on a stable vertical support in a way to provide a constant tangential water flow along the surface of the DGT. Deploy DGT devices in the freshwaters for two to

three weeks in order to accumulate the Pu at a concentration sufficient for measurements.

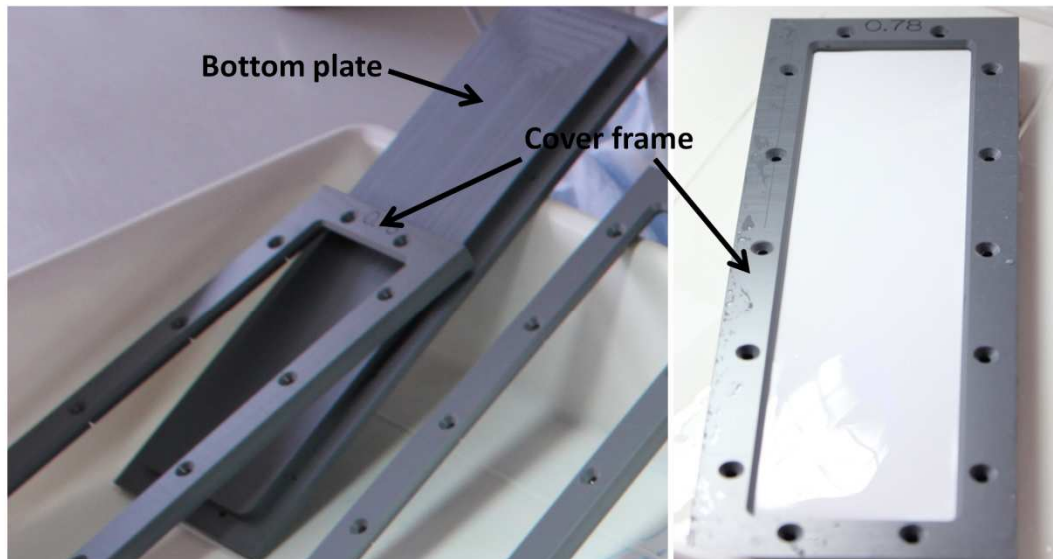


**Figure 3.** Large-surface DGT device for environmental Pu speciation measurements. Parts of the DGT device – the bottom plate and the cover frame – depicted on the left, the assembly with crew holes on the right.



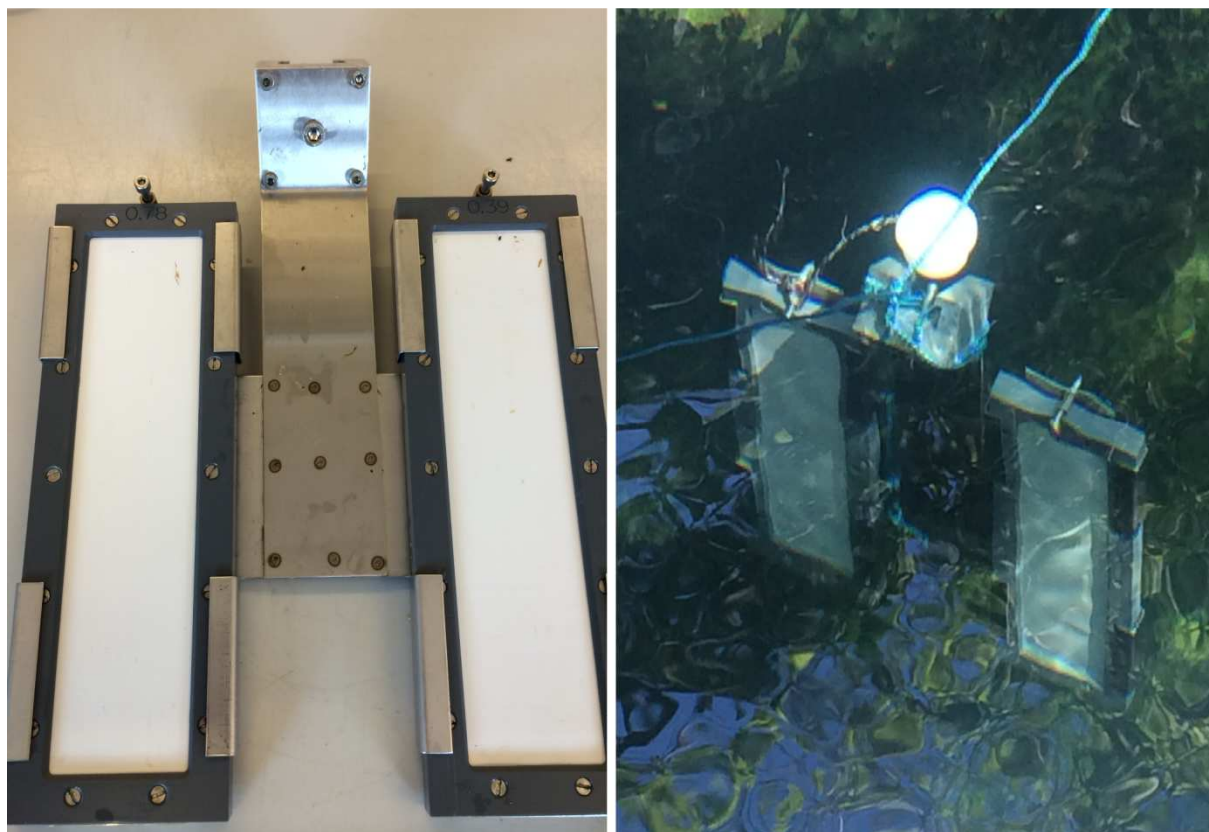


**Figure 4.** DGT sampler devices fixed in the holder (left) exposed in the Venoge spring (right) for Pu bioavailability measurements.

### 3. Treatment of retrieved DGTs

1. Retrieve DGTs from the water. Unscrew the assembly, take out filter membrane and discard. Take out the upper gel layer (PAM diffusive gel) and discard.
2. Transfer the resin gel into a glass beaker containing 20 ml 8 M HNO<sub>3</sub> and spike samples to be analyzed with a yield tracer. Use a spike of 1.00 ml of <sup>242</sup>Pu tracer of 0.25 mBq ml<sup>-1</sup> (1.7 pg ml<sup>-1</sup>) activity concentration for AMS measurements. After having well agitated, leave samples O/N for Pu elution.

### 4. Condition DGT eluates

1. Filter the solutions from the resin gel samples; rinse the remaining resin gels with 5 ml 8 M HNO<sub>3</sub> and combine washouts with samples. Add 20 mg NaNO<sub>2</sub> to each sample, heat the solutions at 70 °C during 10 min. This step allows adjusting the oxidation state of Pu to +IV.

### 5. Solid phase extraction of Pu

1. Wet a quaternary amine-based anion exchange resin cartridge with 10 ml 8 M HNO<sub>3</sub>. Pass the solutions of point 7.4.1 through the exchange resin cartridge with flow rate of about 1 ml min<sup>-1</sup>. Rinse the sample beaker with 5 ml 8 M HNO<sub>3</sub> three times and transfer the washouts to exchange resin cartridge.

### 6. Elute Pu

1. Wash cartridges with 10 ml 9 M HCL. Elute Pu with 15 ml solution 9 M HCl/0.1 M HI. Evaporate eluate on a hot plate. Treat with 2 ml concentrated HNO<sub>3</sub>, evaporate to dryness. Repeat if necessary until the brown iodine color has completely disappeared.
2. Repeat radiochemical separation of Pu one to two more times if higher purification is required — depending on the performance of Pu detecting system. Perform the

second and the third separations on micro-columns made of 1 ml pipette tip with 100 mg of exchange resin conditioned with 1.5 ml 8 M HNO<sub>3</sub>.

3. Determine Pu concentration in the samples. Use the mass-spectrometry techniques to measure <sup>239</sup>Pu because of the very low level of plutonium in the pristine environment.

Note: In this work, use the AMS facility tuned for analysis of actinides at the Laboratory of Ion Beam Physics at the Swiss Federal Institute of Technology in Zurich.

## 8. Analysis of the Data

1. Calculate the concentration ( $C_{DGT}$  in  $\mu\text{Bq ml}^{-1}$ ) of bioavailable (labile) Pu species in the bulk water from the amount of Pu accumulated by DGT during the deployment period.

Use equation (2):

$$C(DGT) = \frac{A \times \Delta g}{D \times S \times t} \quad (2)$$

where  $A$  is the activity ( $\mu\text{Bq}$ ) of Pu accumulated in the binding phase,  $\Delta g$  the diffusion layer (gel + filter membrane) thickness (cm),  $D$  the diffusion coefficient of Pu in the PAM gel ( $\text{cm}^2 \text{sec}^{-1}$ ),  $S$  the diffusion area ( $\text{cm}^2$ ), and  $t$  the duration of deployment (sec).

2. Compare  $C_{DGT}$  of Pu determined by DGTs with total Pu concentration in the bulk water, as well as with other available speciation data.

## 9. Radiochemical Separation for the Determination of Total Pu in the Bulk Water

1. Condition water sample
  1. Pump water from the studied body of water through a 45  $\mu\text{m}$  membrane filter into a plastic recipient. Work with samples of 10 to 50 L for AMS measurements. Acidify

the water to pH 2 with HNO<sub>3</sub> immediately after sampling at the sampling site prior to transporting to the laboratory.

## 2. Precipitate Pu on iron hydroxides

1. In the laboratory introduce an overhead stirrer into the recipient. Spike the sample with Pu yield tracer. Use a spike of 1.00 ml of <sup>242</sup>Pu tracer of 0.25 mBq ml<sup>-1</sup> (1.7 pg ml<sup>-1</sup>) activity concentration for AMS measurements.
2. Add FeCl<sub>3</sub>·6H<sub>2</sub>O taking about 0.25 g per 10 L sample. After having agitated for 30 min, precipitate iron hydroxides with NH<sub>4</sub>OH at pH 8.

## 3. Second precipitation of Pu on iron hydroxides

1. Decant the supernatant from water sample from point 9.2.2. Recover the precipitate of iron hydroxides into a 2 L glass beaker, rinse the recipient with deionized water and combine the washouts with the sample.
2. Dissolve the precipitate in ~100 ml 5 M HCl, heat to 90 °C to decompose carbonates. Filter if necessary when the solution is cooled down. Re-precipitate iron hydroxides with NH<sub>4</sub>OH at pH 8.

## 4. Condition iron hydroxides for analysis

1. Decant the supernatant from the sample from point 9.3.2. Recover the precipitate of iron hydroxide into a centrifugation vessel. Centrifuge, discard the supernatant. Wash the precipitate with deionized water. Repeat 2-3 times.
2. Dissolve the precipitate in 10 ml 8 M HNO<sub>3</sub>, submit to radiochemical separation of Pu as described previously in the sections 7.4-7.6.

## 10. Prepare Samples for AMS Measurements

### 1. Precipitate Pu on iron hydroxides

1. After radiochemical separation, dissolve the final sample in 0.5 ml 1 M HCl, transfer the sample with a plastic pipette into a 2.5 ml glass vial. Rinse the sample beaker twice with 0.5 ml 1 M HCl, transfer washouts to the same vial.
2. Add 0.5 ml of 2 mg ml<sup>-1</sup> Fe<sup>3+</sup> stock solution to provide 1 mg of iron. Precipitate iron hydroxides adding few drops of concentrated NH<sub>4</sub>OH. Centrifuge and decant the supernatant.
3. Wash the precipitate with deionized water, centrifuge and decant the supernatant. Dry the precipitate on the hot plate at 90 °C.

### 2. Prepare target for AMS measurements

1. Bake the hydroxides precipitate from point 10.1.3 in a furnace for 2-3 hr at 650 °C. Thoroughly mix with 3-4 mg of niobium metal powder and press into a Ti target holder for AMS measurements.

Note: We measured the samples with the compact (0.6 MV) AMS system “TANDY” at the Swiss Federal Institute of Technology (ETH Zurich) tuned for measurements of actinides.<sup>15,16</sup>

## 2.3 Representative results

### 2.3.1 Diffusion experiments

Plotting the activities of  $^{239}\text{Pu}$  diffused into the B compartment of the diffusion cell versus time gives a visual representation of the flux of the  $^{239}\text{Pu}$  species diffusing through the PAM gel. Diffusion coefficients calculated from these plots according to equation 1 provide an additional means to compare mobility of different  $^{239}\text{Pu}$  redox species in various chemical environments (Figure 2). Figure 5 illustrates the diffusion experiments with Pu (IV) and Pu (IV)-Pu (V) mixed species, respectively, in the MOPS buffer and in presence of 20 ppm of HA. A comparison of these plots shows that Pu (V) is significantly more mobile than Pu (IV). This is particularly valid for Pu (IV) and Pu (V) when HA (MW 5-40 kDa in our experiments, characterized in the SI by Cusnir *et al.*)<sup>10</sup> is added as complexing molecules. Pu (V) source solution prepared according to the protocol described in this paper contains predominately Pu(V) species. Liquid phase extraction with HDEHP at the end of the diffusion experiment in the MOPS buffered solution found  $80\% \pm 10\%$  of Pu (V). The chemical yield of this extraction is 80%. The solution with Pu (V) in presence of 20 ppm of HA was equilibrated during 24 hr and Pu (V) fraction in this model solution was  $35\% \pm 10\%$ .

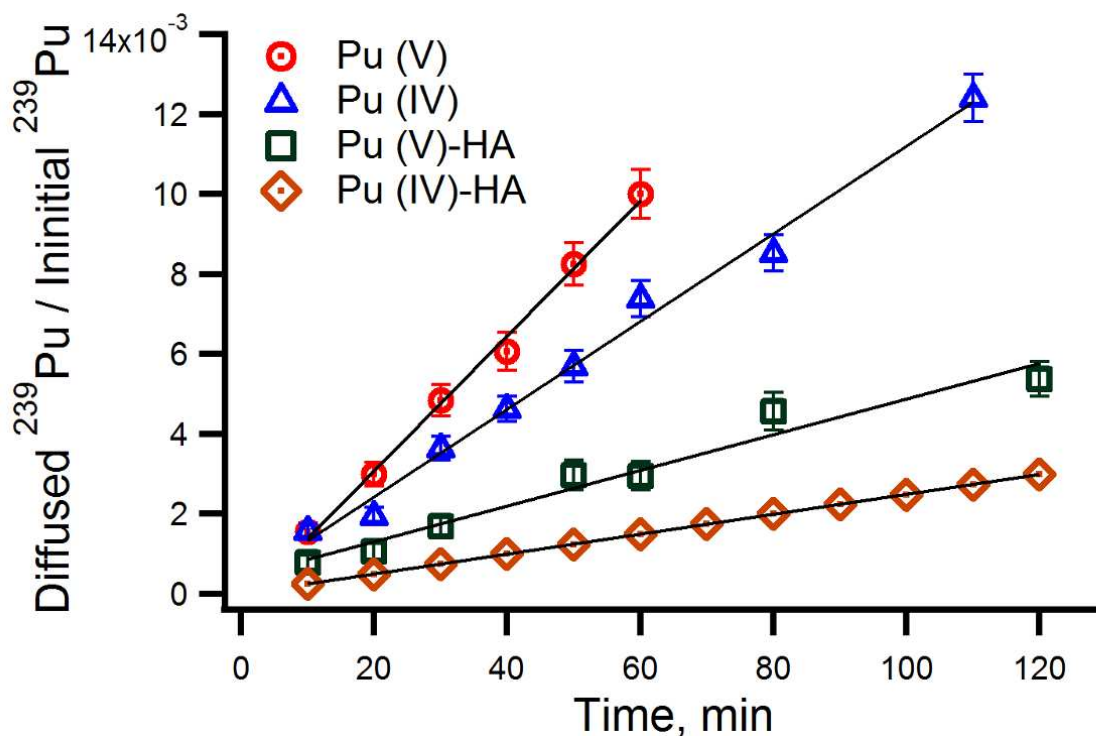


**Figure 5.** Plot of the  $^{239}\text{Pu}$  diffused into B compartment of the diffusion cell in different chemical environments. Experimental data points are presented for  $^{239}\text{Pu}$  (IV) and  $^{239}\text{Pu}$  (V), respectively, in MOPS buffer as well as for  $^{239}\text{Pu}$  (V) in the presence of HA. The line shown for  $^{239}\text{Pu}$  (IV)-HA has been calculated using a diffusion coefficient of  $0.50 \times 10^{-6} \text{ cm}^2 \text{ s}^{-1}$  determined previously<sup>10</sup>. Diffusion coefficients calculated from equation 1 are: Pu (IV) in MOPS buffer –  $2.29 \times 10^{-6} \text{ cm}^2 \text{ s}^{-1}$ , Pu (V) in MOPS buffer –  $3.50 \times 10^{-6} \text{ cm}^2 \text{ s}^{-1}$ , Pu (V) with HA –  $0.92 \times 10^{-6} \text{ cm}^2 \text{ s}^{-1}$ . From top to bottom: Pu (V) in MOPS buffer (red open circle), Pu (IV) in the MOPS buffer (blue open triangles), Pu (V) in presence of 20 ppm of HA (green open squares), Pu (IV) in presence of 20 ppm of HA (brown open diamonds).

### 2.3.2 Studies on Pu bioavailability in natural freshwaters

Several DGT devices constructed in our laboratory were successfully exposed for periods of two to three weeks in a karst spring of the Swiss Jura Mountains. This is a mineral spring with the pH of the water in the range of 6.5-7.5, conductivity above  $400 \mu\text{S cm}^{-1}$  and saturated with oxygen. These experiments demonstrated good applicability and robustness of the gel assemblies with no trace of biofouling, possibly also because of the low temperature of the spring ( $7 \text{ }^\circ\text{C}$ ). DGTs retrieved after the deployments were well preserved, with gel layers intact, conserving the initial form and visual appearance. Pu accumulated by DGTs was analyzed by AMS. AMS provides considerable advantages over other analytical techniques: it is highly sensitive (down to sub-fg levels), and requires much lower initial sample amount than alpha-spectrometry or ICP-MS techniques. In addition, molecular isobaric interferences, such as the uranium hydride ( $^{238}\text{U-H}$ ), or other molecules are efficiently suppressed during the AMS measurement and do not interfere with the  $^{239}\text{Pu}$  detection. For some technical reasons (most probably a contamination with  $^{239}\text{Pu}$  during chemical separations), we were not able to use the data for  $^{239}\text{Pu}$  for the first applications of DGTs in the field. Nevertheless, the  $^{240}\text{Pu}$  results were unbiased. Thus, we calculated the  $^{239}\text{Pu}$  content from the measured  $^{240}\text{Pu}$ , taking 0.18 as  $^{240}\text{Pu}/^{239}\text{Pu}$  atomic ratio for fallout plutonium. The results are summarized in Table 1.

$^{239}\text{Pu}$  concentrations measured in bulk water samples are similar to concentrations previously reported for this aquifer ( $1\text{-}7 \mu\text{Bq L}^{-1}$ )<sup>11</sup>. Furthermore,  $^{239}\text{Pu}$  concentrations calculated from DGT measurements are similar within the uncertainties of the measurement. Since DGTs accumulate only free and labile Pu species, one can estimate the fraction of bioavailable Pu in this water. Data given in Table 1 indicate that all the  $^{239}\text{Pu}$



species present in the bulk water are found in a bioavailable form. This is an interesting result in the light of previous findings<sup>11</sup>, which have revealed the predominant accumulation of <sup>239+240</sup>Pu in the intracellular fraction of the aquatic mosses growing in the spring compared to <sup>241</sup>Am and <sup>90</sup>Sr. The authors<sup>11</sup> suggested that the enhanced mobility of Pu in this natural aquifer was due to formation of a soluble carbonate Pu complex, possibly as a Pu(V) plutonyl form, similar to naturally occurring uranyl-carbonate complex. Water of the Venoge spring is hard water, with high carbonate concentration and very low NOM content (about 1 ppm).

**Table 1.** Representative results for <sup>239</sup>Pu measurements by AMS in the bulk water and DGT samplers. <sup>239</sup>Pu in the bulk water was co-precipitated from 20 L of water with iron hydroxides, extracted on the actinide-specific exchange resin. <sup>239</sup>Pu concentrations for DGT measurements calculated using equation 2 and diffusion coefficient for Pu (IV). Uncertainties for  $k=2$ ;  $u(95)$ .

Sample type	Number of measurements	<sup>239</sup> Pu concentration, $\mu\text{Bq L}^{-1}$
Bulk water	2	1.90±0.55
DGT 0.39 mm	2	1.74±0.90
DGT 0.78 mm	1	1.79±0.90

## 2.4 Discussion

The DGT methodology described here for experiments with Pu using a diffusion cell provides a reliable approach for various studies on Pu redox species and their interactions with organic molecules, colloidal particles and simulated environmental systems. Further applications of DGTs for environmental measurements of Pu will contribute to our understanding of the bioavailability and the fate of this radionuclide in aquatic ecosystems.

### 2.4.1 Laboratory diffusion experiments

In order to perform a successful diffusion experiment with meaningful conclusions on Pu mobility and interactions regarding a specific chemical environment, well defined and controllable conditions must be provided. The adjustment of Pu oxidation states prior to experiment is essential to simplify the data interpretation as well as to simulate various biogeochemical behaviors of Pu redox species. The sensitivity of Pu species to pH variations makes buffering the solutions a must. Particular attention should be drawn to the diffusion cell features and setup: the use of non-sorbing Teflon polymer material avoids adsorption on the cell walls and allows a robust leakproof assembly, preventing loss of Pu from diffusing solutions during the experiment.

The initial Pu concentration to be introduced into the A compartment, as well as the sampling interval and the volume of each sample taken during the diffusion experiment depend on the analytical method available in the laboratory. Any available analytical method can be used for determination of Pu concentration in the samples from the diffusion cell, however this choice is tightly bound to the initial activity of Pu taken for the experiment. 10 Bq of  $^{239}\text{Pu}$  as recommended in this protocol (giving 100-140 mBq ml<sup>-1</sup> or  $\sim 2 \times 10^{-13}$  mol ml<sup>-1</sup>) are sufficient to provide enough sensitivity for measurements by alpha-spectrometry and

generally do not pose particular problems for radiation protection regulations. The initial concentration of Pu can be reduced if other, more sensitive, analytical techniques are available for Pu determination (*e.g.*, mass-spectrometry). Sampling interval can be selected for each diffusion experiment, depending on Pu initial concentration, and the expected rate of diffusion through the PAM gel. In spite of the fact that the aliquots from diffusion experiments do not contain radionuclides other than Pu, the presence of mineral salts and of the MOPS buffer can interfere with analytical procedure, reducing the efficiency and the precision of quantitative analysis. Therefore it is preferable to perform a chemical separation of Pu on these samples.

The diffusion cell provides the best approach to study diffusion in the PAM gel since the gel is exposed directly to a well stirred solution. Thus, the effects of the diffusive boundary layer (DBL) at the gel surface are considered negligible. Good stirring of the solutions during a diffusion experiment is essential, allowing for minimization of the DBL effects. In the same time, one should proceed carefully in order to not disrupt the PAM gel.

#### **2.4.2 Studies of Pu bioavailability in natural freshwaters**

The results produced by this protocol show that measuring plutonium with DGT devices provides an efficient tool to study the bioavailability of plutonium in freshwater. DGT measurements yield time-average concentration of free and labile species, the two most important forms for biological uptake by living organisms. In addition, the kinetics of the interaction of Pu with organic matter can be investigated using gels of different thickness. The time necessary for Pu-NOM species to diffuse through the gel will allow for the most labile complexes to dissociate. DGT measurements can be complemented by ultrafiltration techniques, which yield the percentage of Pu colloidal species above a given size (*e.g.*, 8

kDa). Pu colloidal species are usually considered as non-bioavailable species and are part of the Pu fraction not measurable using DGT.

At this point, the DGT devices were deployed only in freshwater of a karst spring of the Swiss Jura Mountains. Low environmental concentrations of Pu require a long-term deployment of DGT devices, which can encounter potential drawbacks. Biofouling of the DGT surface represents a significant drawback, increasing the DBL thickness and thus limiting the flux of Pu through the PAM gel. Binding phase of the DGTs exposed in marine waters or waters of high mineralization may be rapidly saturated with other trace metals, misrepresenting the data for accumulation of Pu. Determination of trace levels of environmental Pu requires a thorough radiochemical separation and very sensitive analytical methods. AMS measurements applied in this protocol are not widely available, but can be replaced by other mass-spectrometry techniques. However, a rigorous radiochemical separation is necessary to eliminate the isobaric interference  $^{238}\text{U-H}$  from naturally occurring uranium.

Equation 2 shows that the size of the DGT device is an essential parameter that can be tuned to increase the quantity of accumulated Pu during a given deployment time. Commercial gel strips are available only with a maximum surface of 6 cm x 22 cm. Therefore, the window of the DGT sampler has been increased to 105 cm<sup>2</sup> (5 cm × 21 cm), making possible to accumulate enough of Pu species for relatively short deployment times. The assembly of such a DGT sampler requires precision and particular consideration of the PAM gel sheet properties while manipulating. It is of fundamental importance to assemble gel layers into a smooth-faced uniform “sandwich” in order to provide a homogeneous flux of Pu species from the bulk water through the diffusive gel. Good water flow at the DGT

surface is also an important parameter, yet it is mostly determined by flow conditions in the aquifer. It is recommended to place DGT devices for Pu measurements at about 45° towards the direction of water flow in order to provide a steady water supply and minimize the effects of the DBL.

Diffusion coefficient employed in the equation 2 must be corrected if the temperature in the studied body of water is different from the temperature at which the diffusion coefficient was determined. Temperature effects on diffusion coefficients are given by Stokes-Einstein equation (equation 3):

$$\frac{D_1\eta_1}{T_1} = \frac{D_2\eta_2}{T_2} \quad (3)$$

where  $D_1$  and  $D_2$  are diffusion coefficients ( $\text{cm}^2 \text{sec}^{-1}$ ),  $\eta_1$  and  $\eta_2$  are viscosities (mPa sec) of water at temperatures  $T_1$  and  $T_2$  (K) respectively.

Currently, there is no method to investigate Pu speciation in pristine environment, except for thermodynamic calculations based on, *e.g.*, pH and redox parameters. These parameters are only available for macro-components, such as carbonates, iron or manganese cations. Thus, Pu speciation is derived from these measurable species but does not represent a “real” measurement. Here we think that the diffusion in thin PAM gel film technique as presented in this paper is an important step in the resolution of the Pu speciation problem because it allows measuring *in situ* free and labile species and, possibly, evidencing plutonyl species. Although only a few DGT measurements of the environmental Pu in freshwaters have been undertaken so far, the obtained results are encouraging for further applications of the DGT technique for Pu speciation and bioavailability studies. Deployment of DGTs in organic-rich waters will potentially yield important information on Pu

mobility and interactions in presence of NOM molecules. Interesting results should be expected from DGT measurements in contaminated marine environments, such as the coastal seas around the Sellafield nuclear reprocessing plant and the damaged Fukushima Daiichi nuclear power plant.

## **2.5 Disclosures**

The authors have nothing to disclose.

## **2.6 Acknowledgements**

This work was funded by the Swiss National Science Foundation (grant n° 200021-140230) and by the Swiss Federal Office of Public Health (PF and PS). We thank the Swiss Federal Office of Public Health for providing financial support for the open-access publication of this paper.

## 2.7 References

1. Kaplan, D. I., *et al.* Influence of oxidation states on plutonium mobility during long-term transport through an unsaturated subsurface environment. *Environ. Sci. Technol.* **38** (19), 5053-5058, doi: 10.1021/es049406s, (2004).
2. Taylor, D. M. Environmental plutonium - Creation of the universe to twenty-first century mankind in *Plutonium in the Environment*, **1**, 1-14 (2001).
3. Maher, K., Bargar, J. R., Brown, G. E. Environmental Speciation of Actinides. *Inorganic Chemistry*. **52** (7), 3510-3532, doi: 10.1021/ic301686d, (2013).
4. Kurosaki, H., Kaplan, D. I., Clark, S. B. Impact of environmental curium on plutonium migration and isotopic signatures. *Environ. Sci. Technol.* **48** (23), 13985-91, doi: 10.1021/es500968n, (2014).
5. Orlandini, K. A., Penrose, W. R., Nelson, D. M. Pu (V) as the stable form of oxidized plutonium in natural-waters. *Marine Chemistry*. **18** (1), 49-57, doi: 10.1016/0304-4203(86)90075-7, (1986).
6. Kaplan, D. I., *et al.* Eleven-year field study of Pu migration from Pu III, IV, and VI sources. *Environ. Sci. Technol.* **40** (2), 443-448, doi: 10.1021/es050073o, (2006).
7. Morgenstern, A., Choppin, G. R. Kinetics of the oxidation of Pu (IV) by manganese dioxide. *Radiochim. Acta*. **90** (2), 69-74, doi: 10.1524/ract.2002.90.2\_2002.69, (2002).
8. Davison, W., Zhang, H. In-situ speciation measurements of trace components in natural-waters using thin-film gels. *Nature*. **367** (6463), 546-548, doi: 10.1038/367546a0, (1994).
9. Zhang, H., Davison, W. Diffusional characteristics of hydrogels used in DGT and DET techniques. *Anal. Chim. Acta*. **398** (2-3), 329-340, doi: 10.1016/s0003-2670(99)00458-4, (1999).
10. Cusnir, R., Steinmann, P., Bochud, F., Froidevaux, P. A DGT Technique for Plutonium Bioavailability Measurements. *Environ. Sci. Technol.* **48** (18), 10829-10834, doi: 10.1021/es501149v, (2014).
11. Froidevaux, P., Steinmann, P., Pourcelot, L. Long-Term and Long-Range Migration of Radioactive Fallout in a Karst System. *Environ. Sci. Technol.* **44** (22), 8479-8484, doi: 10.1021/es100954h, (2010).
12. Bajo, S., Eikenberg, J. Preparation of a stable tracer solution of plutonium (IV). *Radiochim. Acta*. **91** (9), 495-497, doi: 10.1524/ract.91.9.495.19999, (2003).
13. Saito, A., Roberts, R. A., Choppin, G. R. Preparation of solutions of tracer level plutonium (V). *Anal. Chem.* **57** (1), 390-391, doi: 10.1021/ac00279a096, (1985).
14. Bajo, S., Eikenberg, J. Electrodeposition of actinides for alpha-spectrometry. *Journal of Radioanalytical and Nuclear Chemistry*. **242** (3), 745-751, doi: 10.1007/bf02347389, (1999).
15. Dai, X. X., Christl, M., Kramer-Tremblay, S., Synal, H. A. Ultra-trace determination of plutonium in urine samples using a compact accelerator mass spectrometry system operating at 300 kV. *Journal of Analytical Atomic Spectrometry* **27** (1), 126-130, doi: 10.1039/c1ja10264h, (2012).
16. Christl, M., *et al.* The ETH Zurich AMS facilities: Performance parameters and reference materials. *Nuclear Instruments and Methods in Physics Research B*. **294**, 29-38, doi: 10.1016/j.nimb.2012.03.004, (2013).
17. Blinova, O., *et al.* Redox interactions of Pu(V) in solutions containing different humic substances. *Journal of Alloys and Compounds* **444**, 486-490, doi: 10.1016/j.jallcom.2007.02.117, (2007).





## **Chapter 3: Probing the kinetic parameters of Pu-NOM interactions in freshwaters using the DGT technique**

With Maud Jaccard, Claude Bailat, Philipp Steinmann, Marcus Christl, Max Haldimann, François Bochud and Pascal Froidevaux

Article published in:

*Environmental Science and Technology* (2016), volume 50, issue 10, pp. 5103-5110

DOI: 10.1021/es501149v

### 3.1 Abstract

The interaction of trace metals with naturally-occurring organic matter (NOM) is a key process of the speciation of trace elements in aquatic environments. The rate of dissociation of metal-NOM complexes will impact on the amount of free metal available for biouptake. Assessing the bioavailability of plutonium helps to predict its toxic effects on aquatic biota. However, the rate of dissociation of Pu-NOM complexes in natural freshwaters is currently unknown. Here we used the technique of diffusive gradients in thin films (DGT) with several diffusive layer thicknesses to provide new insights into the dissociation kinetics of Pu-NOM complexes. Results show that Pu complexes with NOM (mainly fulvic acid) are somewhat labile ( $0.2 \leq \xi \leq 0.4$ ), with  $k_{\text{dis}} = 7.5 \times 10^{-3} \text{ s}^{-1}$ . DGT measurements of environmental Pu in organic-rich natural water confirm these findings. In addition, we determined the effective diffusion coefficients of Pu (V) in polyacrylamide (PAM) gel in the presence of humic acid using a diffusion cell ( $D = 1.70 \pm 0.25 \times 10^{-6} \text{ cm}^2 \text{ s}^{-1}$ ). These results show that Pu (V) is a more mobile species than Pu (IV).

### 3.2 Introduction

The end products of decaying organic matter, often referred to as humic (HA) and fulvic (FA) acids, are ubiquitous in natural waters. At concentrations reaching several ppm, they are the major component of dissolved natural organic matter (NOM) and can act as a metal-ion buffer for metals present at trace levels.<sup>1</sup> The formation of soluble complexes with NOM molecules is an essential factor when evaluating the speciation and bioavailability of trace metals in aquatic environments.

Plutonium (Pu) is found at ultratrace levels in aquatic environments as a consequence of the global fallout following nuclear weapons tests and nuclear accidents.<sup>2, 3</sup> Pu is known to form complexes with NOM and natural colloids, however the exact extent of

these interactions remains unclear.<sup>4</sup> The biogeochemical behavior of Pu in natural waters is to some extent comparable to that of other heavy elements, however, there are several distinctive features; Pu can be found in soluble forms in four different oxidation states (+III to +VI) simultaneously, the most common being Pu (IV) and Pu (V).<sup>5, 6</sup> Recent studies have shown that Pu (IV) is prone to bind to NOM and natural colloids, with consequences on its mobility and its bioavailability.<sup>7-9</sup> In turn, Pu (V) is also an environmentally relevant species.<sup>6, 10, 11</sup> The kinetics of Pu (IV) and Pu (V) complex formation and dissociation will affect the bioavailable fraction of Pu in natural waters and its biouptake by aquatic organisms. However, kinetic data on Pu (IV) and Pu (V) interaction with NOM are scarce in the scientific literature and are mostly obtained by ligand exchange techniques.<sup>12</sup>

Recently, we showed that the technique of diffusive gradients in thin films (DGT) was able to provide valuable information on the interaction of plutonium with NOM in environmentally relevant conditions.<sup>7, 13</sup> One quantity which can be easily determined using the DGT technique is the diffusive boundary layer (DBL) thickness: this is a physical quantity, which emerges at the DGT-solution interface, where the metal flux towards the DGT is limited by the diffusive supply from the bulk solution in the absence of complex formation. The DBL thickness is expected to be the same for any metal. However, in the presence of complexing organic molecules, such as NOM, the metal supply to the DGT will also depend on the dissociation kinetics of the metal complexes.<sup>14</sup> Slowly dissociating complexes limit the metal supply to the DGT, thus the apparent diffusive boundary layer (ADBL) thickness will appear greater than the physical DBL and depends on metals. DGT experimental data obtained with various gel thicknesses can provide the dissociation rate constant of metal complexes and their lability degree in natural waters.<sup>15-18</sup>

The aim of the present work was to determine the dissociation rate constant of plutonium complexes with NOM and the lability degree ( $\xi$ ) of the Pu-NOM interaction. We used multiple DGT devices equipped with diffusive gels of different thicknesses to study the accumulation of Pu in the resin gel of DGT devices in absence and presence of NOM. We worked with model solutions containing Pu (IV) at femtomolar concentrations in the presence of a large excess (20 ppm) of FA to reveal the kinetic signature of Pu-FA interactions. The ADBL model was used to estimate the dissociation constant ( $k_{dis}$ ) of the Pu-FA complex<sup>18</sup> while the Penetration Analytical Model (PAM) was used to determine the lability criteria of the Pu-NOM interaction.<sup>15, 17</sup> We used our experimental settings,  $k_{dis}$  and WHAM7 speciation results in a dynamic numerical model to determine the Pu accumulated mass in DGT devices. Further on, we exposed DGT devices of 0.39 and 0.78 mm gel thickness in organic-rich water of a karst brook and used accelerator mass spectrometry (AMS) to determine the bioavailable fraction of Pu accumulated in the DGT resin-gel. Additionally, we determined the effective diffusion coefficients for Pu (V) species alone and Pu (V) in the presence of HA in cell diffusion experiments. The capability of HA to form labile complexes with Pu (V) and to reduce Pu (V) to Pu (IV) was also evaluated.

## **3.3 Experimental**

### **3.3.1 Materials and methods**

All reagents used were of analytical grade from Merck, Fluka, or Sigma-Aldrich. Polyacrylamide (PAM) gel sheets and DGT sampler units (exposed window area 3.08 cm<sup>2</sup>) with gels of five different thicknesses (0.39, 0.78, 1.18, 1.56 and 1.96 mm) and Chelex resin as the binding layer were provided by DGT Research Limited, Lancaster, UK. All solutions were prepared with deionized water (<0.05  $\mu\text{S cm}^{-1}$ ) and used at room temperature (21-25

°C) in equilibrium with atmospheric CO<sub>2</sub>. 3-(N-morpholino)propanesulfonic acid (MOPS) buffer was used at 10 mM concentration to maintain the pH of the solutions. The ionic strength was fixed at 10 mM with NaNO<sub>3</sub> in experiments with Pu (V) and with Na<sub>2</sub>SO<sub>4</sub> in experiments with Pu (IV). NOM (predominately FA, 2-3 kDa) was extracted from the organic-rich water of a brook in the Swiss Jura Mountains (Noiraigue Bied brook) and characterized according to the procedure described in the supplementary information (SI). Humic acid (HA, 5-40 kDa) was alkaline-extracted from an organic soil of an Alpine valley, separated, desalted and characterized as previously described.<sup>7</sup> Dissolved organic matter (DOM) concentrations in the experimental solutions were measured using UV-Vis spectrophotometry and quantified using absorbance at different wavelength according to Carter *et al.*<sup>19</sup> <sup>239</sup>Pu was used in the cell diffusion experiments with Pu in +V oxidation states and <sup>238</sup>Pu was used in +IV oxidation state in experiments with DGTs of different diffusive layer thickness. The reason for this change in isotopes composition was due to the need to use a Pu isotope (here <sup>238</sup>Pu) with higher specific activity when fixing the oxidation state to +IV to lower the Pu concentration, avoiding colloids formation. A <sup>239</sup>Pu reference solution of 10 Bq mL<sup>-1</sup> was provided by the radiometrology group of the Institute of Radiation Physics, Lausanne, Switzerland (source PU239-ELSC10 from CEA), and used at suitable concentrations by dilution. A Pu tracer solution at the +V oxidation state was prepared according to a modified procedure of Xu *et al.*<sup>10</sup> (see SI for details). The <sup>238</sup>Pu (source PU238-ELSC10 from CEA) was adjusted to the +IV oxidation state according to Bajo *et al.*<sup>20</sup> and used in all experiments with FA. To characterize the model solutions in our experiments, the distribution of oxidation states in the initial solution as well as at the end of each diffusion experiment was determined by extracting Pu (IV) into bis-(2-ethylhexyl)phosphoric acid (HDEHP), followed by the analysis of the aqueous phase for Pu (V). Note that the chemical yield of this liquid-liquid

extraction is about 80-90 % and we performed one extraction only. Uncertainties on the Pu (V) activities after extraction by HDEHP were calculated by propagating the counting uncertainty (LSC) and an uncertainty of B-type estimated on the extraction yield. Plutonium analyses were carried out on PIPS (Passivated Implanted Planar Silicon) detectors (450 mm<sup>2</sup>) in an Alpha Analyst spectrometer with Apex Alpha software (Canberra, France).

### 3.3.2 Diffusion experiments

The diffusion of Pu (V) through the PAM gel was studied using a two-compartment diffusion cell as described elsewhere.<sup>7</sup> The freshly prepared Pu (V) tracer solution was dissolved in 75 mL of 10 mM NaNO<sub>3</sub> buffered with 10 mM MOPS, resulting in  $\approx 150$  mBq mL<sup>-1</sup> concentration. The pH was adjusted to 6.50 and the solution used immediately in the diffusion experiment. In the experiments with HA, 1.5 mg of freeze-dried HA was dissolved together with Pu (V) tracer and used immediately in the diffusion experiment. Since Pu (V) is being reduced in the presence of HA,<sup>21</sup> we studied the kinetics of the reduction of Pu (V) to Pu (IV) in one experiment in parallel to diffusion, using samples from the A compartment. In this experiment, 2.00 mL samples from the A compartment (taken simultaneously with samples from the B compartment in order to equilibrate the volumes) were acidified with 1 mL of 2 M HCl and agitated with 3 mL of 0.5 M HDEHP in hexane to extract the Pu (IV). The water phase containing Pu (V) was analyzed by liquid scintillation counting yielding the fraction of Pu (V) remaining at any given time. In another experiment, we kept the Pu (V) in a solution with 20 ppm of HA for 24 h prior to starting the diffusion experiment to reach equilibrium between Pu (IV) and Pu (V) species. The Pu (V) fraction remaining in this solution was determined after extracting the Pu (IV) with HDEHP. Gel discs were retrieved at the end of each diffusion experiment and analyzed for plutonium accumulation. Effective diffusion coefficients  $D$  (cm<sup>2</sup> s<sup>-1</sup>) of Pu (V) were calculated from the classical DGT equation.<sup>22</sup>  $D$  of Pu

obtained using this approach represents an effective diffusion coefficient for Pu species, diffusing through the PAM gel. In all the experiments used to calculate  $D$ , the activity of Pu accumulated in the B compartment in the time frame of a diffusion experiment did not exceed 1.5 % of the initial activity in the A compartment. Uncertainty on the slope was calculated using the linear regression tool of Igor<sup>®</sup> Pro software (WaveMetrics, U.S.). Uncertainties on  $D$  were calculated using a quadratic summation of relative uncertainty on each of the parameters. The coverage factor was  $k = 1$ . A detailed protocol for the cell diffusion experiments with Pu is available open access in a video-article.<sup>13</sup>

### 3.3.3 Deployment of DGTs with different gel thickness

To determine the dissociation constant  $k_{dis}$  and the lability degree ( $\xi$ ) of the interaction of Pu with FA, we deployed a batch of DGT devices of 5 different diffusive layer thicknesses in 2.5 L of a laboratory solution containing 0.73-0.76 mBq mL<sup>-1</sup> Pu (IV), 10 mM Na<sub>2</sub>SO<sub>4</sub>, 2-4 µg L<sup>-1</sup> Co<sup>2+</sup> and 10 mM MOPS buffered at pH 6.5. Co<sup>2+</sup> was used as a bystander species since its kinetic signatures with FA have been characterized previously using the same DGT technique.<sup>18</sup> In addition, Co<sup>2+</sup> is known to interact only weakly with organic matter.<sup>14</sup> In the experiment without FA, <sup>239</sup>Pu (IV) was used at 0.44 mBq mL<sup>-1</sup> concentration in the presence of 2 µg L<sup>-1</sup> Co<sup>2+</sup> in a 5 L beaker during 53 h. Further on, we chose to work with <sup>238</sup>Pu in order to reduce its atomic concentration. In experiments with FA, 50 mg of freeze-dried FA were dissolved together with Pu (IV), resulting in 20 ppm FA concentration (12 ppm DOC measured by UV-Vis); the solution was equilibrated for 24 hours before DGT deployment. The deployment time was 24 h to 7 days. The solution was kept upon permanent stirring with a magnetic stirrer (300 rdn min<sup>-1</sup>) at room temperature. Aliquots of

the test solution were taken every 24 hours and analyzed for Pu, Co<sup>2+</sup> and DOC concentration.

### 3.3.4 ADBL and PAM models to determine the dissociation constant $k_{dis}$ and the lability criteria $\xi$

Natural occurring complexants such as fulvic acid consist of heterogeneous ligands.

Nevertheless, the case of the Pu-NOM interaction has been treated here as the interaction between a metal cation and a ligand considered as unique (*e.g.* with a unique complexation constant,  $K$ ). It is an oversimplification of a problem otherwise difficult to solve. However, the formation of complexes of Pu with FA occurs mostly through interactions with the carboxylic group present on FA at a pH of 6.5. Because of the very large excess of ligand compared to metal, one can consider that the strongest interaction will be preferred.<sup>23</sup>

To interpret the experimental data obtained using DGT of different thicknesses, the accumulated mass is plotted in function of the gel thickness ( $\Delta g$ ). Using the expression derived by Warnken et al. (eq. 13 of reference 18) for the ADBL (eq. 1), one can derive the kinetic parameter  $g_{kin}$ .

$$\frac{b}{m} = \frac{D_M^{gel} (1+e^{gelK'})}{D_M^w (1+e^{wK'})} \delta + g_{kin} = P\delta + g_{kin} \quad (1)$$

$b/m$  is the ratio of the intercept ( $b$ ) over the slope ( $m$ ) of a linear function fitting  $1/M$  as a function of  $\Delta g$ .  $\varepsilon$  is the ratio of the of the diffusion coefficients in gel ( $\varepsilon^{gel} = D_{ML}^{gel}/D_M^{gel}$ ) and water ( $\varepsilon^w = D_{ML}^w/D_M^w$ ), and  $\delta$  is the DBL which can be determined when no ligand is used in the experiment ( $g_{kin} = 0$  and  $K'=0$ ). To determine  $g_{kin}$  requires some knowledge about the speciation of the metal in solution. Here we used the software WHAM7 to determine  $K'$ , with the solution parameters given above. Once  $g_{kin}$  is known, one can compute  $k_{dis}$  using eq. 14 of reference 18.



$$k_{dis} = \frac{(D_{ML}^{gel})^2 K'}{D_M^{gel} g_{kin}^2} \quad (2)$$

This mathematical treatment was carried out on the data obtained using gels of various thickness and solutions with and without FA for both Pu and Co metals. One fundamental parameter of the model is the mobility of the metal-ligand in the diffusive gel, expressed by  $D_{ML}$ . In a previous work,<sup>7</sup> we used the retentate fraction of the ultrafiltration on a 10 kDa membrane of the organic-rich Noiraigue river water spiked with Pu in a diffusion cell to determine  $D_{ML}$  for this particular system. We found a  $D_{ML}$  value of  $1.10 \times 10^{-6} \text{ cm}^2 \text{ s}^{-1}$ . This value is compatible with the value obtained by Zhang and Davison<sup>22</sup> using a similar diffusion cell setting for FA ( $D_{FA} = 1.15 \times 10^{-6} \text{ cm}^2 \text{ s}^{-1}$ ) and was used in all this work. WHAM7 calculation resulted in value for  $K'$  of 3.27 for Co and 164 for Pu (about 96% Pu as Pu-FA). Using the stability constant determined by Zimmerman *et al.*<sup>12</sup> for Pu-HA ( $K = 5.75 \times 10^6 \text{ M}^{-1}$ ) and the ligand concentration used in this work ( $24 \mu\text{mol L}^{-1}$ ) we calculated a  $K'$  of 138, which is in agreement with the WHAM7 value. This difference does not impact significantly the determination of  $P$ .  $\varepsilon^{gel}$  was set to 0.5 and  $\varepsilon^w$  to 0.75. Rigorous expression for the lability degree of a metal-complex in DGT has been proposed by Salvador *et al.*<sup>24</sup> and Galceran and Puy<sup>15</sup> for steady-state finite planar diffusion, resolving the set of equations 9 to 12 presented below. The mathematical treatment and proposed analytical solution are based on the assumption of steady-state conditions and a constant complex concentration in the system. It considers the resin layer as a perfect sink for M and necessitates an excess of ligand ( $[M] \ll [ML]$ ). The steady-state conditions require exposure time significantly longer than the effective time of the transient regime (*e.g.* the time of growing flux) and because we use DGT with large thicknesses, we exposed DGT for 24, 120 and 164 h. When the mobility of

the metal-complex in the gel ( $D_{ML}$ ) and the dissociation constant ( $k_{dis}$ ) are known, the lability degree ( $\xi$ ) can be determined using eq. 19 of reference 15.

$$\xi = 1 - \frac{1 + \varepsilon K'''}{\varepsilon K''' + \frac{g}{m} \coth\left(\frac{g}{m}\right) + \frac{g}{\lambda_{ML}} (1 + \varepsilon K''') \tanh\left(\frac{r}{\lambda_{ML}}\right)} \quad (3)$$

in which  $\lambda_{ML}$  is the penetration parameter given by:

$$\lambda_{ML} = \sqrt{\frac{D_{ML}}{k_{dis}}} \quad (4)$$

And  $m$  is the disequilibrium layer thickness given by:

$$m = \sqrt{\frac{D_{ML}}{k_{dis}(1 + \varepsilon K')}} \quad (5)$$

where  $D_{ML} = 1.1 \times 10^{-6} \text{ cm}^2 \text{ s}^{-1}$  and  $k_{dis}$  is determined following the ADBL mathematical treatment presented above.  $g$  is the thickness of the gel + filter + DBL determined above and  $r$  is the thickness of the resin layer (0.4 mm). On the other hand, and because we performed experiments with and without ligand, the lability degree can be computed from experimental data using eq. 5 of reference 16.

$$\xi = \frac{\frac{n_M}{C_{T,M}^*}}{\frac{(D_{ML})n_M^0}{D_M} \frac{C_M^*}}{C_M^*}} \quad (6)$$

which can be modified into eq. 7 when the exposure time and the gel thickness are different between the experiments carried out with and without ligand, which was the case in this work.

$$\xi = \frac{n_M (D_M C_{T,M}^{*,0}) t^0 g}{n_M^0 (D_{ML} C_{T,M}^*) t g^0} \quad (7)$$

where the symbol  $^0$  relates to experiment without ligand,  $n$  is the number of mole of metal accumulated in the resin,  $g$  is the diffusive gel layer (including DBL) and  $C_{T,M}^*$  refers to the total bulk concentration of metal in the experiment. It is important to notice that eq. 5 is

valid only when making the assumption that the flux of free metal in the bulk solution is negligible. This is clearly the case in our experiments because of the very large excess of ligand compared to Pu.

### 3.3.5 Dynamic numerical model

The behavior of DGT devices in simple metal-ligand synthetic solutions has been numerically modeled by Tusseau-Vuillemin *et al.*<sup>25</sup> and by Lehto *et al.*<sup>26</sup> in some previous studies and we will not describe the model in detail here. These dynamic models make it possible to estimate the evolution of complexes concentrations in the diffusive layer using experimental data from DGT deployments. In our case, the dynamic metal-ligand system is composed of free Pu (IV) species (M), free ligand FA (L), and Pu (IV)-FA complex (ML). The corresponding concentrations in the bulk of the solution are written  $[M_S]$ ,  $[L_S]$ , and  $[ML_S]$ , and are described by the following relationship:

$$\frac{[ML_S]}{[M_S][L_S]} = K = \frac{k_f}{k_{dis}} \quad (8)$$

where  $k$  ((mol/L)<sup>-1</sup>),  $k_{dis}$  (s<sup>-1</sup>), and  $k_f$  ((mol/L)<sup>-1</sup> s<sup>-1</sup>) are respectively the constant of stability, of dissociation and of formation of the metal-ligand complex. The interactions and transport of M, L, and ML in the hydrogel ( $S < x < N$ ) and in the resin ( $N < x < R$ ) are described by:

$$\frac{\partial[M_x]}{\partial t} = D_M \frac{\partial^2[M_x]}{\partial x^2} + (k_{dis}[ML_x] - k_f[M_x][L_x]) \quad (9)$$

$$\frac{\partial[L_x]}{\partial t} = D_L^* \frac{\partial^2[L_x]}{\partial x^2} + (k_{dis}[ML_x] - k_f[M_x][L_x]) \quad (10)$$

$$\frac{\partial[ML_x]}{\partial t} = D_{ML}^* \frac{\partial^2[ML_x]}{\partial x^2} + (k_{dis}[ML_x] - k_f[M_x][L_x]) \quad (11)$$

where  $D_M$  is the diffusion coefficient of M in the hydrogel and  $D_L^*$  and  $D_{ML}^*$  are those of L and ML, which are respectively equal to  $D_L$  and  $D_{ML}$  in the gel ( $S < x < N$ ) and to  $\frac{1}{10} D_L$  and  $\frac{1}{210} D_{ML}$

in the resin ( $N < x < R$ ). It is considered that  $[M_x]$  in the resin is negligible so that  $[M_x]=0$  for  $x > N$ ]. The boundary conditions used for solving the system are the same as in the Tusseau-Vuillemin model:<sup>25</sup>

Then, the metal flux through the gel to the resin ( $\Phi_R$ ) can be expressed by:<sup>25</sup>

$$\Phi_R = \int_N^R k_{dis} [ML_x] S dx - SD_M \left. \frac{\partial [M_x]}{\partial x} \right|_N \quad (12)$$

Equations 8, 9, 10, and 11 form a set of coupled non-linear partial differential equations. They are not solvable analytically and need to be treated numerically. In this study, the system of equations and its boundary conditions were implemented in the commercial software Mathematica® version 10.0. The differential equations were directly solved using the powerful Mathematica® numerical solving tool (NDSolve), which uses a multiple algorithm approach. Additionally, the flux of free Pu (equation 13) was calculated for various parameter values. Finally, the flux is integrated over the deployment duration to obtain the accumulated metal in the resin. The physical parameters used in the calculations to simulate our experimental conditions are summarized in table 1.

### 3.3.6 Deployment of DGTs in field conditions

To measure the bioavailable fraction of Pu in the presence of soluble NOM in environmental conditions, we deployed several DGT devices with Chelex resin as the binding phase in organic-rich freshwater (15-20 ppm DOC, predominately FA 2-3 kDa) of the Noiraigue Bied brook of the Swiss Jura Mountains (see SI for complete description). DGT devices of large exposed window area (105 cm<sup>2</sup>) with 0.39 mm and 0.78 mm diffusive layer thickness were fabricated according to the protocol described earlier.<sup>13</sup> DGTs were mounted in duplicates on a vertical support at 45° angle towards the water flow. Following three

weeks exposure, Pu was eluted from Chelex resin in 8 M HNO<sub>3</sub> and measured with AMS using the compact ETH Zurich low energy system “Tandy” as described previously.<sup>13, 27, 28</sup> The measured Pu concentrations were converted into activities and C<sub>DGT</sub> of Pu was calculated according to the equation 13:

$$\frac{1}{A} = \frac{1}{C_{DGT}St} \left( \frac{\Delta g}{D_M^{gel}} + \frac{\delta}{D_M^w} \right) \quad \text{eq. 13}$$

where  $A$  is the activity in  $\mu\text{Bq}$  of Pu measured in the Chelex resin with AMS,  $\Delta g$  the thickness of the diffusion layer (gel + filter membrane, cm),  $D_M^{gel}$  the diffusion coefficient of Pu (IV) in the PAM gel ( $\text{cm}^2 \text{s}^{-1}$ , taken from Cusnir *et al.*<sup>7</sup>), and  $D_M^w = D_M^{gel}/0.85$ ,  $S$  the diffusion area ( $\text{cm}^2$ ), and  $t$  the duration of deployment (s). According to the underlying model assumptions C<sub>DGT</sub> of Pu represents the effective concentration of metal measured directly by DGT in the river water over the time of deployment. Additionally, Pu concentrations in the bulk water (< 0.45  $\mu\text{m}$ ) at the moment of deployment and at the moment of retrieval of DGTs were determined by co-precipitating with iron hydroxide at pH 8 with subsequent radiochemical separation of Pu and AMS measurements.

## 3.4 Results and discussion

### 3.4.1 Diffusion coefficients of Pu (V) in the PAM gel

The diffusion of Pu (V) species through the PAM gel in the MOPS buffered solution yielded a linear function of time (Figure SI-2). We calculated the effective diffusion coefficient using plot of Figure SI-2, and found that  $D$  for Pu (V) ( $3.29 \pm 0.19 \times 10^{-6} \text{ cm}^2 \text{ s}^{-1}$ ) was higher than  $D$  for Pu (IV) ( $2.29 \pm 0.15 \times 10^{-6} \text{ cm}^2 \text{ s}^{-1}$ ), which was previously determined in identical conditions.<sup>7</sup> Liquid-liquid extraction with HDEHP shows that there was no significant reduction of Pu (V) during the time frame of the experiment (90 min). These findings indicate that Pu (V) species are more mobile than Pu (IV) ones.

Pu (V) can be reduced to Pu (IV) by NOM.<sup>21</sup> When Pu (V) species were diffusing through the PAM gel in the presence of HA, the Pu (V) / Pu (IV) ratio measured at the end of the experiment was lower in the A compartment compared to the B compartment. More specifically, we found  $18 \pm 10 \%$  of Pu (V) left in the A compartment and  $69 \pm 10 \%$  of Pu (V) in the B compartment after a diffusion time of 130 minutes. Moreover, after 30 min in this experiment the diffusion of Pu species becomes clearly non-linear (Figure SI-2, blue open triangles). This behavior reflects the extent of the Pu (V) reduction into Pu (IV), which is more strongly bound to HA, reducing the total flux of Pu through the PAM gel. Using liquid-liquid extraction with HDEHP, we studied the reduction reaction of Pu (V) by HA in the A compartment throughout a diffusion experiment (Figure SI-3). The rate constant of the reduction reaction,  $k$ , was  $0.252 \text{ h}^{-1}$  and the half-life  $\tau$  was 2.75 h, both values very similar to those reported in the literature.<sup>21</sup> The determination of a higher Pu (V) fraction in the compartment B demonstrates the preponderant flux of this species through the PAM gel, compared to Pu (IV), in presence of HA.

Although the reduction of Pu (V) in the presence of HA is an established fact, this is not a complete process.<sup>21</sup> In this work, a Pu (V) solution in the presence of 20 ppm of HA, equilibrated for 24 h, showed the reduction of the major part of the Pu (V) initially introduced, yielding a final solution containing  $31 \pm 10 \%$  of Pu (V) and  $69 \pm 10 \%$  of Pu (IV). When this solution was used in a diffusion experiment, the results of the Pu measurement in compartment B yielded a linear diffusion function (Figure SI-2, green full circles). The calculated  $D_{\text{Pu(V)-Pu(IV)-HA}}$  was  $0.91 \pm 0.07 \times 10^{-6} \text{ cm}^2 \text{ s}^{-1}$ , a value lying in between the  $D_{\text{Pu(IV)-HA}}$  ( $0.50 \times 10^{-6} \text{ cm}^2 \text{ s}^{-1}$ ) and  $D_{\text{Pu(V)-MOPS}}$ . Since the initial solution in this experiment contains a mixed system of [Pu (IV) – Pu (V)] diffusing in the PAM gel and because the diffusion coefficient for [Pu (IV) – HA] is known, it is possible to compute the effective diffusion coefficient for Pu (V) in the presence of HA. The concentration of Pu determined experimentally at any point of time in the B compartment represents the sum of the contributions of the [Pu (IV) – HA] and [Pu (V) – HA] species diffusing through the PAM gel. Subtracting the contribution of [Pu (IV) – HA] species, we obtained a linear plot of the diffused [Pu (V) – HA] species as a function of time (Figure 3, SI). The calculated  $D_{\text{Pu(V)-HA}}$  was  $1.70 \pm 0.25 \times 10^{-6} \text{ cm}^2 \text{ s}^{-1}$ . Compared to a value of  $D$  of  $0.50 \times 10^{-6} \text{ cm}^2 \text{ s}^{-1}$  found for Pu (IV)-HA, Pu (V)-HA species are significantly more mobile and, possibly, more labile.

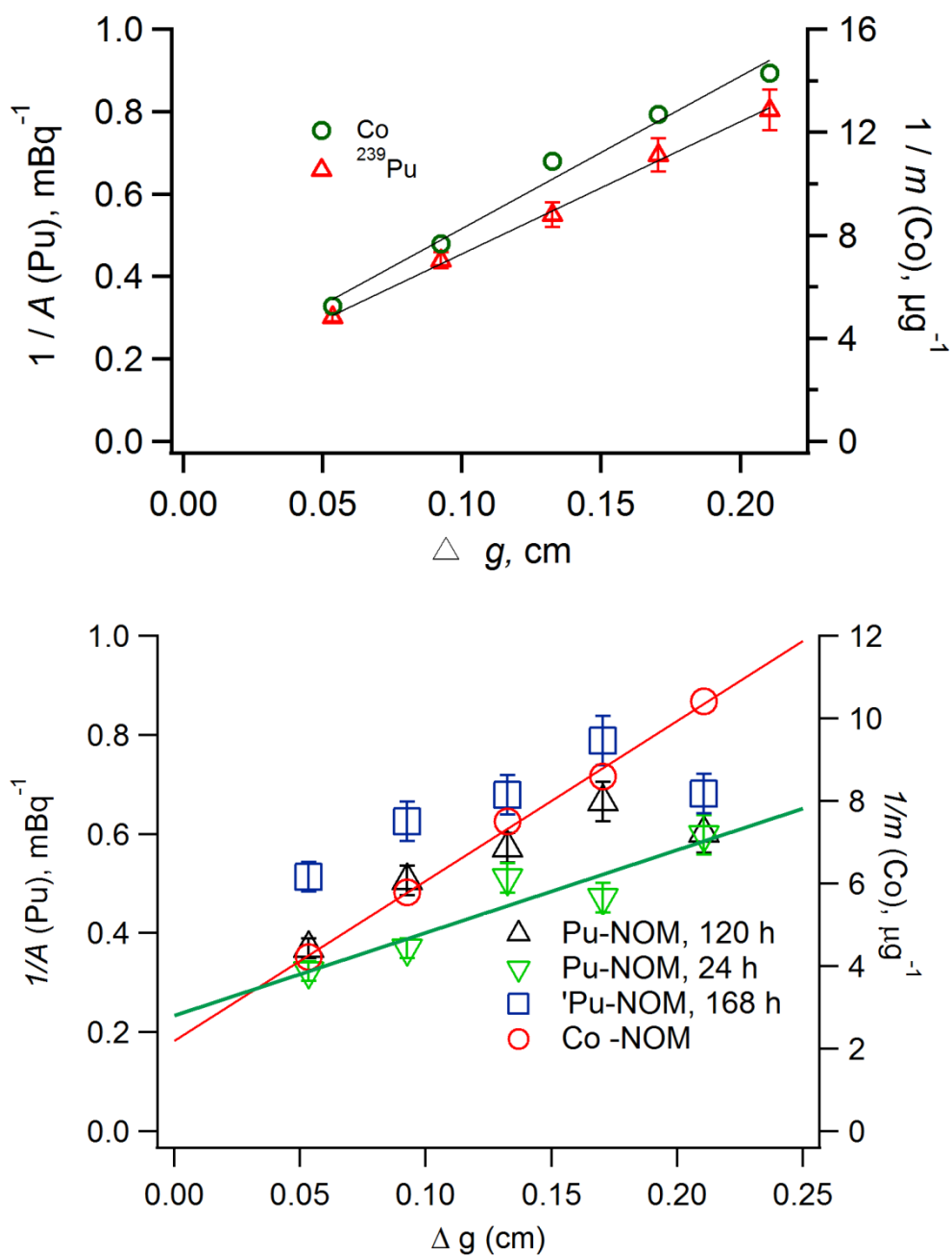
### **3.4.2 Deployment of DGTs with different gel thicknesses and calculation of the dissociation constant ( $k_{\text{dis}}$ ) and of the lability degree ( $\xi$ )**

Figure 1A shows the linear function of the reciprocal of the activity of Pu (IV) accumulated by DGT devices of five diffusive layer thicknesses in the experiment without FA addition.  $\text{Co}^{2+}$  used as a bystander species in the same experiment with Pu (IV) behaves

similarly. Using equation 2, the DBL value is 0.048 cm for Co and 0.049 cm for Pu, showing that DBL is not a parameter depending on the metal.

The reduction of the flux on the surface of the diffusion gel due to complex formation will experimentally be indicated by an increase of the ADBL thickness. The experiment carried out with 20 ppm of FA showed that the reciprocal ( $1/\text{Co}^{2+}$ ) of the mass of  $\text{Co}^{2+}$  accumulated by DGTs increased linearly with the diffusive layer thickness (Figure 1B). Surprisingly, the reciprocal of Pu (IV) activity accumulated in DGTs followed a linear function only for the first four diffusive layer thicknesses. Afterwards, the DGT with the largest diffusive layer (1.96 mm gel) accumulated comparatively more Pu (IV), deviating from linearity (Figure 1B). A repetition of this experiment yielded exactly the same results, showing the reproducibility of this specific behavior. We then performed a series of experiments, deploying DGT devices for different periods of time. When DGT devices were deployed for 24 h, all five diffusive layer thicknesses showed a linear accumulation of Pu (IV). However, linearity was conserved for the four first thicknesses only (up to 1.56 mm), for exposure times of 120 and 168 h. Currently, we do not have a clear explanation for this specific behavior. Nevertheless, the fact that this extra-accumulation of Pu using a gel of large thickness (1.96 mm) happened only when the exposure time was longer than 24 hours, and does not happen with  $\text{Co}^{2+}$ , could indicate that this effect is related to the specificity of the Pu chemistry, *e.g.* oxidation to Pu(V) or hydrolysis.





**Figure 1 (A, top and B, bottom).** Plots of the reciprocal of the activity of Pu (left axis,  $\text{mBq}^{-1}$ ) and of the mass of Co (right axis,  $\mu\text{g}^{-1}$ ) accumulated by DGTs as a function of the total thickness ( $\Delta g$ , cm) of the diffusive layer (gel and filter). A) without ligand (FA) B) with ligand (FA) for different deployment times. Red line: linear regression for Co-FA; green line: linear regression for Pu-FA, 24 h.

We thus carried out the computation of the  $P$ ,  $g_{\text{kin}}$  and  $k_{\text{dis}}$  parameters according to equations 1 and 2 using only the first four layer thicknesses for Pu. Results are presented in Table 2.  $g_{\text{kin}}$  for Co is 0.027 cm, a value significantly higher than the value of 0.015 cm found by Warnken *et al.*<sup>18</sup> for freshwater containing about 12 ppm of DOC. The  $k_{\text{dis}}$  for Co determined in our work is  $9.6 \times 10^{-4} \text{ s}^{-1}$ , a value situated between the value determined by Fasfous *et al.*<sup>23</sup> ( $1.3 \times 10^{-4} \text{ s}^{-1}$ ) and Warnken *et al.*<sup>18</sup> ( $3.1 \times 10^{-3} \text{ s}^{-1}$ ). Average  $g_{\text{kin}}$  for Pu for the three experiments (24 to 168 h) is 0.119 cm, very close to the value of 0.116 cm obtained by Warnken *et al.*<sup>18</sup> for  $\text{Fe}^{3+}$ . The average  $k_{\text{dis}}$  for Pu is  $7.5 \times 10^{-3} \text{ s}^{-1}$ . Thus the  $k_{\text{d}}$  of the Pu-FA complex found in this work is higher than for Ni and Co, but lower than for Cu and Mn.

Having determine  $k_{\text{dis}}$  and knowing the mobility of the Pu-FA complex ( $D_{\text{ML}} = 1.10 \times 10^{-6} \text{ cm}^2 \text{ s}^{-1}$ ) in the gel, we can compute the lability degree,  $\xi$ , according to eq. 3 and, using the accumulate mass in the experiments with and without FA, according to eq. 7. Results show that the lability degree slightly depends on the gel layer thickness (Figure 2A). Linear extrapolation to zero gel thickness yields values situated between 0.21 and 0.4 when eq. 7 is used. When eq. 3 is used, which takes into account the possible penetration of the complex in the resin, the values are situated between 0.84 and 0.88. This large discrepancy between both calculations might express the fact that the model which takes into account the penetration of the complex into the resin gel overestimates the lability of the complex. On the other hand, when the mobility of the metal complex is lowered to  $\varepsilon^{\text{gel}} = 0.2$  in equation 8, calculation yields higher values (Figure 2B), situated between 0.52 and 1.0, with a larger dependency on the gel layer thickness. Thus, as emphasized by Galceran and Puy,<sup>15</sup> one must resist the temptation to interpret DGT measurements only in term of lability, disregarding the changes in mobility. In this respect, the Pu-FA complex investigated in this work is clearly somewhat labile, but probably not fully labile.

### 3.4.3 Dynamic numerical model

The implementation in Mathematica of the non-linear differential system of equations describing the dynamic behavior of Pu-FA in the hydrogel was validated by numerically solving the system for the parameter values of Tusseau-Vuillemin *et al.*<sup>25</sup> Our calculations could reproduce the behavior of metal and ligand found in Tusseau-Vuillemin *et al.* In complement, we implemented the excess ligand approximation (*e.g.* the ligand concentration is constant) and simplified the equation system accordingly. The results obtained in that case are always in agreement with the code solving the full set of equations and validated further our implementation in Mathematica. Following this validation, we calculated the accumulated mass of Pu in the resin, using the experimental parameters of Table 1, including the  $k_{dis}$  value determined previously. Unfortunately, the dynamic numerical model failed to reproduce the accumulated metal in the resin obtained experimentally, producing accumulation in excess of several hundred percent compared to experimental data. It was necessary to reduce drastically the ratio of  $[L]/[Pu]$  from an initial very large value of  $4.76 \times 10^9$  to  $4.76 \times 10^5$  to be able to reproduce correctly the experimental results. As a matter of fact, the calculated amount of accumulated metal in the resin was highly sensitive to the ligand concentration. This fact may reflect the difficulty to model ligand accumulation in the reaction layer when the  $[L]/[M]$  ratio is very large, because the concentrations of the free metal and the complex are not in equilibrium in term of the effective stability constant. Accumulation of free and charged ligand in the gel and resin gel might lead to electrostatic interactions<sup>16</sup> which can hinder the penetration of ML in the gel and resin gel, thus lowering the metal accumulation in the resin, because of the very low concentration of metal.<sup>16</sup> In addition, a slight loss of total Pu in the bulk solution (10-15% after 168 hours) and a slight accumulation of Pu in the diffusive gel (twice than expected

concentration) were experimentally measured. The loss of Pu in the bulk solution and its accumulation in the diffusive gel could be related to a possible hydrolysis of some Pu. Oxidation after dissociation can also occur in our experimental conditions. These side reactions will not be taken into account in the dynamic numerical model and emphasized the difficulty to work in environmentally relevant conditions with a metal with such a complicated chemistry.

**Table 1. Parameters used to calculate the Pu accumulation in the resin using the dynamic numerical model.**

	<b>Symbol</b>	<b>Unit</b>	<b>Value</b>
<b>Stability constant</b>	$K$	$(\text{mol L}^{-1})^{-1}$	$5.75 \times 10^{6 \text{ a)}$
<b>Formation rate constant</b>	$k_f$	$(\text{mol L}^{-1})^{-1} \text{s}^{-1}$	$4.31 \times 10^4$
<b>Diffusion coefficients of M in the gel</b>	$D_M$	$\text{cm}^2 \text{s}^{-1}$	$2.29 \times 10^{-6}$
<b>Diffusion coefficients of ML in the gel</b>	$D_{ML}$	$\text{cm}^2 \text{s}^{-1}$	$1.1 \times 10^{-6}$
<b>Diffusion coefficients of ML in the resin</b>	$D_{ML}$	$\text{cm}^2 \text{s}^{-1}$	$D_{ML}/10$
<b>Surface area of gel</b>	$a$	$\text{cm}^2$	3.08
<b>Thickness of gel + filter</b>	$\Delta g$	mm	0.535-2.105
<b>Concentration of [Pu]</b>	$C_{\text{Pu}}$	$\mu\text{mol L}^{-1}$	$10^{-7}$ - $10^{-9}$
<b>Pu complexation capacity of [NOM]</b>	$C_{\text{NOM}}$	$\mu\text{mol L}^{-1}$	0.0024-24
<b>Dissociation rate constant</b>	$k_{\text{dis}}$	$\text{s}^{-1}$	$7.5 \times 10^{-3}$
<b>Accumulation duration</b>	$t$	h	24-168

<sup>a)</sup> Stability constant for Pu-HA determined by Zimmerman *et al.*<sup>12</sup>

**Table 2. Calculation of the kinetic parameters on the basis of the 1/mass vs  $\Delta g$  plots.**

	metal	$t$ (h)	$b/m$ (cm)	$\delta$ (cm)	$P$	$g_{\text{kin}}$ (cm)	$k_d$ (s <sup>-1</sup> )
Free metal	Co		0.039	0.048			
	Pu		0.042	0.049			
With FA	Co		0.057	0.048	0.65	0.027	<b><math>9.6 \times 10^{-4}</math></b>
	Pu	24	0.140	0.049	0.57	0.119	$6.2 \times 10^{-3}$
	Pu	120	0.104	0.049	0.57	0.083	$1.3 \times 10^{-2}$
	Pu	168	0.177	0.049	0.57	0.156	$3.6 \times 10^{-3}$
	Pu (average)						<b><math>7.5 \times 10^{-3}</math></b>

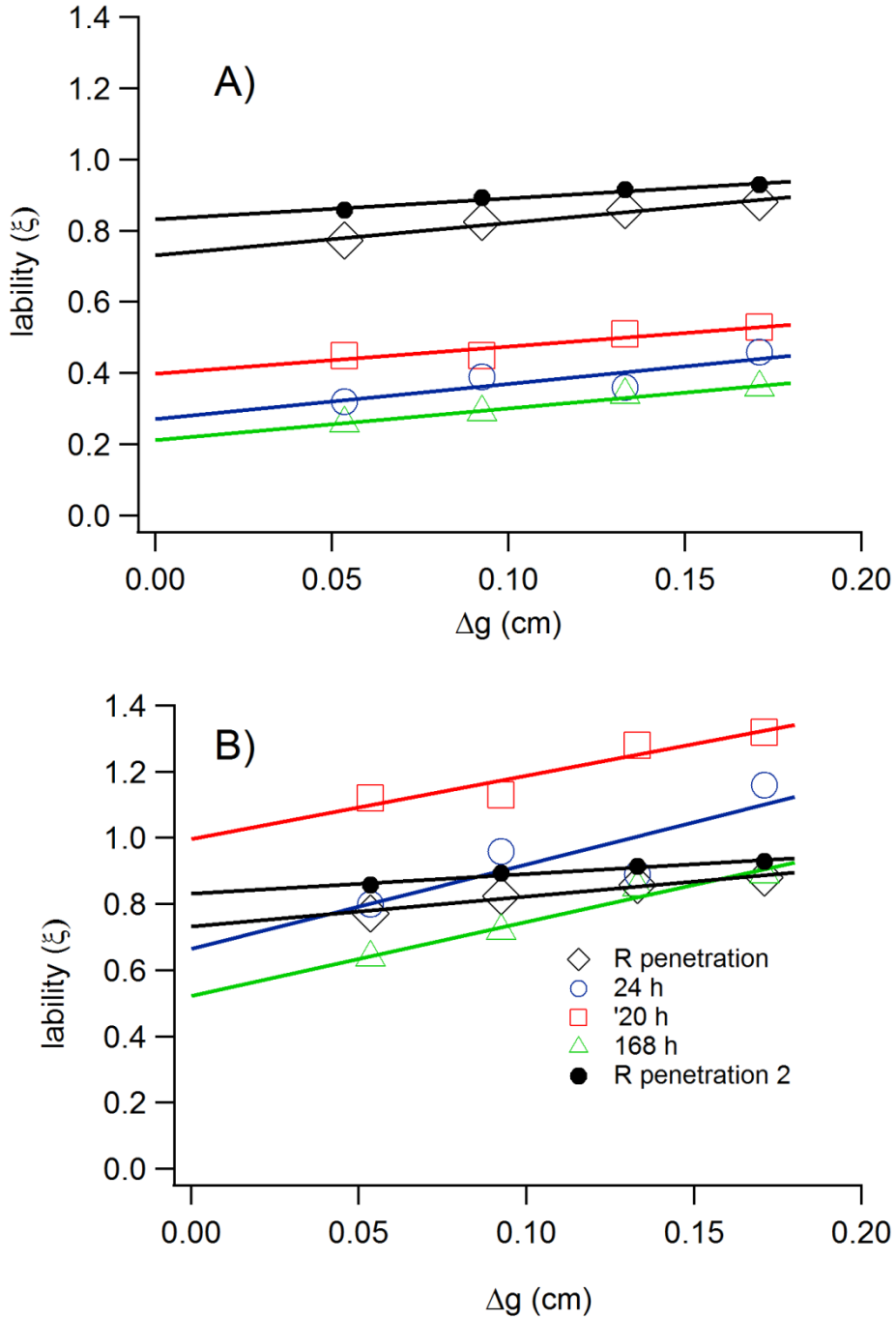


**Figure 2 (A, top and B, bottom).** Lability degree ( $\xi$ ) of the Pu-FA complexes as a function of the total thickness ( $\Delta g$ , cm) of the diffusive layer (gel and filter). A) 24h, 120h, 168h, calculated with eq. 8 and  $\varepsilon = 0.5$ ; B) 24h, 120h, 168h, calculated with eq. 8 and  $\varepsilon = 0.2$ . R penetration calculated with eq. 4 and  $\varepsilon = 0.5$ ; R penetration calculated with eq. 4 and  $\varepsilon = 0.2$ ,

with  $\varepsilon = \frac{D_M^{gel}}{D_{ML}^{gel}}$ .

### 3.4.4 Deployment of DGTs in field conditions

Calculation using WHAM7 and parameters of Table SI-1 shows that 95% of the Pu was associated with carbonates while only 5 % are present as Pu-FA complexes. Accordingly, we expect to find Pu mostly as inorganic metal complex with high lability. The activity of Pu accumulated by DGT devices exposed for three weeks in the Noiraigue Bied brook was comparable to the concentration measured in the bulk water ( $3.27 \pm 0.65 \mu\text{Bq L}^{-1}$ ,  $n=2$ ) during the deployment period. Interestingly, DGTs of 0.78 mm gel thickness accumulated as much Pu ( $10.11 \pm 2.38 \mu\text{Bq}$ ,  $n=2$ ) as DGTs 0.39 mm gel thickness ( $9.67 \pm 2.03 \mu\text{Bq}$ ,  $n=2$ ). Consequently, the  $C_{\text{DGT}}$  of Pu calculated with eq. 14 and a DBL of 0.05 cm was  $2.32 \pm 0.50 \mu\text{Bq L}^{-1}$  for DGT with a gel layer thickness of 0.39 mm ( $n=2$ ) and  $3.40 \pm 0.80 \mu\text{Bq L}^{-1}$  for DGT with a gel layer thickness of 0.78 mm ( $n=2$ ). When compared to the bulk concentration, the  $C_{\text{DGT}}$  measured with 0.39 mm gel showed that 71 % of Pu is bioavailable, while the  $C_{\text{DGT}}$  measured with 0.78 mm gel shows that the Pu is fully bioavailable ( $\cong 100\%$ ) and  $C_{\text{DGT}}$  equals the bulk concentration. The  $C_{\text{DGT-0.78}}/C_{\text{DGT-0.39}}$  ratio of 1.47 suggests that DGTs with greater diffusive gel thickness accumulated more Pu, possibly because a larger gel thickness might increase the lability of Pu-complexes. On the other hand, the fact that DGT with a larger and smaller gel thicknesses accumulated comparable amount of Pu could be an indication of saturation of the resin with major cations for such a long exposure time. However it must be notice that the Pu concentration in freshwater in this pristine environment is very low so that the accumulated mass of Pu is determined with a standard uncertainty close to 30% ( $k=1$ ).

This work has shown the potential of DGT with different layer thickness to determine the dissociation constant and lability of the Pu-FA complex in environmentally relevant conditions. Calculation demonstrated that the Pu-FA complexes are somewhat labile, with a

dissociation rate constant in the range of other metal cations such as  $\text{Co}^{2+}$  and  $\text{Fe}^{3+}$ . However, the multifarious redox and hydrolysis chemistry of Pu adds complexity in quantitatively modeling and interpreting DGT data. Nevertheless, our work with Pu, a very toxic element issued from the nuclear industry, demonstrates that it behaves similarly to other heavy metals in freshwater containing high concentration (up to 20 ppm) of dissolved organic matter. Accordingly, Pu should be regarded as a potentially mobile and bioavailable species in environmentally relevant conditions of carbonated and organic-rich waters.

### **3.5 Supporting information**

Detailed description of the extraction, desalting and characterization of the NOM from organic-rich water of the Noiraigue Bied brook (Fig. SI-1). Detailed description of the plutonium determination. Figure SI-2 showing Pu(V) diffusion experiments. Figure SI-3 showing the reduction of Pu (V) in the presence of HA and figure SI-4, showing the kinetic signature of Pu (IV) in the presence of FA. This material is available free of charge via the Internet at <http://pubs.acs.org>.

### **3.6 Acknowledgements**

This work was funded by the Swiss National Science Foundation (grant n° 200021-140230) and by the Swiss Federal Office of Public Health (PF and PS). Two reviewers are thanked for helping us to better interpret our experimental data.



### 3.7 References

1. Saar, R. A.; Weber, J. H., Fulvic-acid modifier of metal-ion chemistry. *Environ. Sci. Technol.* **1982**, *16*, (9), A510-A517.
2. Taylor, D. M., Environmental plutonium - Creation of the universe to twenty-first century mankind. *Plutonium in the Environment* **2001**, *1*, 1-14.
3. Alvarado, J. A. C.; Steinmann, P.; Estier, S.; Bochud, F.; Haldimann, M.; Froidevaux, P., Anthropogenic radionuclides in atmospheric air over Switzerland during the last few decades. *Nature Commun.* **2014**, *5*, 3030-3030.
4. Santschi, P. H.; Roberts, K. A.; Guo, L. D., Organic nature of colloidal actinides transported in surface water environments. *Environ. Sci. Technol.* **2002**, *36*, (17), 3711-3719.
5. Choppin, G. R.; Bond, A. H.; Hromadka, P. M., Redox speciation of plutonium. *J. Radioanal. Nucl. Ch.* **1997**, *219*, (2), 203-210.
6. Choppin, G. R., Redox speciation of plutonium in natural waters. *J. Radioanal. Nucl. Ch.* **1991**, *147*, (1), 109-116.
7. Cusnir, R.; Steinmann, P.; Bochud, F.; Froidevaux, P., A DGT Technique for Plutonium Bioavailability Measurements. *Environ. Sci. Technol.* **2014**, *48*, (18), 10829-10834.
8. Kersting, A. B.; Efurud, D. W.; Finnegan, D. L.; Rokop, D. J.; Smith, D. K.; Thompson, J. L., Migration of plutonium in ground water at the Nevada Test Site. *Nature* **1999**, *397*, (6714), 56-59.
9. Kersting, A. B., Plutonium Transport in the Environment. *Inorg. Chem.* **2013**, *52*, (7), 3533-3546.
10. Xu, C.; Athon, M.; Ho, Y.-F.; Chang, H.-S.; Zhang, S.; Kaplan, D. I.; Schwehr, K. A.; DiDonato, N.; Hatcher, P. G.; Santschi, P. H., Plutonium Immobilization and Remobilization by Soil Mineral and Organic Matter in the Far-Field of the Savannah River Site, US. *Environ. Sci. Technol.* **2014**, *48*, (6), 3186-3195.
11. Orlandini, K. A.; Penrose, W. R.; Nelson, D. M., Pu(V) as the stable form of oxidized plutonium in natural waters. *Mar. Chem.* **1986**, *18*, (1), 49-57.
12. Zimmerman, T.; Zavarin, M.; Powell, B. A., Influence of humic acid on plutonium sorption to gibbsite: Determination of Pu-humic acid complexation constants and ternary sorption studies. *Radiochim. Acta* **2014**, *102*, (7), 629-643.
13. Cusnir, R.; Steinmann, P.; Christl, M.; Bochud, F.; Froidevaux, P., Speciation and Bioavailability Measurements of Environmental Plutonium Using Diffusion in Thin Films. *J. Vis. Experim.* **2015**, (105). <http://www.jove.com/video/53188>.
14. Levy, J. L.; Zhang, H.; Davison, W.; Galceran, J.; Puy, J., Kinetic Signatures of Metals in the Presence of Suwannee River Fulvic Acid. *Environ. Sci. Technol.* **2012**, *46*, (6), 3335-3342.
15. Galceran, J.; Puy, J., Interpretation of diffusion gradients in thin films (DGT) measurements: a systematic approach. *Environ. Chem.* **2015**, *12*, (2), 112-122.
16. Puy, J.; Galceran, J.; Cruz-Gonzalez, S.; David, C. A.; Uribe, R.; Lin, C.; Zhang, H.; Davison, W., Measurement of Metals Using DGT: Impact of Ionic Strength and Kinetics of Dissociation of Complexes in the Resin Domain. *Anal. Chem.* **2014**, *86*, (15), 7740-7748.
17. Puy, J.; Uribe, R.; Mongin, S.; Galceran, J.; Cecilia, J.; Levy, J.; Zhang, H.; Davison, W., Lability Criteria in Diffusive Gradients in Thin Films. *J. Phys. Chem. A* **2012**, *116*, (25), 6564-6573.
18. Warnken, K. W.; Davison, W.; Zhang, H.; Galceran, J.; Puy, J., In situ measurements of metal complex exchange kinetics in freshwater. *Environ. Sci. Technol.* **2007**, *41*, (9), 3179-3185.
19. Carter, H. T.; Tipping, E.; Koprivnjak, J. F.; Miller, M. P.; Cookson, B.; Hamilton-Taylor, J., Freshwater DOM quantity and quality from a two-component model of UV absorbance. *Water Res.* **2012**, *46*, (14), 4532-4542.
20. Bajo, S.; Eikenberg, J., Preparation of a stable tracer solution of plutonium(IV). *Radiochim. Acta* **2003**, *91*, (9), 495-497.
21. Blinova, O.; Novikov, A.; Perminova, I.; Goryachenkova, T.; Haire, R., Redox interactions of Pu(V) in solutions containing different humic substances. *J. Alloy Compd.* **2007**, *444*, 486-490.
22. Zhang, H.; Davison, W., Diffusional characteristics of hydrogels used in DGT and DET techniques. *Anal. Chim. Acta* **1999**, *398*, (2-3), 329-340.
23. Fafous, I.; Yapici, T.; Murimboh, J.; Hassan, I. M.; Chakrabarti, C. L.; Back, M. H.; Lean, D. R. S.; Gregoire, D. C., Kinetics of trace metal competition in the freshwater environment: Some fundamental characteristics. *Environ. Sci. Technol.* **2004**, *38*, (19), 4979-4986.
24. Salvador, J.; Puy, J.; Cecilia, J.; Galceran, J., Lability of complexes in steady-state finite planar diffusion. *J. Electroanal. Chem.* **2006**, *588*, (2), 303-313.

25. Tusseau-Vuillemin, M. H.; Gilbin, R.; Taillefert, M., A dynamic numerical model to characterize labile metal complexes collected with diffusion gradient in thin films devices. *Environ. Sci.Technol.* **2003**, *37*, (8), 1645-1652.
26. Lehto, N. J.; Davison, W.; Zhang, H.; Tych, W., An evaluation of DGT performance using a dynamic numerical model. *Environ. Sci.Technol.* **2006**, *40*, (20), 6368-6376.
27. Christl, M.; Vockenhuber, C.; Kubik, P. W.; Wacker, L.; Lachner, J.; Alfimov, V.; Synal, H. A., The ETH Zurich AMS facilities: Performance parameters and reference materials. *Nucl. Instrum. Meth. B* **2013**, *294*, 29-38.
28. Dai, X. X.; Christl, M.; Kramer-Tremblay, S.; Synal, H. A., Ultra-trace determination of plutonium in urine samples using a compact accelerator mass spectrometry system operating at 300 kV. *J. Anal. Atom. Spectrom.* **2012**, *27*, (1), 126-130.

## **Chapter 4: Plutonium is bioavailable in karstic freshwater environments**

With Marcus Christl, Philipp Steinmann, François Bochud and Pascal Froidevaux

Article in preparation for *Geochimica et Cosmochimica Acta*

## 4.1 Abstract

The interaction of trace environmental plutonium with dissolved natural organic matter (NOM) plays an important role on its mobility and bioavailability in freshwater environments. Here we explore the speciation and biogeochemical behavior of Pu in freshwaters of the karst system in the Swiss Jura Mountains. Chemical extraction and ultrafiltration methods were complemented by diffusive gradients in thin films technique (DGT) to measure the dissolved and bioavailable Pu fraction in water. Accelerator mass spectrometry (AMS) was used to accurately determine Pu in this pristine environment. Selective adsorption of Pu (III, IV) on silica gel showed that 88 % of Pu in the mineral water is found in +V oxidation state, possibly in a highly soluble  $[\text{PuO}_2^+(\text{CO}_3)_n]^{m-}$  form. Ultrafiltration experiments at 10 kDa yielded a slightly higher fraction of colloid-bound Pu in the organic-rich water (25 %) compared to mineral water (18 %). We also found that the concentrations of Pu measured by DGT in mineral water are similar to the bulk concentration, suggesting that the dissolved phase Pu is readily available for biouptake. Sequential elution (SE) of Pu from aquatic plants revealed that the co-precipitation with calcite on leaves is the major contribution (60 to 75 %) of Pu to the biomass. Hence, we suggest that plutonium is fully available for biological uptake in both mineral and organic-rich karstic freshwaters.

## 4.2 Introduction

Plutonium is an artificial element found in the environment mainly as a result of atmospheric nuclear weapons tests, nuclear accidents or authorized discharges (Taylor, 2001; Hunt et al., 2013; Alvarado et al., 2014). Pu represents a radiological risk if incorporated through the food chain because of its long biological half-life (Froidevaux et al., 2010) and emission of high energy alpha-particles. The speciation of plutonium in freshwaters defines its radiological risk for aquatic biota and humans. Pu has complex redox

chemistry and occurs under a variety of physico-chemical forms in the environment. Consequently, it is challenging to accurately predict its biogeochemical behavior and bioavailability in aquatic ecosystems without precise knowledge of its physico-chemical form. Environmental Pu can be found simultaneously in both reduced (+III and +IV) and oxidized (+V and +VI) forms, with +IV and +V being the most common species in natural waters (Choppin et al., 1997; Xu et al., 2014). Pu (IV) is generally considered a low-mobility species, tending to precipitate into immobile phases, to form intrinsic colloids at significant concentration or to sorb onto organic and inorganic natural colloids at lower concentrations (Santschi et al., 2002; Novikov et al., 2006; Utsunomiya et al., 2007; Chawla et al., 2010). Nevertheless, field experiments have shown that Pu (IV) can be readily oxidized to Pu (V) in oxic conditions prevalent in the environment (Kaplan et al., 2004). Conversely, Pu (V) is much less sensitive to hydrolysis, has much lower partition coefficients to solid phase and has lower stability constants with organic ligands (*e.g.* with EDTA) (Katz et al., 1986). Thus, sorbed Pu (IV) can be remobilized as soluble and labile Pu (V) species, which then increase Pu transport and biouptake in aquatic ecosystems (Kaplan et al., 2004; Xu et al., 2014). In addition to the oxidative dissolution of Pu (IV), interactions with naturally-occurring organic matter have critical implications on its sorption and desorption kinetics in the subsurface water environments (Tinnacher et al., 2015). The lability of Pu complexes with fulvic acid (FA) recently demonstrated in laboratory experiments provides new reasons for reconsidering the role of NOM for Pu bioavailability in natural freshwater environments (Cusnir et al., 2014; Cusnir et al., 2016).

Our preliminary work on the use of the DGT technique to determine the lability of the Pu-FA complexes paved the way for direct *in-situ* measurements of the labile environmental Pu (Cusnir et al., 2014; Cusnir et al., 2015). A DGT device for Pu bioavailability

measurements contains a polyacrylamide (PAM) gel assembly with a Chelex resin-gel as binding phase, protected with a filter (Davison and Zhang, 1994). The PAM gel layer enables the diffusion of the free and labile Pu species only, which are accumulated in the binding phase for subsequent analysis. Within reasonably short deployment time (2-3 weeks), DGT devices with a large surface area (*e.g.* 105 cm<sup>2</sup>) accumulate sufficient Pu for accelerator mass spectrometry measurements. Varying PAM gel thicknesses enable probing the dynamics of the molecular interactions of Pu with FA in natural waters *in-situ*, since the greater gel thickness increases the residence time and dissociation of Pu-FA complexes within the gel (Cusnir et al., 2016), thus contributing to the uptake of Pu. To predict the toxic effects of plutonium on aquatic organisms in the presence of dissolved NOM, the *in-situ* assessment of its bioavailability is required.

This paper reports on the use of the DGT and ultrafiltration techniques to determine the bioavailability of Pu in freshwaters of the karst system located in the Swiss Jura Mountains. A previous study on this system demonstrated a higher mobility of <sup>239+240</sup>Pu compared to <sup>241</sup>Am and <sup>137</sup>Cs (Froidevaux, Steinmann, et al., 2010), suggesting that carbonate-rich vadose waters might contain Pu in a soluble, plutonyl-carbonated form similar to [UO<sub>2</sub>(CO<sub>3</sub>)<sub>n</sub>]<sup>m-</sup>. We hypothesized that DGT would fully accumulate this species in carbonated waters because of a high mobility and lability of the carbonate and Pu-FA complexes. Our main objectives were to (1) provide evidence of the lability of the Pu-carbonate and Pu-FA complexes using the DGT and ultrafiltration techniques, (2) identify Pu-calcite depositions on aquatic plant leaves as a consequence of CO<sub>2</sub> water degassing, (3) quantify an additional flux of Pu from water to plants caused by the diffusion and dissociation of small Pu-FA complexes. Furthermore, we complemented the DGT results with the sequential elution of Pu from different fractions of aquatic mosses and plants. These

results help to construct a comprehensive geochemical model of Pu mobility and bioavailability in carbonated mineral and organic-rich waters.

## 4.3 STUDY AREA

### 4.3.1 The karst freshwater system

To investigate the speciation of Pu in freshwaters, we chose two distinct aquatic environments located in the Swiss Jura Mountains (Fig. 1). In general, karst systems are characterized by high water permeability, with underground waters highly enriched in carbonates. Their Pu content comes only from the fallout of the atmospheric nuclear bomb tests of the sixties, as demonstrated in a previous study by an average  $^{238}\text{Pu}/^{239+240}\text{Pu}$  activity ratio of  $0.031 \pm 0.0089$  ( $n = 49$ ) (Froidevaux, Steinmann, et al., 2010).

The first aquatic environment was at the Venoge spring, which is located in the commune of L'Isle, about 20 km northwest of the city of Lausanne, and collects water from a karstic catchment area situated between 700 and 1400 m asl. The hydrological regime of the spring is mixed, with the highest flow rate in April-May (up to  $7.50 \text{ m}^3 \text{ s}^{-1}$ ) and the lowest in the summer period (down to  $0.01 \text{ m}^3 \text{ s}^{-1}$ ). The pH of the water varies between 6.5 and 7.5; at a temperature of *ca* 7-8 °C, water is saturated with oxygen and CO<sub>2</sub>. Water of this mineral spring is oxic (Eh 490 mV NHE), carbonate-rich, and has a low NOM content (1 ppm at most). Detailed physico-chemical parameters of the water, as well as the precipitation regime during the sampling and field measurements campaign are given in the Supplementary Information (SI).

The second environment was the Noiraigue Bied brook, which is located at the Vallée-des-Ponts site at 1000 m asl altitude. The complex watershed of the valley is formed by densely drained peat bogs and a river (Grand Bied), which collects atmospheric waters

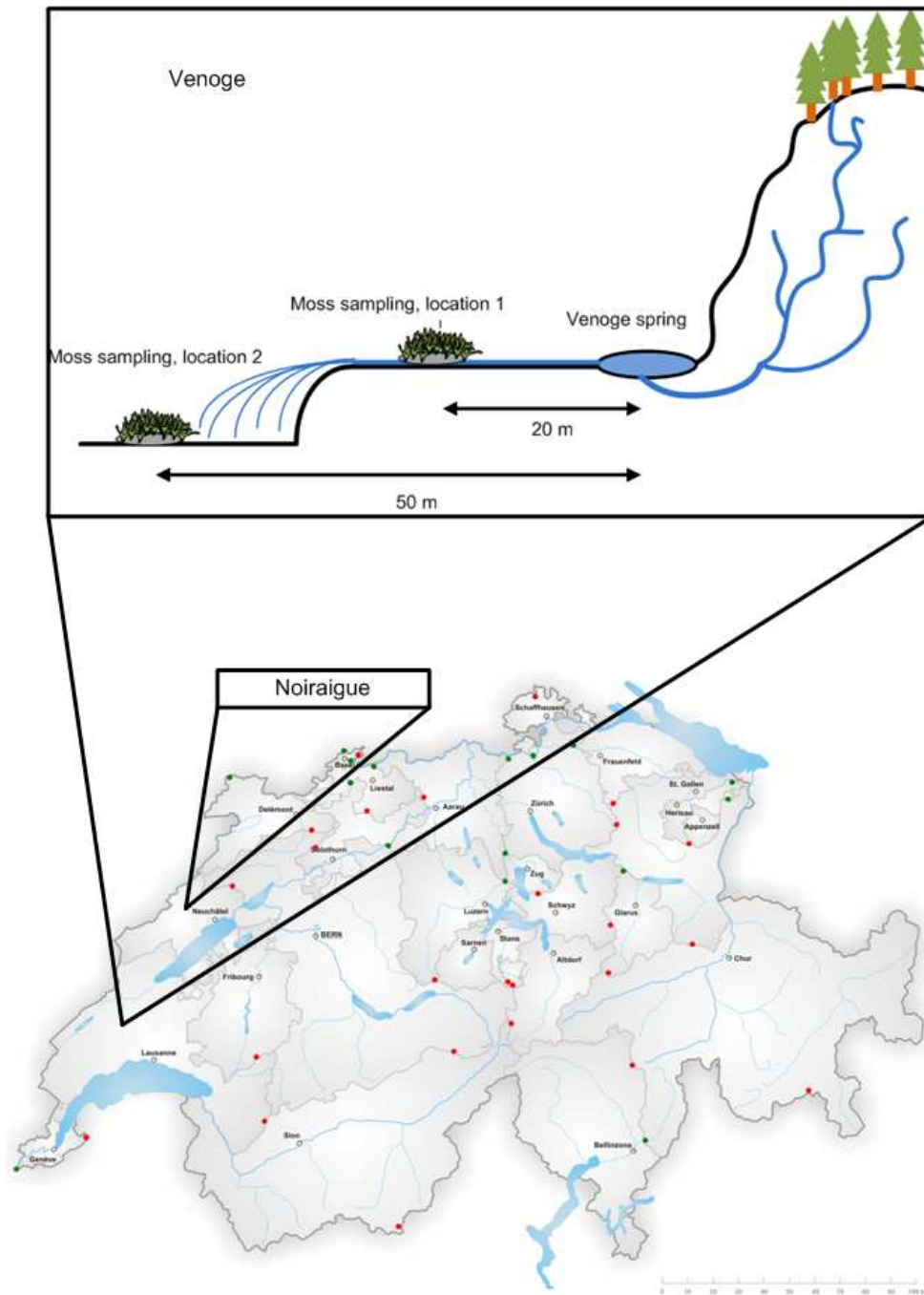


Figure 1. Study and sampling area.



from the catchment and flows into the karstic sinkhole, giving rise to the Noiraigue spring at a distance of 4 km and an altitude of 736 m. The hydrological regime of the brook is strongly dependent on precipitation, with a lowest flow rate of  $0.03 \text{ m}^3 \text{ s}^{-1}$  and a highest flow rate of  $4.50\text{-}6.00 \text{ m}^3 \text{ s}^{-1}$ . The pH of the water is *ca* 6.5-7.5, the temperature varies from 0 °C in the winter season to +15 °C in the summer months. Water of the Noiraigue Bied brook is characterized by a high NOM content – up to 15-20 ppm. Detailed physico-chemical parameters of the water, as well as the precipitation regime during sampling and field measurements campaign are given in SI.

#### **4.4 MATERIALS AND METHODS**

All reagents used were of analytical grade from Merck, Fluka, or Sigma-Aldrich. Polyacrylamide gel sheets (6 × 22 cm) of 0.39 mm and 0.78 mm thickness and Chelex resin gels were provided by DGT Research Limited, Lancaster, UK. Local physico-chemical parameters of the water (pH, *t* °C, Eh, conductivity, dissolved oxygen) in the field were measured with a universal Multi 340i pocket meter equipped with a standard TetraCon<sup>®</sup> 325 conductivity cell and CelloX<sup>®</sup> oxygen sensor. NOM concentrations in water (as total DOC) were quantified using UV-Vis spectrophotometry according to Carter *et al.* (Carter *et al.*, 2012) WHAM 7 equilibrium model was used to calculate the chemical speciation of Pu in natural waters using the input data from Table SI-5.

##### **4.4.1 SAMPLE PREPARATION**

###### **4.4.1.1 WATER SAMPLES**

To determine the Pu concentration in water, we measured  $^{239}\text{Pu}$  and  $^{240}\text{Pu}$  using AMS (see § 3.3) in the bulk water samples from the Venoge spring and Noiraigue Bied brook (hereafter the activities are only given for  $^{239}\text{Pu}$ ). Water samples (10-50 L) were collected by

pumping, filtered on line through a 0.5  $\mu\text{m}$  Milligard<sup>®</sup> Nominal MCE cartridge and acidified on the spot with 1 mL conc.  $\text{HNO}_3$  per L of water. Each sample was spiked with 1.7 pg of  $^{242}\text{Pu}$  (source Pu242 Nr. 790 from LNSIRR), internal standard for AMS measurements.  $\text{FeCl}_3 \cdot 6\text{H}_2\text{O}$  was dissolved in the water sample (0.25 g per 10 L) and Pu was co-precipitated with iron hydroxides at pH 8, by adding conc.  $\text{NH}_4\text{OH}$ . After decanting, the precipitate was dissolved in 5 M HCl and the solution heated to 80 °C under stirring to eliminate carbonates. 5 mL of a solution of  $\text{Ca}^{2+}$  of 100  $\text{mg mL}^{-1}$  and 15 g of  $\text{H}_2\text{C}_2\text{O}_4 \cdot 2\text{H}_2\text{O}$  were then added to the solution and calcium oxalate was precipitated at pH 2. After decanting and centrifugation, calcium oxalate was destroyed using microwave-assisted digestion (Milestone Ultraclave IV) in 20 mL of conc.  $\text{HNO}_3$  (Luisier et al., 2009). 50 mg of  $\text{FeCl}_3 \cdot 6\text{H}_2\text{O}$  was added to the sample after digestion and iron hydroxides were precipitated at pH 8. This precipitate was centrifuged and washed with deionized water ( $<0.05 \mu\text{S cm}^{-1}$ ) and dissolved in 20 mL of 8 M  $\text{HNO}_3$  for radiochemical separation of Pu. The radiochemical separation of Pu for AMS measurements was done by solid-phase extraction using AG 1-X4 anion exchange resin (chloride form) from Bio-Rad Laboratories Inc. as described by Cusnir et al. (2015).

To determine the Pu (V) fraction in natural water, we used selective adsorption of Pu (IV) and Pu (VI) on silica gel as described by Orlandini et al. (1986). Briefly, 100 g of silica gel (Fluka, 70-230 mesh) was added to 50 L of bulk water sample and left under vigorous stirring for 5 min. Afterwards the sample was decanted for 10 min and filtered to remove the silica gel. Pu (V) was co-precipitated from the filtrate and analyzed as described above.

To determine the colloid-bound and dissolved fractions of Pu, 50 L water samples from the Venoge spring and Noiraigue Bied brook were submitted to cross-flow ultrafiltration through a 10 kDa Millipore Prep/Scale-TFF membrane (surface area 1  $\text{ft}^2$ ) to reach the concentration factor (cf) of 5. The retentate and permeate fractions were acidified, spiked with  $^{242}\text{Pu}$  and submitted to radiochemical separation of Pu as described above.

#### 4.4.1.2 AQUATIC PLANTS SAMPLES

Aquatic mosses (mainly *Fontinalis antipyretica*) were collected in two locations at the Venoge spring (Fig. 1). Each sample was subsequently divided into two sub-samples for Pu sequential elution and measurements. The first location (L1) was in the close proximity to the Venoge spring's outlet, *ca* 20 m downstream from the outlet. The second (L2) was *ca* 50 m down the stream, next to a 2 meter-high waterfall. Vascular aquatic plants (*Phragmites australis*) were collected in one location in the Noiraigue Bied brook near the DGT samplers. Only plants totally covered by water were carefully collected. The sample was divided into two sub-samples for Pu sequential elution and measurements. Pu in these sub-samples was determined separately for leaves permanently exposed in water, and roots growing within the sediment.

Mosses and plants for sequential elution (Scheme SI-1) of Pu were thoroughly washed with deionized water to remove any adhering sediment particles. To determine the fraction of Pu co-precipitated with calcite in aquatic mosses and plants, the sample was dispersed in a citrate buffer (0.1 M citric acid anhydrous / 0.1 M sodium citrate tribasic dihydrate at pH 4.3) for 1 hour, then the plants were removed and the citrate solution filtered to form the citrate fraction. Next, the plant sample was exposed to a 10 mM EDTA (pH 7) solution for one hour. The resulting solution formed the extracellular Pu fraction. Afterwards, the plant sample was dried at 80 °C for 24 h to destroy cell walls and the intracellular Pu was eluted with 1 M HNO<sub>3</sub>. Finally, the sample was dried, ashed, and the residual Pu was extracted in 8 M HNO<sub>3</sub> following a microwave digestion under pressure (50 bars) at 180°C. Between each elution step, the plant sample was rinsed with deionized water and the washouts combined with the respective fraction. SE fractions were spiked with 1.7 pg of <sup>242</sup>Pu and submitted to radiochemical separation for Pu. The calcium content in the citrate fraction was measured using ICP-OES. In addition, a sub-sample of plants was weighed, dried at 80 °C and ashed. Pu was extracted from the ashes using microwave-assisted digestion (Luisier et al., 2009).

After microwave digestion the solution was filtered and submitted to radiochemical separation of Pu as described above to determine the bulk concentration of Pu.

#### 4.4.2 DGTs

The fabrication and deployment of large surface (105 cm<sup>2</sup>) DGT devices for *in-situ* Pu bioavailability measurements were described and demonstrated by us earlier (Cusnir et al., 2015). To measure the bioavailable fraction of Pu in karstic freshwaters *in-situ*, we deployed large surface DGT devices of 0.39 mm and 0.78 mm gel layer thickness for 2 to 3 weeks in the two water systems. In the Venoge spring, DGTs were ballasted and suspended for deployment in the spring outlet. In the Noiraigue Bied brook, DGTs were deployed on a vertical support, at a 45 ° angle to the water flow. After deployment, the DGTs were disassembled and the Chelex resin-gel layers were retrieved for Pu elution. Each Chelex resin-gel sample was spiked with 1.7 pg of <sup>242</sup>Pu internal standard and then 10 mL of 8 M HNO<sub>3</sub> was added. After 24 h elution, the samples were centrifuged, decanted and washed twice with 5 mL of 8 M HNO<sub>3</sub>. The sample solutions were filtered through glass-fiber 0.45 µm Nalgene syringe filters when necessary and submitted to radiochemical separation of Pu for AMS measurements as described previously (Cusnir et al., 2015). The concentration of bioavailable (labile) Pu species in water  $C_{DGT}$  (µBq mL<sup>-1</sup>) was calculated from the equation 1 (Warnken et al., 2007; Cusnir et al., 2016):

$$\frac{1}{A} = \frac{1}{C_{DGT}St} \left( \frac{\Delta g}{D_M^{gel}} + \frac{\delta}{D_M^w} \right) \quad (1)$$

where  $A$  is the activity (µBq) of Pu accumulated in the binding phase (converted from the Pu concentration (at g<sup>-1</sup>) measured by AMS),  $\Delta g$  is the diffusion layer (gel + filter membrane) thickness (cm),  $D_M^{gel}$  is the diffusion coefficient of Pu in the PAM gel (cm<sup>2</sup> s<sup>-1</sup>, taken from Cusnir et al. (2014),  $D_M^w$  is the diffusion coefficient of Pu in water ( $D_M^w = D_M^{gel}/0.85$ ),  $\delta$  the diffusive boundary layer (0.03 cm from Warnken et al., 2007),  $S$  the diffusion area (cm<sup>2</sup>), and

$t$  the duration of deployment (s). We used average  $C_{DGT}$  determined with DGT devices of the same resin-gel thickness for each deployment campaign. Similarly, to compare the  $C_{DGT}$  with total Pu in the bulk water, we used average Pu concentration, determined for each period of DGT deployments.

#### **4.4.3 Pu MEASUREMENTS by AMS**

The AMS measurements of the Pu isotopes were performed at ETH Zurich using the low energy system “Tandy” (Christl et al., 2013). The compact (lab-sized) AMS system is ideally suited for determining ultra-trace amounts of actinides because it combines a high sensitivity (the transmission for actinides is up to 40%, Vockenhuber et al., 2013) with an efficient suppression of neighboring masses (the abundance sensitivity is at a level of  $10^{-12}$  for the actinides, Christl et al., 2015). With the current setup of the AMS system, detection limits in the sub-femtogram range are reached for Pu isotopes (Dai et al., 2012). Details of the AMS measurement of Pu isotopes are described in Christl et al. (2013). Briefly, the xPu-isotopes ( $x=239, 240,$  and  $242$ ) were measured sequentially (typically 10s, 20s, and 6s, respectively). The isotopic ratios of interest (here  $^{239}\text{Pu}/^{242}\text{Pu}$  and  $^{240}\text{Pu}/^{242}\text{Pu}$ ) were calculated from the repeated sequential measurement of samples, standards, and blanks. A possible interference of  $^{238}\text{U}$  ions with  $^{239}\text{Pu}$  (caused by “tailing” of  $^{238}\text{U}$ ) was carefully monitored and turned out to be negligible for all Pu-samples of this study. Each Pu-sample was measured between 1h and 1½h in total. The measured Pu-ratios were normalized to the ETH in-house standard “CNA” (Christl et al., 2013). The uncertainty of the reported Pu concentrations includes counting statistics and the variability of the measured isotopic ratios during the repeated measurement (of samples and standards).

## 4.5 RESULTS

### 4.5.1 Pu CONCENTRATIONS IN BULK WATER

A total of fourteen bulk water samples (20-50 L) were measured, yielding an average  $^{240}\text{Pu}/^{239}\text{Pu}$  isotopic ratio of  $0.194 \pm 0.014$  ( $n = 14$ ). This result demonstrates that the origin of the Pu in the karst system is the fallout of the atmospheric nuclear tests of the sixties. The concentration of  $^{239}\text{Pu}$  in the Venoge spring ranged from 0.43 to  $3.44 \mu\text{Bq L}^{-1}$  ( $n = 10$ ), similar to concentrations determined previously with alpha-spectrometry ( $1-7 \mu\text{Bq L}^{-1}$ , Froidevaux et al. (2010)). The concentration of  $^{239}\text{Pu}$  in karstic freshwaters obviously depends on the precipitation regime, however it was challenging to identify a straightforward relationship. When compared to precipitation data, the lowest  $^{239}\text{Pu}$  concentration ( $0.43 \pm 0.03 \mu\text{Bq L}^{-1}$ ) was correlated with a precipitation regime *ca* 72% of the monthly precipitation norm (MPN). Nevertheless, a relatively low concentration ( $0.83 \pm 0.17 \mu\text{Bq L}^{-1}$ ) was also measured on the day following a major rain event (40 % of the total monthly precipitations), possibly due to a significant dilution. The highest  $^{239}\text{Pu}$  concentration ( $3.44 \pm 0.14 \mu\text{Bq L}^{-1}$ ) in the Venoge spring was measured when monthly precipitations were close to the MPN and about one week later following a flood event. A similar pattern of  $^{239}\text{Pu}$  concentrations was observed for the Noiraigue Bied brook. The lowest  $^{239}\text{Pu}$  ( $0.39 \pm 0.02 \mu\text{Bq L}^{-1}$ ) was measured in water sampled during a dry summer month with only 59 % of the MPN. The absence of rainfall had a similar effect on the NOM content – it dropped from 15 ppm to 10 ppm during this dry period. Higher  $^{239}\text{Pu}$  concentrations ( $3.13-3.40 \mu\text{Bq L}^{-1}$ ) were measured in water sampled during periods with a precipitation regime closer to normal (MPN 70-85 %) – this effect being probably due to the elution of  $^{239}\text{Pu}$  deposited and retained in the organic-rich soil of the valley.

#### 4.5.2 Pu SPECIATION IN NATURAL WATERS

Selective adsorption experiments enabled the determination of Pu (V) fraction in the natural water of the Venoge spring. We found 88 % ( $n=2$ , with a measurement uncertainty of 8 %) of the plutonium as  $^{239}\text{Pu}$  (V) in water; this supports the hypothesis that in the carbonate-rich vadose waters the predominant form of Pu is a highly soluble  $[\text{PuO}_2^+(\text{CO}_3)_n]^{m-}$ , similar to uranyl-carbonate species. In the Noiraigue Bied brook water, it was not possible to carry out similar sorption experiments due to the high NOM content (15-20 ppm).

Calculation using WHAM7 and parameters of Table SI-5 shows that in the mineral water of the Venoge spring all the Pu was associated with carbonates in a soluble form, at both pH 6.5 and 7.0. Though, in the presence of soluble FA in the Noiraigue Bied brook the speciation is dependant of pH as well as  $\text{CO}_3^{2-}$  and FA concentrations. Varying FA and carbonate concentrations input in WHAM7 shows that at elevated carbonate concentration of  $150 \text{ mg L}^{-1}$  in the presence of  $15 \text{ mg L}^{-1}$  FA 72 % of Pu was associated with carbonates at pH 6.5, while it increased to 94 % at pH 7. When carbonate concentration drops to  $90 \text{ mg L}^{-1}$  at the same FA concentration of  $15 \text{ mg L}^{-1}$ , 48 % of Pu are found associated to carbonates at pH 6.5 and 84 % at pH 7.0. Detailed output of WHAM7 calculations is given in the Table SI-8. As a general trend, increasing the FA concentration from 15 to  $18 \text{ mg L}^{-1}$  slightly lowers the Pu-carbonate fraction at the same concentration of carbonate at both pH 6.50 and 7.00; increasing the pH from 6.5 to 7.0 and  $\text{CO}_3^{2-}$  concentration from 90 to  $150 \text{ mg L}^{-1}$  yields higher Pu-carbonate fractions.

#### 4.5.3 Pu CONCENTRATIONS IN ULTRAFILTERED FRACTIONS

The results of the measurements of the  $^{239}\text{Pu}$  in the ultrafiltered fractions of water sampled in the Venoge spring and the Noiraigue brook showed that Pu is present mostly in the dissolved phase (Fig. 2). We found a slightly higher colloid-bound  $^{239}\text{Pu}$  fraction in organic-rich water from Noiraigue (25 %,  $n=2$ ) compared to mineral water from Venoge (18

%,  $n=3$ ). The full mass balance of  $^{239}\text{Pu}$  as a performance characteristic of cross-flow ultrafiltration (CFUF) yielded 83-105 % recoveries ( $n=3$ ) for the Venoge water and 76-84 % ( $n=2$ ) for the Noiraigue water. These performances were considered satisfactory, taking into account the very low  $^{239}\text{Pu}$  concentration in our environmental water samples and the fact that Pu tends to sorb onto the filter membrane (Chawla et al., 2010).

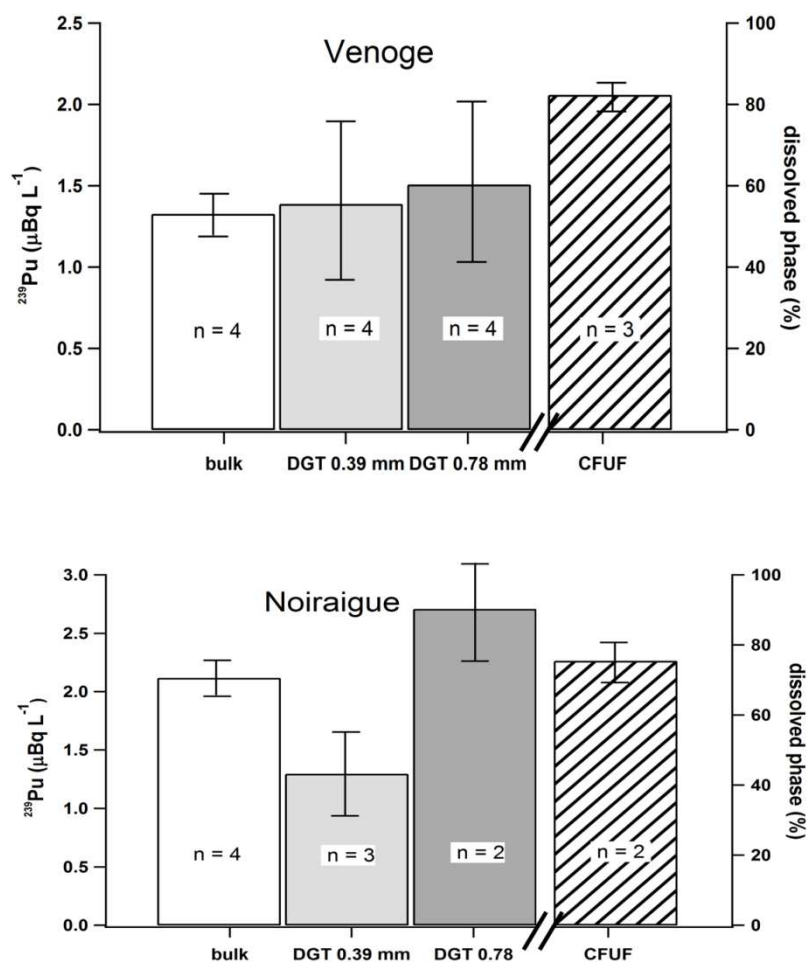


**Figure 2. Determination of Pu as bioavailable species.** Total  $^{239}\text{Pu}$  measured in the bulk water during deployment of DGTs, concentrations of free and labile  $^{239}\text{Pu}$  species measured with DGTs (left scale) and percentage of  $^{239}\text{Pu}$  in the dissolved phase measured by CFUF (right scale) in the Venoge waters (top) and Noiraigue waters (bottom). Results are the average of  $n$  measurements and uncertainties are the sum of the absolute uncertainty of each measurement divided by  $n$ .



#### 4.5.4 DGT MEASUREMENTS OF FREE AND LABILE PU SPECIES

In total, we deployed 13 DGTs in the Venoge spring and 9 DGTs in the Noiraigue Bied brook during two field campaigns in April-September 2014 and April-June 2015. Detailed information of each deployment campaign is given in the SI. DGTs retrieved after the deployment did not show traces of biofouling, probably due to the low temperature recorded for these waters, and preserved the initial form and condition of the gel assemblies. Figure 2 compares the  $C_{DGT}$  of  $^{239}\text{Pu}$  with total  $^{239}\text{Pu}$  and dissolved phase  $^{239}\text{Pu}$ , measured in both Venoge and Noiraigue waters. The average  $C_{DGT}$  of the  $^{239}\text{Pu}$  measured in the Venoge spring was  $1.39 \pm 1.03 \mu\text{Bq L}^{-1}$  ( $n=4$ ) with a gel thickness of 0.39 mm and  $1.51 \pm 1.04 \mu\text{Bq L}^{-1}$  ( $n=4$ ) with a gel thickness of 0.78 mm. These concentrations correlated well with the total  $^{239}\text{Pu}$  measured in the bulk water during the deployment period ( $1.33 \pm 0.24 \mu\text{Bq L}^{-1}$ ,  $n=4$ ) as well as with the dissolved phase  $^{239}\text{Pu}$ .

DGTs deployed in the organic-rich waters of the Noiraigue Bied brook showed a different pattern of Pu accumulation. The  $C_{DGT}$  of the  $^{239}\text{Pu}$  measured with a gel thickness of 0.39 mm was  $1.30 \pm 0.76 \mu\text{Bq L}^{-1}$  ( $n=3$ ), which made only 60 % of the total  $^{239}\text{Pu}$  measured in the bulk water during the deployment period ( $2.12 \pm 0.35 \mu\text{Bq L}^{-1}$ ,  $n=4$ ), while the  $C_{DGT}$  of the  $^{239}\text{Pu}$  measured with a gel thickness of 0.78 mm was  $2.71 \pm 1.50 \mu\text{Bq L}^{-1}$  ( $n=2$ ). This value overestimates the bioavailable fraction and is higher than total  $^{239}\text{Pu}$  measured in the Noiraigue waters. DGTs with a gel thickness of 0.78 mm deployed in the Noiraigue Bied brook systematically accumulated similar amounts of Pu as DGTs with a gel thickness of 0.39 mm. According to Equation 1 this yields a two times higher concentration of labile Pu in the river water.

#### 4.5.5 DISTRIBUTION OF Pu IN DIFFERENT COMPARTMENTS OF AQUATIC MOSSES AND PLANTS

The activity of the  $^{239}\text{Pu}$  per g of bulk fresh weight of mosses from Venoge measured in L1 was  $6.20 \pm 0.06 \mu\text{Bq g}^{-1}$  ( $n=2$ ) – five times lower compared to mosses sampled in L2

( $31.2 \pm 0.32 \text{ } \mu\text{Bq g}^{-1}$ ,  $n=2$ ). The major fraction of Pu (60 %) in both locations was present within the calcite precipitated on the surface of mosses and extracted in the citrate buffer fraction (Figure 3). However, the activity of  $^{239}\text{Pu}$  per mg of Ca measured in the calcite fraction varied between the two locations. We found  $3.20 \pm 0.03 \text{ } \mu\text{Bq}$  of  $^{239}\text{Pu}$  per mg of Ca in mosses near the spring and  $5.30 \pm 0.12 \text{ } \mu\text{Bq}$  of  $^{239}\text{Pu}$  per mg of Ca in mosses sampled next to the waterfall.

Measurements of Pu in aquatic plants from Noiraigue revealed a distribution similar to that in the Venoge mosses. Figure 3 shows that the major fraction of Pu eluted from the leaves was concentrated within the calcite, even to a greater extent (75 %) compared to mosses from the Venoge spring (60 %). In the roots, we only measured  $^{239}\text{Pu}$  in extra- and intracellular compartments, as well as in the residue. We found a comparable activity of  $^{239}\text{Pu}$  per g of fresh weight (Fig. 3 and Table SI-7) in these three fractions.

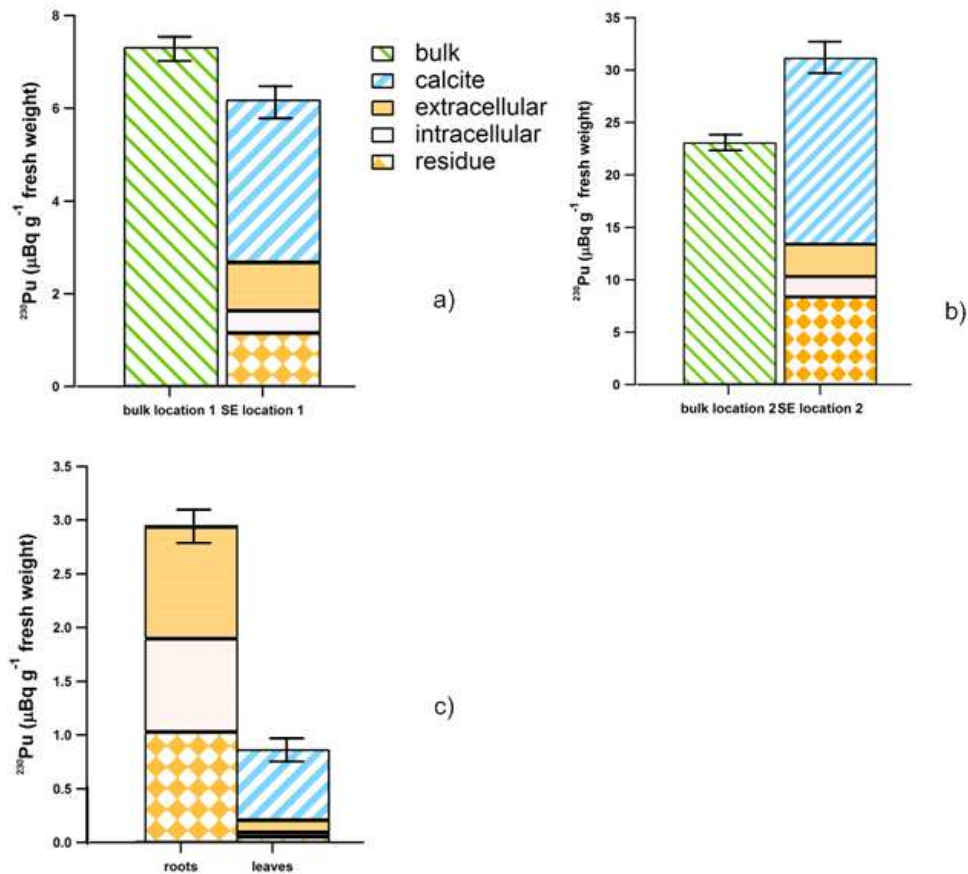


**Figure 3. Sequential elution of Pu from different compartments of aquatic mosses and plants.** Activity of  $^{239}\text{Pu}$  ( $\mu\text{Bq g}^{-1}$ ) measured in mosses sampled at the Venoge spring (top, a and b) and in aquatic plants sampled at the Noiraigue Bied brook (bottom, c). Each result is the average of 2 measurements and uncertainties are the sum of the absolute uncertainty of each measurement divided by 2. Activity of  $^{239}\text{Pu}$  in the bulk are failing to perfectly match with the sum of fractions in mosses (a and b) due to uncertainty of type B and heterogeneity of calcite depositions in the different subsamples.

## 4.6 DISCUSSION

As shown by the ultrafiltration experiments, a rather constant 15-20 % of the total Pu is associated with colloids > 10 kDa, with slightly higher colloid-bound  $^{239}\text{Pu}$  fraction at the Noiraigue site (25 %,  $n=2$ ) compared to the Venoge site (18 %,  $n=3$ ). Waters gathered from the organic-rich agricultural soils and peat bogs of the Vallée-des-Ponts are enriched in NOM and NOM-complexed Fe-Ca colloids (Atteia and Kozel, 1997; Mavrocordatos et al., 2000). We characterized the NOM from Noiraigue earlier with size-exclusion chromatography (Cusnir et al., 2016). These results showed mostly the presence of fulvic acids less than 3 kDa in molecular weight. In this respect, the lower recovery yield for the Noiraigue ultrafiltration experiments might be due to a slight adsorption of Pu-FA material onto the filtering membrane.

Soluble carbonated complexes of Pu predicted by WHAM7 for Venoge spring are expected to be fully measurable with DGTs. It should be noted that WHAM7 allows only calculations for Pu (IV) and the complex reported is  $[\text{Pu(IV)(CO}_3)_2]^0$ , while we found experimentally that 88 % of Pu in this water is in +V oxidation state. According to Novikov et al.(2006) a plutonyl-carbonate  $[\text{PuO}_2^+(\text{CO}_3)_n]^{m-}$  form, similar to  $[\text{UO}_2(\text{CO}_3)_n]^{m-}$ , can be found in water at equilibrium with atmospheric  $\text{CO}_2$ . The concentration of  $^{239}\text{Pu}$  in water, calculated from DGT measurements ( $C_{DGT}$ ) of accumulated  $^{239}\text{Pu}$ , represents the effective concentration of metal measured directly by DGT in the river water during the time of deployment. At the Venoge site, DGT with gel thicknesses of 0.39 mm and 0.78 mm give similar  $C_{DGT}$ , which are coherent with the total Pu concentrations. Therefore, under “Venoge conditions”, most dissolved Pu exists in a readily available form – likely a plutonyl carbonate complex measurable by DGT, e.g. fully labile inorganic complexes.

In contrast, at the Noiraigue site WHAM7 predicts that carbonate and soluble FA are competing for Pu, with up to 50 % of Pu bound to FA at pH 6.50 and  $18 \text{ mg L}^{-1}$  of FA (Table SI-8). Additionally, DGTs with gel thickness of 0.078 mm accumulated more Pu than

expected from DGT theory. While the diffusive flux of free metals is obviously greater through a thinner gel, this can be compensated by an additional flux of Pu from labile Pu-FA complexes in the thicker gels, where enough time is available for these complexes to dissociate (Levy et al., 2012). We have previously shown in laboratory experiments that DGTs with a diffusive layer thickness of 1.96 mm actually accumulated more Pu in the presence of dissolved FA (Cusnir et al., 2016). More specifically, this study showed that larger gel thicknesses increased the lability degree of the Pu-FA complexes. Small FA molecules have been shown to diffuse into the PAM gel (Van der Veecken et al., 2010), as well as into plants (Nardi et al., 2002), while a greater diffusive layer thickness of a DGT sampler increases the diffusion time of Pu-FA complexes within the gel. A relatively high dissociation constant of Pu-FA complexes, as measured by Cusnir et al. (2016), contributes to free Pu species, available for accumulation in the Chelex binding phase. The good agreement of DGT (0.78 mm) results and bulk Pu concentrations in the Noiraigue Bied brook revealed that Pu in the presence of dissolved FA in karstic freshwaters is fully available for biouptake and that the interaction of Pu with dissolved FA in the organic-rich water is a dynamic process.

The sequential elution of Pu from aquatic mosses and vascular plants showed that in permanently immersed plants, more than 60-75 % of the Pu is associated with calcite precipitations on the plants leaves. In the case of mosses from Venoge spring this could be supported by the greater extent of calcite precipitation – involving also Pu as co-precipitate – due to CO<sub>2</sub>-degassing of the carbonate-rich water falling down the cascade (L2). As a matter of fact, the amount of Ca eluted with calcite in mosses sampled in L2 was also three times higher, compared to mosses sampled in L1. Only some 5 to 10 % of the total Pu is found in the intracellular fraction. Therefore, in these calcareous waters, calcite precipitation out-competes biouptake of Pu by plants. In the case of the Venoge spring, the Pu/Ca ratio in the

water is roughly  $0.01 \mu\text{Bq Pu mg}^{-1} \text{ Ca}$ , whereas in the calcite precipitates on the mosses Pu is relatively enriched, with a Pu/Ca ratio of approximately  $1 \mu\text{Bq Pu mg}^{-1} \text{ Ca}$ . The calcite co-precipitation of Pu in organic-rich water of the Noiraigue Bied brook most probably involves Pu-FA complexes. This corroborates our assumption that the local environment on the plant surface (similar to the DGT gel) promotes the dissociation of the Pu-FA complex and the formation of a solid carbonate phase. While it was not possible to determine experimentally the Pu (V) fraction in this water, we suggest that a certain fraction might still be found as  $[\text{PuO}_2^+(\text{CO}_3)_n]^{m-}$  form.

#### **4.7 CONCLUSION**

The ultrasensitive determination of trace Pu with AMS in a pristine environment has provided a model of Pu speciation in natural freshwaters. A tentative sketch of the biogeochemical behavior of Pu in a karstic spring environment is given in the Fig. 4. With a rather constant colloid-bound fraction, Pu is found predominately in the dissolved phase in both bicarbonate-rich and organic-rich water. Although Pu (V) has been experimentally evidenced in the mineral water, its reduction to Pu (IV) obviously takes place in the presence of soluble NOM, which is competing for Pu with carbonates as NOM concentration in water increases. The exact speciation of Pu in these conditions can only be estimated using modeling approach. Additionally, the dependence on the rainfall of Pu and NOM concentrations in water implies important consequences on predicting the long-range Pu transport.

Loss of dissolved  $\text{CO}_2$  due to degassing promotes the precipitation of calcite on aquatic plants, involving Pu, both in mineral and organic-rich water. This co-precipitation constitutes the main input of Pu to aquatic plants biomass, with only minute amounts of Pu found in the intracellular fractions. However, secondary dissociation of Pu-NOM complexes

co-precipitated on plants surface should also be considered in the bioaccumulation of Pu in these conditions.

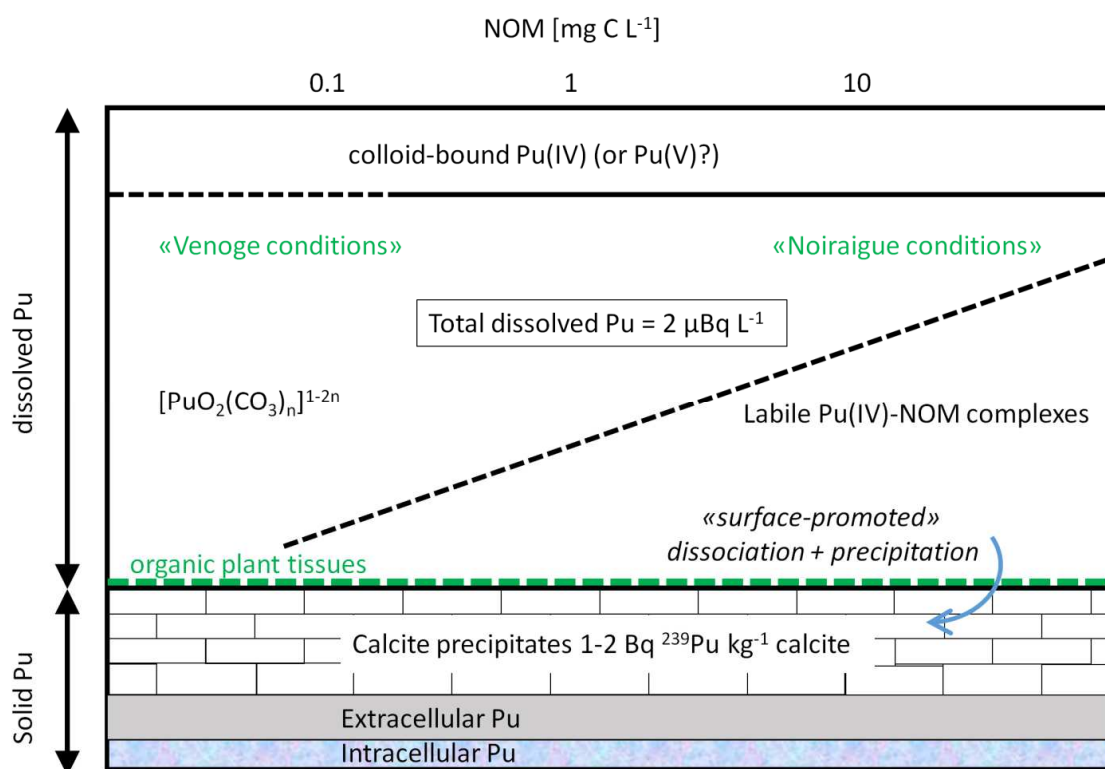


**Figure 4. Tentative sketch of the biogeochemical behavior of Pu in karstic freshwater environments.** Under “Venoge conditions”, in bicarbonate-rich and Ca-rich waters with a low content of NOM, Pu is found mainly in a +V oxidation state as soluble plutonyl-carbonate complexes. With the increase of soluble FA concentration in water, such as in “Noiraigue conditions”, carbonate competes with FA for Pu. Furthermore, the Pu (V) is being reduced to Pu (IV), which forms labile Pu-FA complexes, available for bioaccumulation. Due to the release of CO<sub>2</sub> from the water, the precipitation of the calcite (involving the Pu as co-precipitate) is a major input of Pu to aquatic plants in both environments.

This work demonstrates the value of using the DGT technique for Pu bioavailability measurements *in situ*. The determination of Pu as fully labile species in the mineral Venoge spring using DGTs correlated well with the finding of a soluble plutonyl-carbonate  $[\text{PuO}_2^+(\text{CO}_3)_n]^{m-}$  form and with a low proportion of colloid-bound Pu in water. Overestimated  $C_{DGT}$  of Pu in the organic-rich Noiraigue water has demonstrated the possibility of Pu-NOM complexes to contribute to the bioaccumulation of Pu via dissociation. While DGTs applied for trace Pu measurements in pristine environments require highly sensitive analytical techniques, this approach can prove useful in continuous monitoring and in contaminated environments with higher Pu concentrations.

#### **4.8 Acknowledgements**

This work was funded by the Swiss National Science Foundation (grant n° 200021-140230) and by the Swiss Federal Office of Public Health (PF and PS).

#### **4.9 Contributions**

R. C. carried out the experiments and field work and wrote the paper. M. C. performed AMS measurements and contributed to the paper. P. S. brought the biogeochemical model and made figure 3. F. B. took part in discussion of the results and contributed to the paper. P. F. conceived the study, took part in field work and co-wrote the manuscript.



## 4.10 References

- Alvarado J. A. C., Steinmann P., Estier S., Bochud F., Haldimann M. and Froidevaux P. (2014) Anthropogenic radionuclides in atmospheric air over Switzerland during the last few decades. *Nat. Commun.* **5**, 3030.
- Atteia O. and Kozel R. (1997) Particle size distributions in waters from a karstic aquifer: from particles to colloids. *J. Hydrol.* **201**, 102–119.
- Carter H. T., Tipping E., Koprivnjak J.-F., Miller M. P., Cookson B. and Hamilton-Taylor J. (2012) Freshwater DOM quantity and quality from a two-component model of UV absorbance. *Water Res.* **46**, 4532–4542.
- Chawla F., Steinmann P., Loizeau J.-L., Hassouna M. and Froidevaux P. (2010) Binding of Pu-239 and Sr-90 to Organic Colloids in Soil Solutions: Evidence from a Field Experiment. *Environ. Sci. Technol.* **44**, 8509–8514.
- Choppin G. R., Bond A. H. and Hromadka P. M. (1997) Redox speciation of plutonium. *J. Radioanal. Nucl. Chem.* **219**, 203–210.
- Christl M., Casacuberta N., Lachner J., Maxeiner S., Vockenhuber C., Synal H.-A., Goroncy I., Herrmann J., Daraoui A., Walther C. and Michel R. (2015) Status of U-236 analyses at ETH Zurich and the distribution of U-236 and I-129 in the North Sea in 2009. *Nucl. Instrum. Methods Phys. Res. Sect. B-Beam Interact. Mater. At.* **361**, 510–516.
- Christl M., Vockenhuber C., Kubik P. W., Wacker L., Lachner J., Alfimov V. and Synal H.-A. (2013) The ETH Zurich AMS facilities: Performance parameters and reference materials. *Nucl. Instrum. Methods Phys. Res. Sect. B-Beam Interact. Mater. At.* **294**, 29–38.
- Cusnir R., Jaccard M., Bailat C., Christl M., Steinmann P., Haldimann M., Bochud F. and Froidevaux P. (2016) Probing the Kinetic Parameters of Plutonium–Naturally Occurring Organic Matter Interactions in Freshwaters Using the Diffusive Gradients in Thin Films Technique. *Environ. Sci. Technol.* **50**, 5103–5110.
- Cusnir R., Steinmann P., Bochud F. and Froidevaux P. (2014) A DGT Technique for Plutonium Bioavailability Measurements. *Environ. Sci. Technol.* **48**, 10829–10834.
- Cusnir R., Steinmann P., Christl M., Bochud F. and Froidevaux P. (2015) Speciation and Bioavailability Measurements of Environmental Plutonium Using Diffusion in Thin Films. *J. Vis. Exp. JoVE*, e53188.
- Dai X., Christl M., Kramer-Tremblay S. and Synal H.-A. (2012) Ultra-trace determination of plutonium in urine samples using a compact accelerator mass spectrometry system operating at 300 kV. *J. Anal. At. Spectrom.* **27**, 126–130.
- Davison W. and Zhang H. (1994) In situ speciation measurements of trace components in natural waters using thin-film gels. *Nature* **367**, 546–548.
- Froidevaux P., Bochud F. and Haldimann M. (2010) Retention half times in the skeleton of plutonium and <sup>90</sup>Sr from above-ground nuclear tests: A retrospective study of the Swiss population. *Chemosphere* **80**, 519 – 524.
- Froidevaux P., Steinmann P. and Pourcelot L. (2010) Long-Term and Long-Range Migration of Radioactive Fallout in a Karst System. *Environ. Sci. Technol.* **44**, 8479–8484.
- Hunt J., Leonard K. and Hughes L. (2013) Artificial radionuclides in the Irish Sea from Sellafield: remobilisation revisited. *J. Radiol. Prot.* **33**, 261–279.
- Kaplan D. I., Powell B. A., Demirkanli D. I., Fjeld R. A., Molz F. J., Serkiz S. M. and Coates J. T. (2004) Influence of oxidation states on plutonium mobility during long-term transport through an unsaturated subsurface environment. *Environ. Sci. Technol.* **38**, 5053–5058.
- Katz J., Seaborg G. and Morss L. (1986) The chemistry of the actinide elements. In *The chemistry of the actinide elements* Chapman and Hall Ltd, London New York.

- Levy J. L., Zhang H., Davison W., Galceran J. and Puy J. (2012) Kinetic Signatures of Metals in the Presence of Suwannee River Fulvic Acid. *Environ. Sci. Technol.* **46**, 3335–3342.
- Luisier F., Alvarado J. A. C., Steinmann P., Krachler M. and Froidevaux P. (2009) A new method for the determination of plutonium and americium using high pressure microwave digestion and alpha-spectrometry or ICP-SMS. *J. Radioanal. Nucl. Chem.* **281**, 425–432.
- Mavrocordatos D., Mondy-Couture C., Atteia O., Leppard G. G. and Perret D. (2000) Formation of a distinct class of Fe-Ca(-C-org)-rich particles in a complex peat-karst system. *J. Hydrol.* **237**, 234–247.
- Nardi S., Pizzeghello D., Muscolo A. and Vianello A. (2002) Physiological effects of humic substances on higher plants. *Soil Biol. Biochem.* **34**, 1527–1536.
- Novikov A. P., Kalmykov S. N., Utsunomiya S., Ewing R. C., Horreard F., Merkulov A., Clark S. B., Tkachev V. V. and Myasoedov B. F. (2006) Colloid transport of plutonium in the far-field of the Mayak Production Association, Russia. *Science* **314**, 638–641.
- Orlandini K., Penrose W. and Nelson D. (1986) Pu(v) as the Stable Form of Oxidized Plutonium in Natural-Waters. *Mar. Chem.* **18**, 49–57.
- Santschi P. H., Roberts K. A. and Guo L. D. (2002) Organic nature of colloidal actinides transported in surface water environments. *Environ. Sci. Technol.* **36**, 3711–3719.
- Taylor D. M. (2001) Environmental Plutonium - Creation of the Universe to Twenty-first Century Mankind. In *Plutonium in the Environment* Elsevier, Oxford. pp. 1–14. Available at: <Go to WoS>://WOS:000168875100001.
- Tinnacher R. M., Begg J. D., Mason H., Ranville J., Powell B. A., Wong J. C., Kersting A. B. and Zavarin M. (2015) Effect of Fulvic Acid Surface Coatings on Plutonium Sorption and Desorption Kinetics on Goethite. *Environ. Sci. Technol.* **49**, 2776–2785.
- Utsunomiya S., Ewing R. C., Novikov A. P., Kalmykov S. N., Horreard F., Merkulov A., Clark S. B., Myasoedov B. F. and Tkachev V. V. (2007) Colloid transport of plutonium in the far-field of the Mayak Production Association, Russia. *Abstr. Pap. Am. Chem. Soc.* **233**.
- Van der Veecken P. L. R., Chakraborty P. and Van Leeuwen H. P. (2010) Accumulation of Humic Acid in DET/DGT Gels. *Environ. Sci. Technol.* **44**, 4253–4257.
- Vockenhuber C., Alfimov V., Christi M., Lachner J., Schulze-Koenig T., Suter M. and Synal H.-A. (2013) The potential of He stripping in heavy ion AMS. *Nucl. Instrum. Methods Phys. Res. Sect. B-Beam Interact. Mater. At.* **294**, 382–386.
- Warnken K. W., Davison W., Zhang H., Galceran J. and Puy J. (2007) In situ measurements of metal complex exchange kinetics in freshwater. *Environ. Sci. Technol.* **41**, 3179–3185.
- Xu C., Athon M., Ho Y.-F., Chang H.-S., Zhang S., Kaplan D. I., Schwehr K. A., DiDonato N., Hatcher P. G. and Santschi P. H. (2014) Plutonium Immobilization and Remobilization by Soil Mineral and Organic Matter in the Far-Field of the Savannah River Site, US. *Environ. Sci. Technol.* **48**, 3186–3195.



## Conclusions and prospects

The purpose of this doctoral thesis was to develop a DGT technique for bioavailability measurements of Pu and to apply this technique *in-situ* in order to measure the free and labile Pu fraction in natural freshwaters of the karst system of the Swiss Jura Mountains. We aimed to achieve several milestones: to determine the diffusion coefficients of Pu in the PAM gel; to calibrate the DGT technique for Pu bioavailability measurements in laboratory conditions; to apply the DGT technique for Pu speciation studies in natural fresh water environments; to determine the bio-uptake and bioaccumulation of Pu by aquatic plants and mosses; and, finally, to integrate the above findings in a model of the Pu speciation in karstic freshwater environments.

As a result of this project, the diffusion coefficients of Pu in the PAM gel determined in cell diffusion experiments appear for the first time in the scientific literature.  $D$  is a parameter necessary to interpret the data of DGT measurements, and can henceforth be used by environmental scientists in further studies. Earlier laboratory studies on Pu speciation and aqueous chemistry were typically carried out at high Pu concentrations and are not directly transferrable to environmental conditions. Numerous authors acknowledge the concentration-dependant behavior of Pu species in natural waters. In this study, we show that environmentally relevant concentrations can be used in laboratory experiments with Pu, using a specially fabricated diffusion cell, to provide experimental protocols for studies of molecular interactions of Pu species with humic and fulvic substances, as well as with natural colloids.

Earlier speciation studies on Pu, based essentially on thermodynamic calculations and modeling in function of several physico-chemical parameters (pH, Eh, water chemistry) were hardly correlated to field measurements, due to strong influence of local biogeochemical

characteristics on Pu speciation. Additionally, the concentration ratio approach, used to predict the bioavailability of Pu, suffers from a high variability of CR values, undermining the possibility to accurately predict the Pu biouptake from its bulk concentration. The findings of this thesis demonstrate that the DGT technique can be applied for *in-situ* Pu bioavailability measurements in freshwater environments, with Chelex resin as a binding phase. The DGT technique developed and tested within this project makes possible to overcome these shortcomings, since the DGT sampler continuously integrates the uptake of Pu from water in function of changing local physico-chemical parameters and, eventually, discharges varying in time. Finally, DGT measurements in the field are supported by laboratory experiments in controlled conditions, providing a tool for investigation of various working hypotheses in environmentally relevant conditions.

The occurrence of Pu in +V oxidation state in the form of highly soluble, uranyl-like  $[\text{PuO}_2^+(\text{CO}_3)_n]^{m-}$  complexes in carbonate-rich oxic waters has been suggested in earlier works. Although our measurements confirm the presence of Pu mainly as Pu (V) in the Venoge spring, it was not experimentally possible to separate the Pu (V) in the organic-rich Noiraigue water. Based on similar physico-chemical parameters, we suggest that a certain fraction of Pu (V) can also be found in this organic-rich water. Laboratory experiments with NOM extracted from Noiraigue water and Pu at environmentally relevant concentrations yielded a relatively high  $k_{dis}$  for Pu-NOM complexes, correlating with findings from field measurements. DGTs deployed in the Noiraigue Bied brook show that Pu complexes are labile and fully available for biouptake.

The outcome of this doctoral thesis paves the way for future applications of the DGT technique for bioavailability and speciation studies of Pu, and possible other transuranic actinides, in the aquatic environments. Large-surface DGT samplers, developed and tested in

freshwaters, enable for accumulation of Pu at ultra-trace environmental concentrations, sufficient for AMS measurements. Of particular interest is the application of the DGT technique for continuous monitoring of Pu in seawater and in contaminated areas, such as the bay adjacent to the damaged Fukushima Daiichi nuclear power plant, and nearby La Hague or Sellafield nuclear reprocessing plants. Some of these areas (La Hague, Sellafield) are contaminated with quite high amounts of Pu, however, as discussed earlier, the bulk concentration is not indicative of bioavailability and cannot provide exhaustive information on potential radiological and exposure risks. On the other hand, some areas are susceptible to receive discrete inputs of Pu from accidental leakages (Fukushima) or re-suspended sediments (Irish Sea). Such inputs can be looked over with grab sampling, while DGTs provide a continuous integrated record, accumulating the Pu throughout deployment period. Similarly, the CR approach is not a reliable tool either, while the determination of CRs for each contaminated area would be laborious, expensive and time-consuming. DGTs serve as a rapid, simple and inexpensive tool to measure the bioavailable fraction of Pu *in-situ* in such areas, providing exhaustive information for assessment of radiological risks.

Experimental determination of CRs in a given aquatic ecosystem in parallel with DGT measurements would make possible to elucidate an empirical relationship between CRs and the measure of bioavailability, thus providing an improved approach for understanding the radionuclides transfer to living organisms. However, at this point of research, actinides which attract most of interest among radioactive contaminants have only been studied with DGTs in water, including our work on Pu. Actinides transfer from soil to terrestrial plants is an issue of greatest pertinence for contaminated areas, and the greatest variability of CRs is common for soil-to-plant radionuclides transfer. Measurement of actinides with DGTs in

soils and sediments can be a challenging task due to slower than in water mass transport to the sampler device and potentially long deployment time needed.

The capacity of the binding phase to efficiently bind contaminant species in a wide range of field conditions is of greatest importance for the specific application of the DGT technique. For instance, DGT devices with Chelex resin as binding phase deployed in carbonate-rich waters for Pu measurements in our field studies did not accumulate any U (data not shown). Yet the concentration of U in water was similar or even higher than that of Pu. This observation suggests that U is not bound to Chelex resin in carbonate-rich waters at pH in the range 6.5 – 7.5 and to provide accurate measurements a binding phase of another type is needed. Additionally, some daughter radionuclides produced in contaminated sites from decaying sources can have oxidation states different from their parent nuclides. Binding efficiencies of some ion-exchange resins are sensitive to the oxidation state of the metal ion and this issue should be taken into account when developing DGT devices for environmental surveillance applications. Use of ion-imprinted exchange resins or mineral phases ( $\text{MnO}_2$ ,  $\text{TiO}_2$ ) should be explored for applications as binding phases in DGTs.





## **Appendix**

## **Appendix 1: Supporting information for Chapter 1**

### **Extraction, desalting and characterisation of fulvic and humic acids from an organic**

#### **soil of an Alpine valley, Switzerland**

##### **Extraction**

10 g of soil was weighted in a flask obscured by an aluminium foil and 100 ml of degassed and Ar saturated 0.1 M NaOH solution was added. The flask was closed tight under Ar and the mixture was agitated for 4 hours. After centrifugation during ½ h at 3000 r/ min, the supernatant was filtered at 0.45 µm and acidified to pH 1 with concentrated HCl. The solution was left overnight at 4°C in the refrigerator and then centrifuged during ½ h at 3000 r/min. The supernatant contains the fulvic acid (FA) fraction, while the precipitate contains the humic acid (HA) fraction. This fraction was shaken once again in 100 ml ultrapure water and centrifuged as before.

##### **Desalting**

**Fulvic acid:** the FA fraction was pumped on a DAX-Supelite column (Omnifit of 10 ml; d=1 cm ; h= 10 cm, 1ml/min). FA was extracted on the head of the column. The column was washed with water (about 20 ml), controlling from time to time with an AgNO<sub>3</sub> test the presence of chloride. The washing was stopped as soon as the formation of an AgCl precipitate stopped. The column is then turned bottom-top and the FA was back-extracted using 20 ml of 0.1 M NaOH. The NaOH solution was pumped on a Dowex AG50w-x8 (Bio-Rad 30 ml; d=1.5 cm; h=14.5cm, H<sup>+</sup> form, 1ml/min). From time to time, the pH was checked for acidity, meaning that cations are extracted on the column. The column was then washed with 3 x 10 ml of water. All the fractions were collected, freeze-dried, and kept in the refrigerator at 4°C until used.

**Humic acid:** the precipitated HA fraction was dissolved in a minimum of an Ar degassed 0.1 M NaOH solution. This solution was pumped on a Dowex AG50w-x8 (Bio-Rad 30 ml; d=1.5 cm ; h=14.5cm, H<sup>+</sup> form, 1ml/min). From time to time, the pH was checked for acidity, meaning that cations are extracted on the column. The column was then washed with 3 x 10 ml of water. All the fractions were collected, freeze-dried, and kept in the refrigerator at 4°C until used.

### **Characterization**

**Size exclusion chromatography:** 1 mg of fulvic or humic acid was dissolved in 1 ml of 5 mM Na<sub>2</sub>B<sub>4</sub>O<sub>7</sub> (5 mM and 0.5 mM Na<sub>4</sub>P<sub>2</sub>O<sub>7</sub> in 25 mM Tris buffer at pH 8.3. The solution was loaded in a 1 m column (internal diameter of 0.5 cm) of Sephadex gel and the organic matter eluted with the same buffer. The output of the column was connected to a quartz Suprasil continuous flow UV-VIS cuvette inserted in a spectrometer with a wavelength fixed at 254 nm. Chromatograms were calibrated for size with polystyrene standards between 3000 and 40'000 Da. Results of the size exclusion experiments are presented in Figure S1.

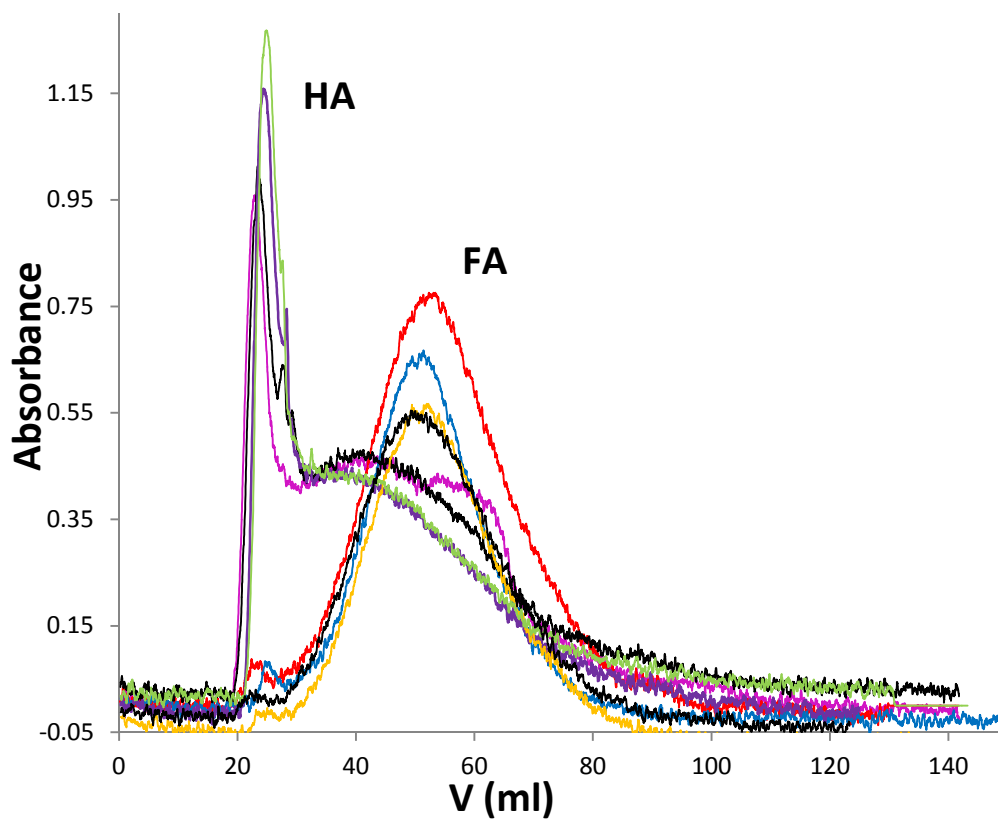


**Figure S1.** Size exclusion chromatography of the HA and FA fractions. The calibration by a 3500 Da shows a distribution centered on the 50 ml exclusion volume while the calibration by a 40'000 Da shows a distribution centered on a 20 ml exclusion volume.

### Plutonium activity determination

2 mL aliquots from the compartment B of the diffusion cell were collected throughout the experiment in 20 mL glass beakers and spiked with 1 mL  $^{242}\text{Pu}$  yield tracer (25 mBq). Samples were subjected to several cycles of wet ashing with 2 mL of concentrated  $\text{HNO}_3$  and 1 mL of concentrated  $\text{HClO}_4$  alternately on a hot plate at temperatures of 200°C-300°C. Finally, a white residue is obtained after ashing on the hot plate at 400°C. Plutonium was electrodeposited on a stainless steel disk from a  $\text{NaHSO}_4$ - $\text{Na}_2\text{SO}_4$  buffer solution according to Bajo *et al.*<sup>1</sup>. The disks were counted during 864'000 s in an Alpha Analyst spectrometer on PIPS detector (450 mm<sup>2</sup>) and analyzed with Apex Alpha software (Canberra, France).

Polyacrylamide diffusive gel discs retrieved from the diffusion cell were subjected to the same procedure of wet ashing and electrodeposition prior to Pu analysis.

Chelex resin gel discs retrieved from commercially available DGT devices were spiked with 1 mL of  $^{242}\text{Pu}$  yield tracer (25 mBq) and wet ashed by microwave digestion under pressure of 60 bars at 170°C in a Milestone MLS Ultraclave IV digester (MLS GmbH, Leutkirch, Germany) for 40 min in 20 mL of concentrated  $\text{HNO}_3$ . After filtration through a 25 mm Nalgene-SFCA membrane, plutonium was electrodeposited from a  $\text{NaHSO}_4$ - $\text{Na}_2\text{SO}_4$  buffer solution according to Bajo *et al.*<sup>1</sup> and analyzed as previously described.

## Natural water sampling

The Noiraigue Bied brook is located in the Vallée-des-Ponts of the Swiss Jura Mountains. The complex watershed of the valley is formed by densely drained peat bogs and a river (Grand Bied), which collects atmospheric waters from the catchment and flows into the karstic sinkhole, giving the Noiraigue spring about 400 m down the stream. Waters gathered from the organic-rich agricultural soils and peat bogs are enriched in humic substances and humics-complexed Fe-Ca colloids. Detailed study on natural colloids in the Noiraigue Bied Brook is given by Mavrocordatos *et al.*<sup>2</sup>. The main physico-chemical parameters were measured in our sampling campaign and are shown in Table S1.

Waters collected from a karstic catchment area situated at the altitude between 700-1400 m in the Swiss Jura Mountains about 20 km north-western from Lausanne give rise to Venoge spring, located at L'Isle. The spring is characterized by nivo-pluvial regime with the highest flow rate around April and lower water levels in the period between June and October. We sampled water from a perennial vaclusian spring (Le Chaudron), with flow rates varying from 0.01 m<sup>3</sup>/s in dry period up to 7.5 m<sup>3</sup>/s during flood events.<sup>3,4</sup> The karstic nature of the Venoge watershed determines the chemical composition of this carbonate-rich, mineralized water with low DOM content. Main physico-chemical parameters were measured in our sampling campaign and are shown in the Table S1.

**Table S1.** Main physico-chemical parameters of natural waters used in laboratory diffusion experiments with  $^{239}\text{Pu}$  (IV). pH, t°C and conductivity measured at the spot with universal pocket meter Multi 340i equipped with a standard conductivity cell TetraCon® 325.

Parameter	Noiraigue Bied brook	Venoge spring
Sampling date	03.12.2013	28.08.2013
pH	7.8	7.1
t°C	+0.7°C	+8°C
Conductivity ( $\mu\text{S}/\text{cm}$ )	560	370
Mg (ppm)	6.0	5.4
Ca (ppm)	104.9	75.5
K (ppm)	1.3	0.3
Cl (ppm)	9.4	3.2
NO <sub>3</sub> (ppm)	4.2	5.7
SO <sub>4</sub> (ppm)	6.3	4.7
DOM (ppm)	13.3	1.0

### Natural water ultrafiltration

Raw waters sampled at the Venoge spring and Noiraigue Bied brook were subjected to ultrafiltration through an 8 kDa Millipore Pellicon XL polyethersulphone membrane (surface area 50 cm<sup>2</sup>) to reach the concentration factor (*cf*) of 5. Retentate flow rate was 30 mL/min and permeate flow rate was 5 mL/min. Retentate fractions were then spiked with  $^{239}\text{Pu}$  (IV) and used in diffusion experiments as described above.

### Stability of the diffusing solutions

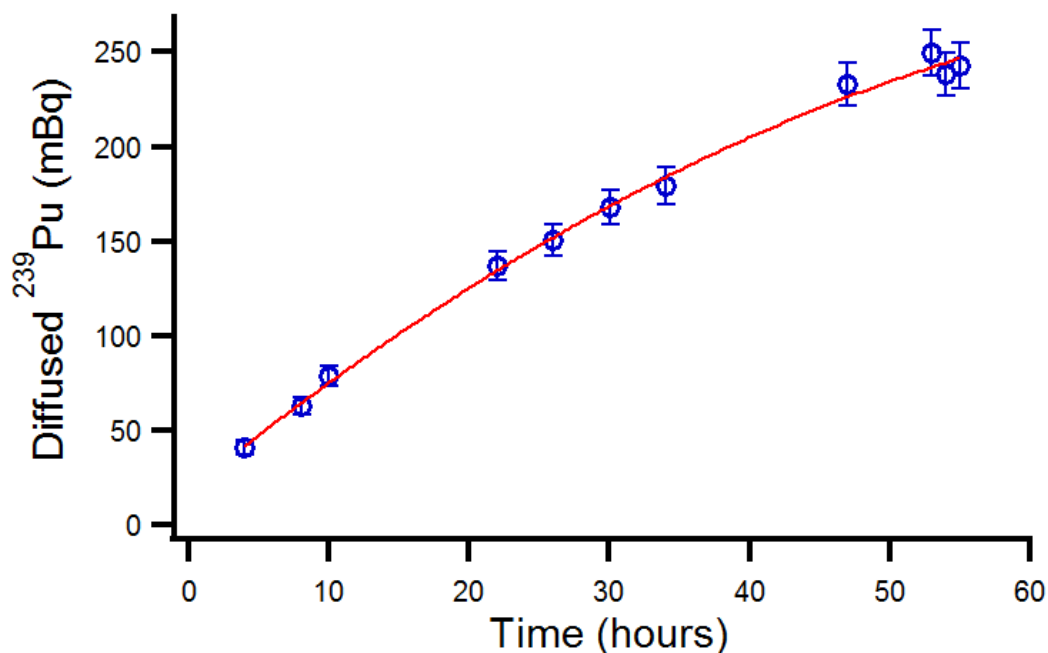


**Figure S2.** <sup>239</sup>Pu (IV) accumulation in the compartment B of the diffusion cell in the timeframe of 55 hours. Compartment A initially contained 964.47 mBq of <sup>239</sup>Pu (IV) and 242.62 mBq of <sup>239</sup>Pu (IV) were diffused into the compartment B (25 %) after 55 hours. While the first three points follow a linear function, further points throughout the duration of the experiment deviate from linearity and acquire the shape of a typical diffusion function with an important contribution of back diffusion. Diffusion coefficient calculated with the first three points is  $2.13 \times 10^{-6} \text{ cm}^2 \text{ s}^{-1}$ . The diffusion experiment was performed in 50 mM Tris buffered solution at pH 5.50 with 0.39 mm PAM gel at room temperature. In these conditions, no adsorption of plutonium onto the cell walls was observed ( $C/C_0=0.95-1.03$ ).



### DGTs in a glass beaker

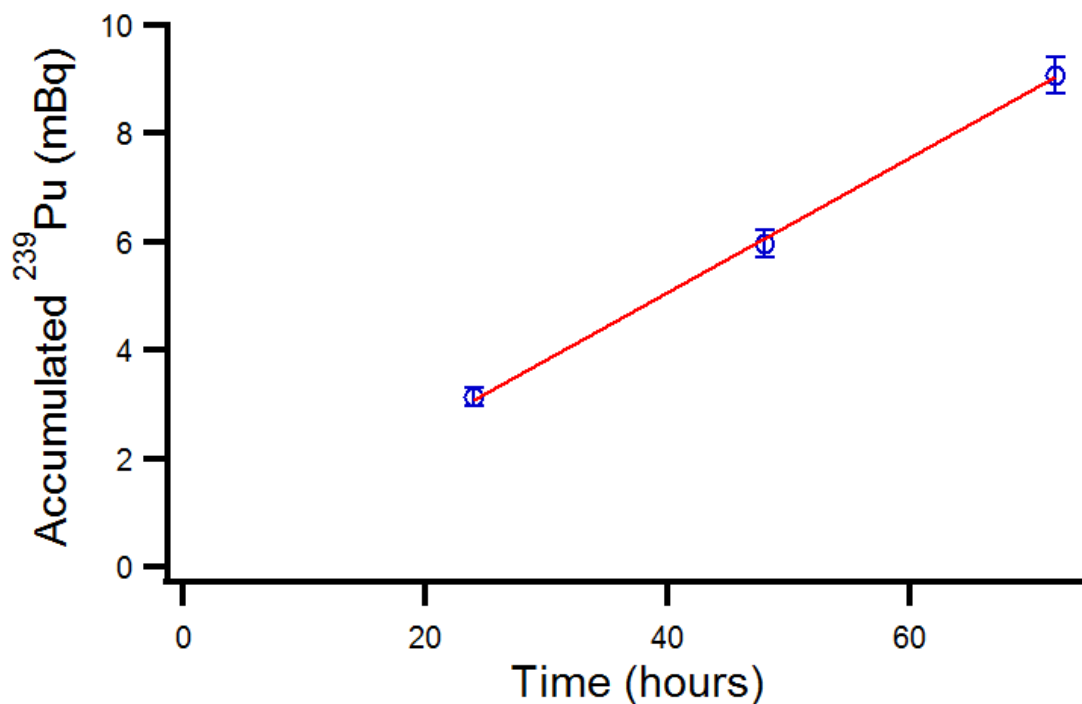


**Figure S3.** DGT uptake of <sup>239</sup>Pu (IV) from laboratory solution of 0.44 mBq/mL concentration. DGT samplers with 0.39 mm diffusive gel thickness and Chelex resin gel as binding phase were deployed in the 5 L glass beaker. Straight line represents linear uptake of <sup>239</sup>Pu (IV) in time, however, accumulated activities is much lower than expected, evoking problem of <sup>239</sup>Pu (IV) adsorption on the glass labware ( $C/C_0=0.70$ ).

**Details on experimental conditions for <sup>239</sup>Pu (IV) diffusion coefficient determination**

**Table S2.** Diffusion coefficient measurements of <sup>239</sup>Pu (IV) in the PAM gel. Experiments carried out in the two-compartment diffusion cell with single gel thickness of 0.39 mm in solutions of different composition. DGT devices deployed in 5 L standardized solution.

Experimental conditions	pH	T, °C	C <sub>0</sub> , mBq/mL	Sampling interval, min	D, ×10 <sup>-6</sup> cm <sup>2</sup> s <sup>-1</sup>
10 mM Tris/10 mM NaNO <sub>3</sub>	7.25	24	103.81	10	2.06±0.15
10 mM MOPS/10 mM Na <sub>2</sub> SO <sub>4</sub>	6.50	25	113.55	10	2.29±0.15
10 mM MOPS/10 mM Na <sub>2</sub> SO <sub>4</sub>	6.50	22	124.00	10	2.02±0.15 <sup>a)</sup>
10 mM MOPS/10 mM Na <sub>2</sub> SO <sub>4</sub>	6.50	25	247.26	10	2.06±0.13 <sup>b)</sup>
10 mM MOPS/20 mM Na <sub>2</sub> SO <sub>4</sub> / 20 ppm FA	7.00	23	125.00	240	2.03±0.19
10 mM MOPS/20 mM Na <sub>2</sub> SO <sub>4</sub> / 20 ppm HA	6.80	22	126.88	720	0.50±0.03 <sup>c)</sup>
10 mM MOPS / 10 mM Na <sub>2</sub> SO <sub>4</sub> / Venoge spring bulk water	7.00	25	135.48	10	1.89±0.11
10 mM MOPS / 10 mM Na <sub>2</sub> SO <sub>4</sub> / Venoge spring retentate	7.00	23	105.02	10	1.60±0.21
10 mM MOPS / 10 mM Na <sub>2</sub> SO <sub>4</sub> / Noiraigue Bied brook bulk	7.00	22	120	10	1.38±0.12
10 mM MOPS / 10 mM Na <sub>2</sub> SO <sub>4</sub> / Noiraigue Bied brook retentate	7.00	22	120	10	1.10±0.10
0.39 mm DGTs / 10 mM MOPS / 10 mM NaNO <sub>3</sub> / glass beaker	7.00	22	0.44	1440	1.33±0.10
0.78 mm DGTs / 10 mM MOPS / 10 mM NaNO <sub>3</sub> / plastic beaker	6.50	28	0.43	1440	2.45±0.30

<sup>a)</sup> Diffusion experiment carried out in a glove box in the nitrogen atmosphere

<sup>b)</sup> Diffusion experiment carried out with <sup>238</sup>Pu (IV)

<sup>c)</sup> Diffusion coefficient of <sup>239</sup>Pu (IV) in presence of 20 ppm HA was calculated with the first three points lying in the linear domain.

## References

1. Bajo, S.; Eikenberg, J., Electrodeposition of actinides for alpha-spectrometry. *Journal of Radioanalytical and Nuclear Chemistry* **1999**, *242*, (3), 745-751.
2. Mavrocordatos, D.; Mondy-Couture, C.; Atteia, O.; Leppard, G. G.; Perret, D., Formation of a distinct class of Fe-Ca(-C-org)-rich particles in a complex peat-karst system. *Journal of Hydrology* **2000**, *237*, (3-4), 234-247.
3. Franca, M. J.; Ferreira, R. M. L.; Lemmin, U., Parameterization of the logarithmic layer of double-averaged streamwise velocity profiles in gravel-bed river flows. *Advances in Water Resources* **2008**, *31*, (6), 915-925.
4. Trevisan, D.; Quetin, P.; Barbet, D.; Dorioz, J. M., POPEYE: A river-load oriented model to evaluate the efficiency of environmental policy measures for reducing phosphorus losses. *Journal of Hydrology* **2012**, *450*, 254-266.

## Appendix 2: Supporting information for Chapter 2

### Materials List for:

## Speciation and Bioavailability Measurements of Environmental Plutonium Using Diffusion in Thin Films

Ruslan Cusnir<sup>1</sup>, Philipp Steinmann<sup>2</sup>, Marcus Christl<sup>3</sup>, François Bochud<sup>1</sup>, Pascal Froidevaux<sup>1</sup>

<sup>1</sup>Institute of Radiation Physics, Lausanne University Hospital

<sup>2</sup>Federal Office of Public Health, Bern, Switzerland

<sup>3</sup>Laboratory of Ion Beam Physics, ETH Zurich

Correspondence to: Pascal Froidevaux at [Pascal.Froidevaux@chuv.ch](mailto:Pascal.Froidevaux@chuv.ch)

URL: <http://www.jove.com/video/53188>

DOI: [doi:10.3791/53188](https://doi.org/10.3791/53188)

### Materials

Name	Company	Catalog Number	Comments
<sup>239</sup> Pu tracer	CEA		Source PU239-ELSC10
<sup>242</sup> Pu tracer	LNSIRR		Source Pu242 N° 790 from Laboratory for National Standards of Ionizing Radiation of Russia
25 ml Beakers			
Pipette	Socorex		
Disposable plastic pipettes	Semadeni		
20 ml Plastic scintillation vial	Semadeni		
Aluminium foil			
Hot plate			
Tweezers			
Actinide exchange resin - TEVA - B	Triskem	TE-B50-A	
Actinide exchange resin - TEVA - R cartridges	Triskem	TE-R10-S	
1 ml Pipette tips	Socorex		
PAM gel strip 6×21 cm	DGT Research Ltd		0.39 mm and 0.78 mm thickness / <a href="http://www.dgtresearch.com">www.dgtresearch.com</a>
Chelex gel strip 6×21 cm	DGT Research Ltd		0.40 mm thickness / <a href="http://www.dgtresearch.com">www.dgtresearch.com</a>
Diffusion cell			Fabricated / in-house workshop
Ø 27 mm Punch			Fabricated / in-house workshop
Plastic tray			
DGT set-up			Fabricated / in-house workshop
Membrane filter	PALL Corporation		HT-450 Tuffryn Polysulfone Membrane Disc Filter 0.45 µm / 145 µm thickness
Nitric acid	Carlo Erba	408025	
Sulfuric acid	Sigma-Aldrich	84720	
Hydrochloric acid	Carlo Erba	403981	
Hydriodic acid	Merck	100341	
Potassium permanganate	Merck	105082	
Sodium hydrogen sulfate	Merck	106352	
Sodium sulfate	Merck	106647	
Sodium nitrate	Sigma-Aldrich	31440	

Sodium nitrite	Fluka	71759	
Sodium acetate	Merck	106281	
Ammonium oxalate	Fluka	9900	
Bis-(2-ethyl hexyl) phosphoric acid (HDEHP)	Merck	177092	
2-thenyltrifluoroacetone (TTA)	Fluka	88300	
MOPS buffer	Sigma-Aldrich	M9381	MOPS sodium salt
Cyclohexane	Carlo Erba		
Humic acid			Extracted from an organic-rich soil of an Alpine Valley, freeze-dried, MW 5-40 kDa
NH <sub>4</sub> OH	Carlo Erba	419943	
FeCl <sub>3</sub> · H <sub>2</sub> O	Sigma-Aldrich	44944	

## **Appendix 3: Supporting information for Chapter 3**

### **Extraction, desalting and characterisation of naturally occurring organic matter**

#### **(NOM) from an organic-rich water of a brook of the Swiss Jura Mountains**

##### **Extraction**

The water was sampled at the Noiraigue Bied brook of the Swiss Jura Mountains and filtered through a 0.5 µm Milligard® cartridge filter at the spot. 15 L of water were adjusted to pH 2.0 with 5 M HCl and pumped on a DAX-Supelite column at 1 mL min<sup>-1</sup> flow rate (Omnifit of 10 mL; d = 1 cm; h = 10 cm; 1 mL min<sup>-1</sup>). NOM was extracted on the head of the column.

##### **Desalting**

The column was washed with water (about 20 mL), controlling from time to time with an AgNO<sub>3</sub> test the presence of chloride. The washing was stopped as soon as the formation of an AgCl precipitate stopped. The column is then turned bottom-top and the NOM was back-extracted using 20 mL of 0.1 M NaOH. The NaOH solution was pumped on a Dowex AG50w-x8 (Bio-Rad 30 mL; d = 1.5 cm; h = 14.5cm, H<sup>+</sup> form, 1 mL min<sup>-1</sup>). From time to time, the pH was checked for acidity, meaning that cations are extracted on the column. The column was then washed with 3 x 10 mL of water. All the fractions were collected, freeze-dried, and kept in the refrigerator at 4 °C until used.

##### **Characterization**

**Size exclusion chromatography:** 5 mg of freeze-dried NOM were dissolved in 1 mL of 5 mM Na<sub>2</sub>B<sub>4</sub>O<sub>7</sub> (5 mM and 0.5 mM Na<sub>4</sub>P<sub>2</sub>O<sub>7</sub> in 25 mM Tris buffer at pH 8.3). The solution was loaded on a 1 m column (internal diameter of 0.5 cm) of Sephadex gel and the organic matter eluted with the same buffer. The output of the column was connected to a quartz Suprasil continuous flow UV-VIS cuvette inserted in a spectrophotometer with a wavelength

fixed at 254 nm. Chromatograms were calibrated for size with polystyrene standards of 3.5 kDa and 40 kDa. Results of the size exclusion experiments are presented in Figure SI 1.

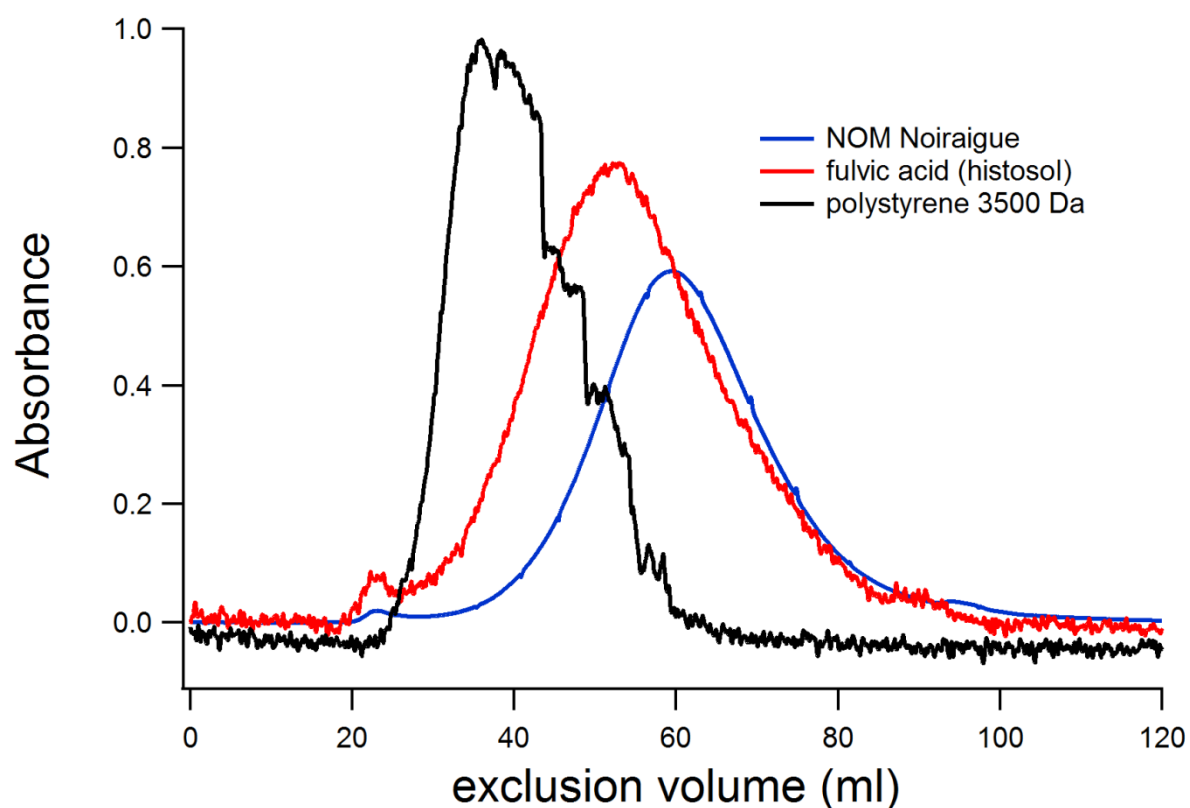


**Figure SI 1.** Size exclusion chromatography of the NOM extracted from the organic-rich natural water.

#### **Preparation of the Pu(V) standard solution**

Briefly, an aliquot of Pu was evaporated in a glass vial, the dry residue dissolved in 0.5 mL of 0.1 M CH<sub>3</sub>COONa at pH 4.7. The vial was wrapped with aluminum foil to protect from light. 0.05 mL of 0.01 M KMnO<sub>4</sub> was then added to oxidize the Pu overnight. 2.5 mL of 0.1 M CH<sub>3</sub>COONa at pH 4.7 and 2.5 mL of freshly prepared 0.5 M 2-thenoyltrifluoroacetone (TTA) in cyclohexane were then added to the solution. The mixture was agitated in the dark for 5 min to extract Pu (IV) and Pu (VI) into the organic phase. The water phase containing Pu (V) was then separated and Pu was measured in an aliquot by liquid scintillation counting in a Wallac 1220 Quantulus (PerkinElmer) ultralow level liquid scintillation (LSC) spectrometer.

We found about 80 % of the total Pu in the water phase following this extraction. Different authors acknowledge the relative stability of Pu (V) solutions up to several months.<sup>1,2</sup> Nevertheless, we used fresh Pu (V) tracer prepared shortly prior to each diffusion experiment.

### **Plutonium activity determination**

2 mL aliquots from the compartment B of the diffusion cell were collected throughout the experiment in 20 mL glass beakers and spiked with 1 mL <sup>242</sup>Pu yield tracer (25 mBq). Samples were subjected to several cycles of wet ashing with 2 mL of concentrated HNO<sub>3</sub> on a hot plate at temperatures of 200°C-300°C. Finally, a dry residue is obtained after ashing on the hot plate at 400°C. The residue was dissolved in 5 mL of 8 M HNO<sub>3</sub>, 20 mg of NaNO<sub>2</sub> were added and the solution was heated at 70 °C for 10 min. Plutonium was extracted on a quaternary amine-based anion exchange resin (TEVA) column, preconditioned with 8 M HNO<sub>3</sub>. After washing the column with 8 M HNO<sub>3</sub> and 9 M HCl, plutonium was eluted with 9 M HCl/0.1 M HI. The samples were evaporated on the hot plate with few mL of concentrated HNO<sub>3</sub> until the brown iodine color disappeared. Plutonium was electrodeposited on a stainless steel disk from a NaHSO<sub>4</sub>-Na<sub>2</sub>SO<sub>4</sub> buffer solution according to Bajo *et al.*<sup>1</sup>. The disks were counted during 864'000 s in an Alpha Analyst spectrometer on PIPS detector (450 mm<sup>2</sup>) and analyzed with Apex Alpha software (Canberra, France).

Polyacrylamide diffusive gel discs retrieved from the diffusion cell were subjected to the same procedure of wet ashing, radiochemical separation and electrodeposition prior to Pu analysis.

<sup>239</sup>Pu (V) aliquots of water phase after liquid phase extraction of <sup>239</sup>Pu (IV) with HDEHP were thoroughly mixed with Ultima Gold™ AB liquid scintillation cocktail to the final volume of 20



mL in a scintillation vial.  $^{239}\text{Pu}$  was measured by liquid scintillation counting in a PerkinElmer ultralow level liquid scintillation spectrometer Wallac 1220 Quantulus.

Chelex resin gel discs retrieved from commercially available DGT devices were spiked with 1 mL of  $^{242}\text{Pu}$  yield tracer (25 mBq) and wet ashed by microwave digestion under pressure of 60 bars at 170°C in a Milestone MLS Ultraclave IV digester (MLS GmbH, Leutkirch, Germany) for 40 min in 20 mL of concentrated  $\text{HNO}_3$ . After filtration through a 25 mm Nalgene-SFCA membrane, plutonium was extracted on TEVA resin, eluted and electrodeposited from a  $\text{NaHSO}_4$ - $\text{Na}_2\text{SO}_4$  buffer solution according to Bajo *et al.* and analyzed as previously described.

### **Natural water sampling**

The Noiraigue Bied brook is located in the Vallée-des-Ponts of the Swiss Jura Mountains. The complex watershed of the valley is formed by densely drained peat bogs and a river (Grand Bied), which collects atmospheric waters from the catchment and flows into the karstic sinkhole, giving the Noiraigue spring about 400 m down the stream. Waters gathered from the organic-rich agricultural soils and peat bogs are enriched in humic substances and humics-complexed Fe-Ca colloids. Detailed study on natural colloids in the Noiraigue Bied Brook is given by Mavrocordatos *et al.* The main physico-chemical parameters were measured in our sampling campaign and are shown in Table SI 1.

**Table SI 1.** Main physico-chemical parameters of the natural water sampled on the 26.05.2014 at the Noiraigue Bied brook and used for extraction of the NOM. pH, t °C and conductivity measured on-the-spot with universal pocket meter Multi 340i equipped with a standard conductivity cell TetraCon® 325.

---

pH	7.4
t°C	+9.5°C
Conductivity (µS/cm)	469
Mg (ppm)	6.0
Ca (ppm)	105.0
K (ppm)	1.3
Cl (ppm)	9.0
NO <sub>3</sub> (ppm)	4.5
SO <sub>4</sub> (ppm)	6.5
DOM (ppm)	13.2

---

### Diffusion coefficients of Pu (V) in the PAM gel

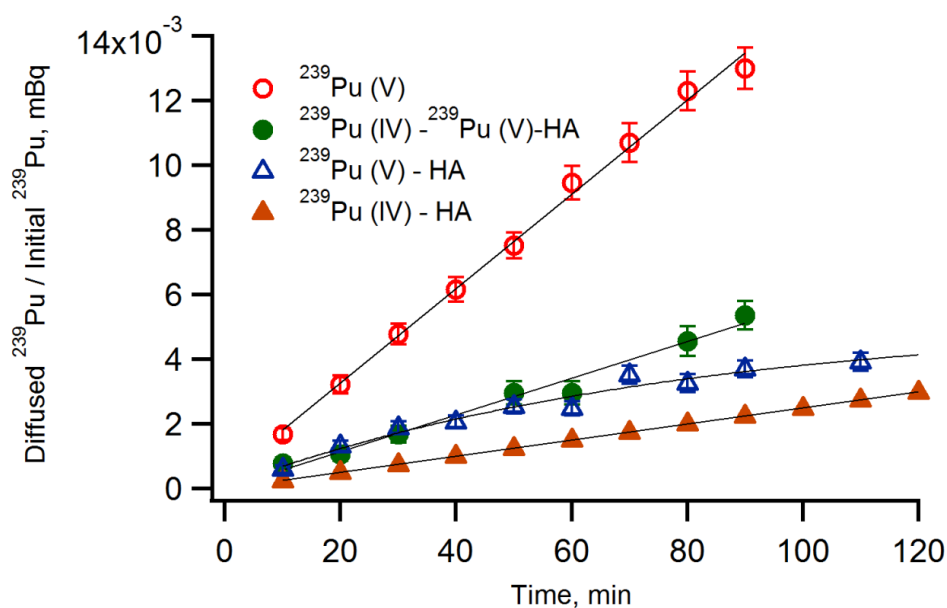


**Figure SI 2.** Plot of normalized activities (mBq) of Pu diffused into the initially zero concentration compartment B of the diffusion cell as a function of time. Experimental data plots are given for Pu (V) in the MOPS buffered solution (red open circle), for a mixed Pu (IV)-Pu (V) model solution containing  $31 \pm 10\%$  of Pu (V) in the presence of 20 ppm of HA (green full circle) and Pu (V) in the presence of 20 ppm of HA (blue open triangle). The line shown for Pu (IV)-HA has been simulated using a diffusion coefficient of  $0.50 \times 10^{-6} \text{ cm}^2 \text{ s}^{-1}$  as determined previously.<sup>3</sup>

The concentration of Pu determined in the PAM gel discs retrieved at the end of each diffusion experiment did not exceed 50 % of the Pu concentration in the initial (A compartment) solution. In experiments with 20 ppm of HA the Pu concentration in the PAM gel disc was 80 % of the initial Pu concentration. This indicates that there was no significant Pu-HA accumulation within the PAM gel during the time frame of the diffusion experiment (90-130 min).<sup>3</sup>

### Kinetics of $^{239}\text{Pu}$ (V) reduction by HA

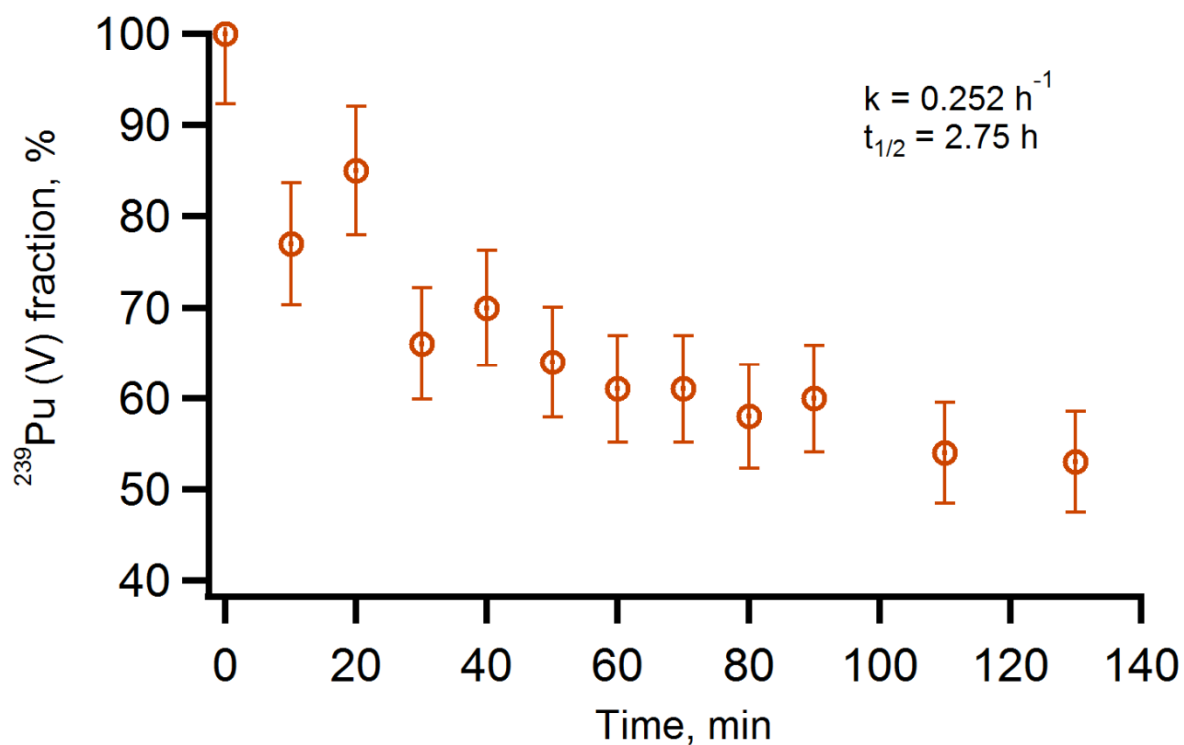


**Figure SI 3.** Kinetics of  $^{239}\text{Pu}$  (V) reduction in presence of 20 ppm of HA studied in the A compartment of the diffusion cell at pH 6.5 and initial  $^{239}\text{Pu}$  (V) concentration  $2.8 \times 10^{-10}$  M. The reduction follows a first-order kinetics with  $k = 0.252 \text{ h}^{-1}$  and  $t_{1/2} = 2.75 \text{ h}$ . Uncertainties on  $^{239}\text{Pu}$  (V) concentration were calculated by a quadratic summation of relative uncertainty on the number of counts for  $^{239}\text{Pu}$ .

### Details of experimental conditions for $^{239}\text{Pu}$ (V) diffusion coefficient determination

**Table SI 2.** Diffusion coefficient measurements of  $^{239}\text{Pu}$  (V) in the PAM gel. Experiments carried out in the two-compartment diffusion cell with single gel thickness of 0.39 mm in the 10 mM MOPS buffered solution and in presence of 20 ppm of HA.

Experimental conditions	pH	t °C	$C_0$ mBq mL <sup>-1</sup>	Sampling interval, min	$D \times 10^{-6}$ cm <sup>2</sup> s <sup>-1</sup>
10 mM MOPS/10 mM Na <sub>2</sub> SO <sub>4</sub> $^{239}\text{Pu}$ (V) 80±10 %	5.5	24	42.60	10	3.38±0.34
10 mM MOPS/10 mM NaNO <sub>3</sub> $^{239}\text{Pu}$ (V) 79±10 %	5.5	24	74.40	10	3.49±0.35
10 mM MOPS/10 mM NaNO <sub>3</sub> $^{239}\text{Pu}$ (V) 87±10 %	6.5	20	157.70	10	2.98±0.17 <sup>a)</sup>
10 mM MOPS/10 mM NaNO <sub>3</sub> / 20 ppm HA/ $^{239}\text{Pu}$ (V) 35±10 % <sup>b)</sup>	5.5	24	65.10	10	0.92±0.07
10 mM MOPS / 10 mM NaNO <sub>3</sub> / 20 ppm HA/ $^{239}\text{Pu}$ (V) 97±10 % <sup>c)</sup>	6.5	20	152.60	10	1.33±0.12 <sup>d)</sup>

a) D recalculated for 24 °C is  $3.29 \times 10^{-6}$  cm<sup>2</sup> s<sup>-1</sup>.

b) The initial solution was equilibrated for 24 h to reach the steady state between  $^{239}\text{Pu}$  (V) and  $^{239}\text{Pu}$  (IV).

c) The solution was used in the experiment immediately after preparation. Reduction of  $^{239}\text{Pu}$  (V) by HA was studied in this experiment.

d) Diffusion coefficient of  $^{239}\text{Pu}$  (V) in presence of 20 ppm HA was calculated with the first three points lying in the linear domain. D recalculated for 24 °C is  $1.45 \times 10^{-6}$  cm<sup>2</sup> s<sup>-1</sup>.

### Diffusion of Pu (V) through PAM gel in a Pu (IV) – Pu (V) mixture

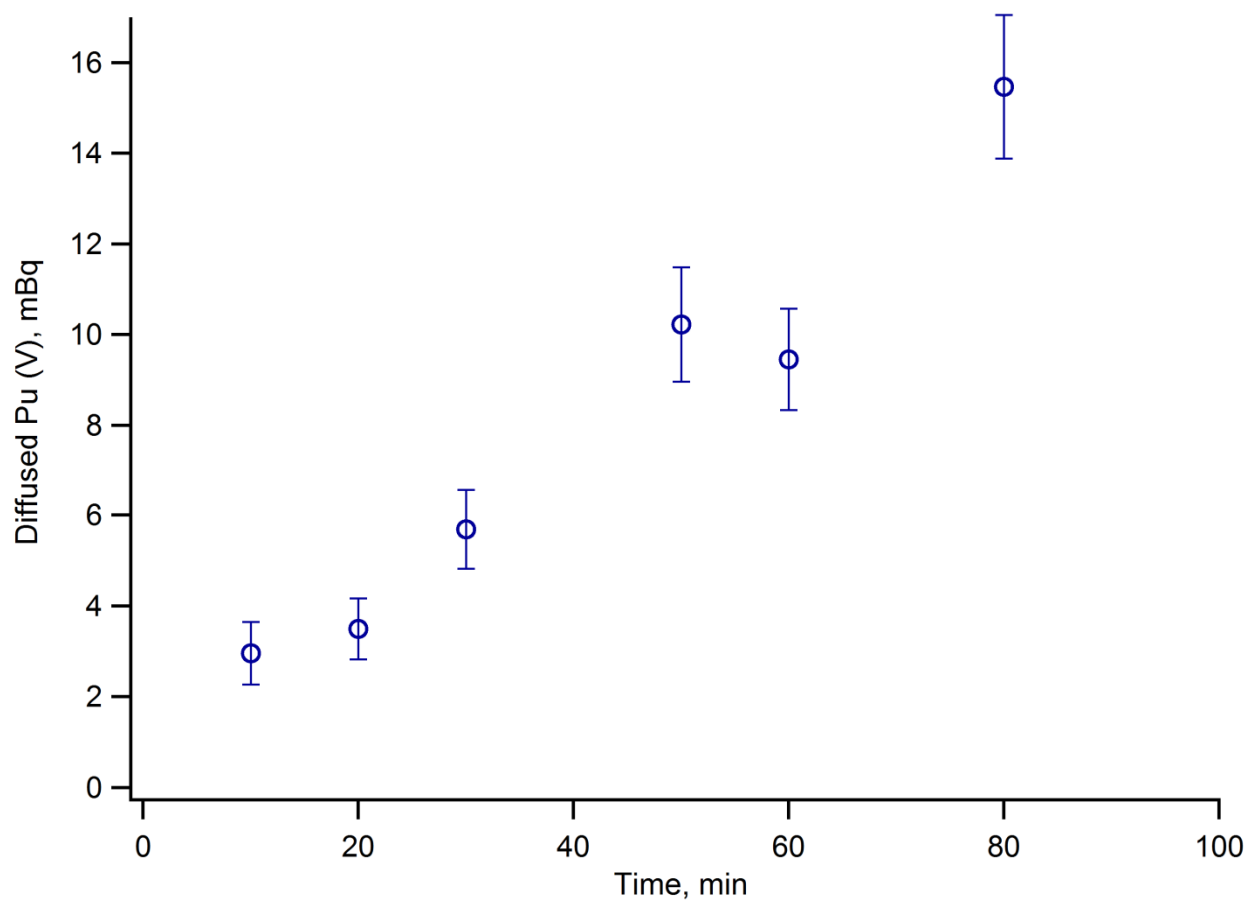


**Figure SI 3.** Plot of  $^{239}\text{Pu}$  (V) activities (mBq) diffusing into the B compartment of the diffusion cell in a  $^{239}\text{Pu}$  (IV)- $^{239}\text{Pu}$  (V)-HA mixture.  $^{239}\text{Pu}$  (V) diffused at any point of time determined by subtraction of  $^{239}\text{Pu}$  (IV)-HA contribution from the total  $^{239}\text{Pu}$  measured experimentally.

**Details of experimental conditions for ADBL measurements with  $^{238}\text{Pu}$  (IV) in presence of NOM**

**Table SI 3.** ADBL thickness measured for Pu (IV) and Co using DGT devices of 5 diffusive layer thicknesses.  $\delta$  (cm) calculated according to Warnken *et al.*<sup>4</sup>

Experimental conditions	pH	t °C	C <sub>0</sub> mBq mL <sup>-1</sup>	Deployment time, h	Pu-ADBL, cm	Co-ADBL, cm
10 mM MOPS/10 mM NaNO <sub>3</sub> Co <sup>2+</sup> 2 μg L <sup>-1</sup> / <sup>239</sup> Pu (IV)	7.0	22	0.44	53	0.06±0.005	0.05±0.006
10 mM MOPS/10 mM Na <sub>2</sub> SO <sub>4</sub> Co <sup>2+</sup> 4 μg L <sup>-1</sup> / <sup>238</sup> Pu (IV)	6.5	27	0.76	120	0.14±0.019	0.08±0.006
NOM 20 ppm 10 mM MOPS/10 mM Na <sub>2</sub> SO <sub>4</sub> <sup>238</sup> Pu (IV) / NOM 20 ppm	6.5	27	0.80	168	0.24±0.029	-
10 mM MOPS/10 mM Na <sub>2</sub> SO <sub>4</sub> <sup>238</sup> Pu (IV) / NOM 20 ppm	6.5	20	6.40	24	0.19±0.019	-

### Kinetic signature of Pu (IV)

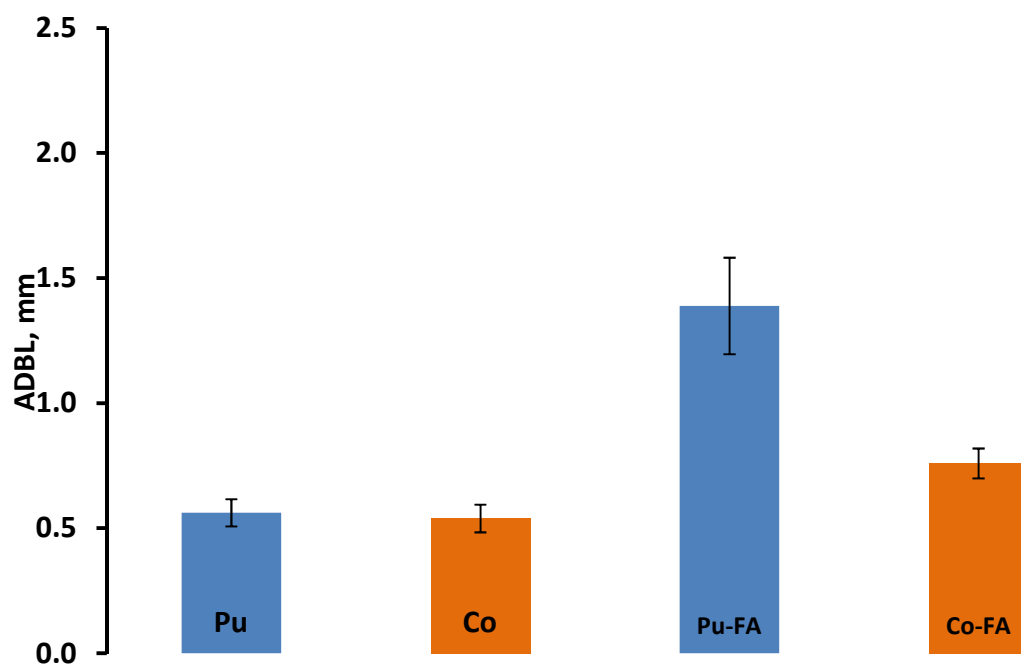


**Figure SI 4.** Kinetic signature of Pu (IV). ADBL in the experiment without FA for Pu ( $0.49 \pm 0.05$  mm) and Co ( $0.48 \pm 0.06$  mm) calculated using the plot given on Fig. 2-A. ADBL in the experiment with Pu ( $1.4 \pm 0.19$  mm) and Co ( $0.8 \pm 0.06$  mm) in presence of 20 ppm FA calculated using four first points of the linear domain of the plot given on Fig. 2-B.



## References

1. Blinova, O.; Novikov, A.; Perminova, I.; Goryachenkova, T.; Haire, R., Redox interactions of Pu(V) in solutions containing different humic substances. *Journal of Alloys and Compounds* **2007**, *444*, 486-490.
2. Saito, A.; Roberts, R. A.; Choppin, G. R., Preparation of solutions of tracer level plutonium (V). *Analytical Chemistry* **1985**, *57*, (1), 390-391.
3. Cusnir, R.; Steinmann, P.; Bochud, F.; Froidevaux, P., A DGT Technique for Plutonium Bioavailability Measurements. *Environmental Science & Technology* **2014**, *48*, (18), 10829-10834.
4. Warnken, K. W.; Davison, W.; Zhang, H.; Galceran, J.; Puy, J., In situ measurements of metal complex exchange kinetics in freshwater. *Environmental Science & Technology* **2007**, *41*, (9), 3179-3185.

## Appendix 4: Supporting information for Chapter 4

### Precipitations regime during field measurements campaigns

**Table SI 1. Precipitations data for the Venoge spring catchment basin.** Recorded at the station Bière (CH 1903), altitude 684 m asl, coordinates 515'889 / 153'207.

Month / Year	Sum monthly precipitations, mm	Sum/Norm monthly precipitations, %	Max of precipitations, mm
April / 2014	57.70	64	11.60
May / 2014	74.40	76	30.80
June / 2014	90.80	87	30.40
September / 2014	26.80		9.50
October / 2014	123.60		49.40
April / 2015	69.40	77	17.50
May / 2015	117.40	112	60.70
June / 2015	75.30	72	21.90
July / 2015	47.90		18.70

**Table SI 2. Precipitations data for the Noiraigue Bied brook catchment basin.** Recorded at the station Les Ponts-de-Martel (CH 1903), altitude 1052 m asl, coordinates 545'880 / 205'400.

Month / Year	Sum monthly precipitations, mm	Sum/Norm monthly precipitations, %	Max of precipitations, mm
April / 2014	113.00	100	37.70
May / 2014	155.80	111	47.70
June / 2014	104.20	82	48.80
September / 2014	82.70	68	14.30
October / 2014	109.00	85	15.50
April / 2015	122.20	108	30.70
May / 2015	128.00	91	46.80
June / 2015	140.80	110	43.40
July / 2015	75.30	59	27.80

## DGT deployments in the Venoge spring and Noiraigue Bied brook

DGTs were deployed in duplicates (0.39 mm x 2 and 0.78 mm x 2) by suspending in the karstic Venoge spring or by fixing on the vertical support on the brook's bed of the Noiraigue Bied.  $C_{DGT}$  ( $\mu\text{Bq L}^{-1}$ ) of  $^{239}\text{Pu}$  was calculated from the equation 1 (Cusnir et al., 2016):

$$\frac{1}{A} = \frac{1}{C_{DGT} S t} \left( \frac{\Delta g}{D_M^{gel}} + \frac{\delta}{D_M^w} \right) \quad (1),$$

where  $A$  is the activity ( $\mu\text{Bq}$ ) of Pu accumulated in the binding phase (converted from the Pu concentration (at  $\text{g}^{-1}$ ) measured by AMS),  $\Delta g$  the diffusion layer (gel + filter membrane) thickness (cm),  $D_M^{gel}$  the diffusion coefficient of Pu in the PAM gel ( $\text{cm}^2 \text{s}^{-1}$ , taken from Cusnir et al. (2014)),  $D_M^w$  the diffusion coefficient of Pu in water ( $D_M^w = D_M^{gel} / 0.85$ ),  $\delta$  the diffusive boundary layer (0.03 cm from Warnken et al., 2007),  $S$  the diffusion area ( $\text{cm}^2$ ), and  $t$  the duration of deployment (s). For calculation of  $C_{DGT}$  of Pu in the Venoge spring we used the  $D$  for Pu (V) (Cusnir et al., 2016), and for calculation of  $C_{DGT}$  of Pu in the Noiraigue Bied we used the  $D$  for Pu (IV), adjusted respectively to water temperature (Cusnir et al., 2015).

Data from 2014 field campaign show relatively high uncertainties on  $^{239}\text{Pu}$  measurements. Indeed, the isotopic ratio  $^{240}\text{Pu}/^{239}\text{Pu}$  measured with AMS for these samples was *circa* 0.02, due to a contamination of TEVA resin cartridges with a tiny amount of  $^{239}\text{Pu}$ . Nevertheless, the  $^{240}\text{Pu}$  results were unbiased and we were able to calculate the  $^{239}\text{Pu}$  content from the measured  $^{240}\text{Pu}$ , taking 0.18 as  $^{240}\text{Pu}/^{239}\text{Pu}$  isotopic ratio for fallout plutonium. Thereafter (2015 field campaign) we used the AG 1-X4 anion exchange resin (chloride form) from Bio-Rad Laboratories Inc., which shows no  $^{239}\text{Pu}$  contamination, to measure the  $^{239}\text{Pu}$  and to validate our previous data based on  $^{240}\text{Pu}$ .

**Table SI 3. DGT deployments in the Venoge spring.** Uncertainties on  $C_{DGT}$  were calculated

using a quadratic summation of relative uncertainty on each of the parameters. The

coverage factor was  $k = 1$ .

Deployment dates (from-to)	Precipitations sum, mm	DGT thickness, mm	$^{239}\text{Pu}$ average per DGT, $\mu\text{Bq}$	$C_{DGT}$ , $\mu\text{Bq L}^{-1}$	$C_{\text{bulk}}$ average for deployment period, $\mu\text{Bq L}^{-1}$
17.04.2014	45.2	0.39 (n=2)	5.95±3.19	1.81±1.96	1.90±0.55 (n=2)
01.05.2014		0.78 (n=2)	2.52±1.14	2.26±2.07	
17.09.2014	71.7	0.39 (n=2)	10.55±3.03	2.14±1.28	1.47±0.26 (n=2)
08.10.2014		0.78 (n=2)	8.11±1.98	2.45±1.29	
21.04.2015	159.8	0.39 (n=1)	5.17±1.40	1.00±0.57	1.51±0.11 (n=2)
13.05.2015		0.78 (n=1)	2.43±0.99	0.70±0.59	
08.06.2015	65.9	0.39 (n=2)	2.95±0.75	0.60±0.32	0.43±0.03 (n=1)
29.06.2015		0.78 (n=1)	2.09±0.43	0.63±0.29	

**Table SI 4. DGT deployments in the Noiraigue Bied brook.** Uncertainties on  $C_{DGT}$  were

calculated using a quadratic summation of relative uncertainty on each of the parameters.

The coverage factor was  $k = 1$ .

Deployment dates	Precipitations sum, mm	DGT thickness, mm	$^{239}\text{Pu}$ average per DGT, $\mu\text{Bq}$	$C_{DGT}$ , $\mu\text{Bq L}^{-1}$	$C_{\text{bulk}}$ average for deployment period, $\mu\text{Bq L}^{-1}$
06.06.2014 26.06.2014	63.8	0.39 (n=1)	2.01±1.19	0.61±0.72	
17.09.2014	68.5	0.39 (n=2)	9.67±2.03	2.79±1.30	3.27±0.65 (n=2)
08.10.2014		0.78 (n=2)	10.11±2.38	4.35±2.27	
10.06.2015	76.4	0.39 (n=2)	1.78±1.32	0.49±0.27	0.96±0.04 (n=2)
02.07.2015		0.78 (n=2)	2.62±0.85	1.07±0.73	

**Main physico-chemical characteristics of water in the Venoge spring and Noiraigue Bied brook**

**Table SI 5. Main physico-chemical characteristics of water measured in water in the Venoge spring and Noiraigue Bied brook during field campaign.**

Parameter	Noiraigue Bied brook	Venoge spring
pH	6.5-7.5	6.5-7.5
t °C	0 °C + 15 °C	+5 °C +7.5 °C
Conductivity ( $\mu\text{S cm}^{-1}$ )	495-589	321-585
Mg <sup>2+</sup> (ppm)	4-6	4-5
Ca <sup>2+</sup> (ppm)	80-105	75-110
K <sup>+</sup> (ppm)	1-3	0.5-2
Cl <sup>-</sup> (ppm)	5-9	3-4
NO <sub>3</sub> <sup>-</sup> (ppm)	4-6	4-5
SO <sub>4</sub> <sup>2-</sup> (ppm)	5-7	2-5
NOM (ppm)	10-18	0-1.0

## Sequential elution of Pu from aquatic mosses and plants

**Table SI 6. Distribution of  $^{239}\text{Pu}$  measured in different compartments of the aquatic moss**

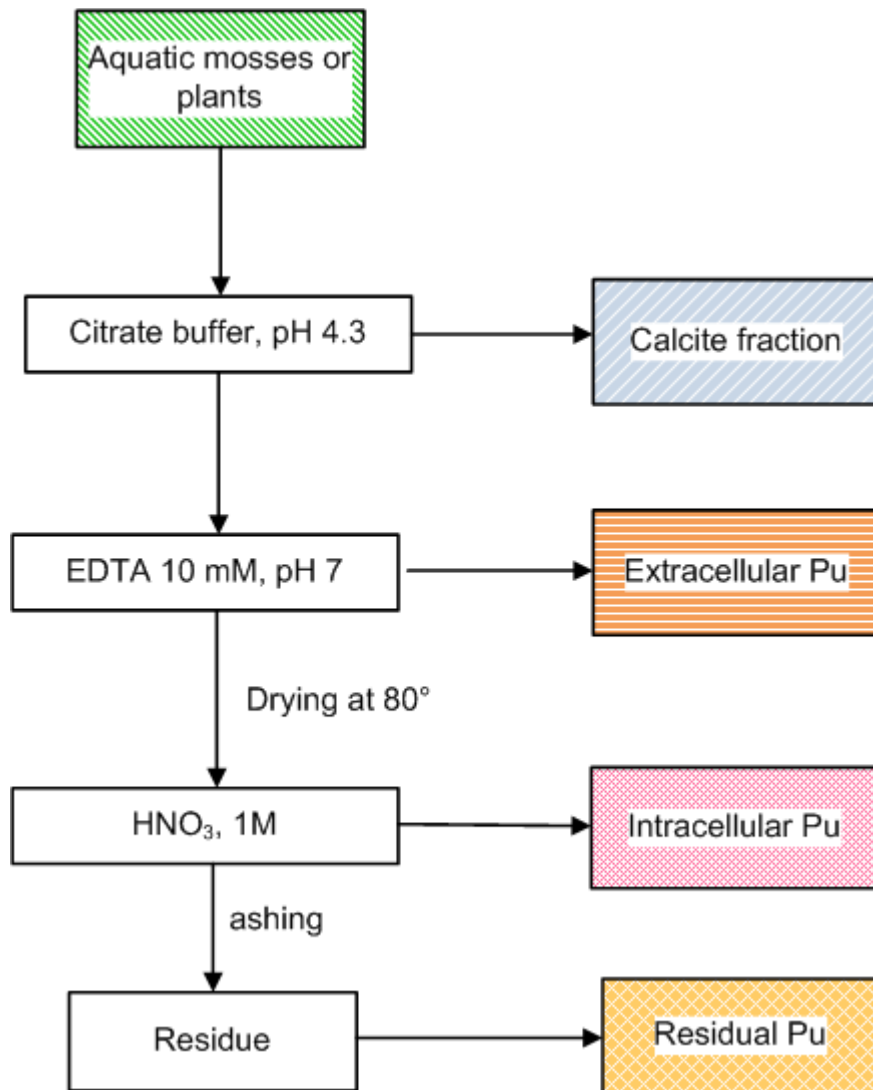
***Fontinalis antipyretica* in the Venoge spring.**

Fraction	$^{239}\text{Pu}$ , $\mu\text{Bq g}^{-1}$ fresh weight	
	Location 1	Location 2
Calcite (n=2)	3.53±0.09	17.82±0.40
Extracellular (n=2)	1.04±0.04	3.08±0.09
Intracellular (n=2)	0.48±0.05	1.32±0.55
Residual (n=2)	1.16±0.04	8.41±0.22
Sum of fractions	6.20±0.22	30.63±0.32
Bulk (n=2)	7.33±0.16	23.14±0.53

**Table SI 7. Distribution of  $^{239}\text{Pu}$  measured in different compartments of the aquatic plant**

***Phragmites australis* in the Noiraigue Bied brook.**

Fraction	$^{239}\text{Pu}$ , $\mu\text{Bq g}^{-1}$ fresh weight	
	Leaves	Roots
Calcite (n=2)	0.66±0.020	N/A
Extracellular (n=2)	0.12±0.007	1.04±0.031
Intracellular (n=2)	0.04±0.004	0.88±0.031
Residual (n=2)	0.06±0.016	1.04±0.103
Sum of fractions	0.87±0.047	2.95±0.165



**Scheme SI 1. Sequential elution of Pu from a sample of aquatic plants or mosses.** Pattern and color correspond to the fractions represented in Figure 3 of the main text.

## WHAM7 calculation of the chemical speciation of Pu in natural water

**Table SI 8. Chemical speciation of Pu in the Noiraigue Bied brook water calculated using**

**WHAM7.** Input parameters taken from table SI 5, initial concentration of Pu  $4.00 \times 10^{-18}$  M.

pH	CO <sub>3</sub> <sup>2-</sup> , mg L <sup>-1</sup>	FA, mg L <sup>-1</sup>	[Pu(IV)(CO <sub>3</sub> ) <sub>2</sub> ] <sup>0</sup> , %	Fraction bound to colloidal FA: Pu(IV), %
6.50	90	15	48	52
6.50	150	15	72	28
6.50	90	18	44	56
6.50	150	18	68	32
7.00	90	15	84	16
7.00	150	15	94	6
7.00	90	18	82	18
7.00	150	18	92	8

## References

Cusnir R., Jaccard M., Bailat C., Christl M., Steinmann P., Haldimann M., Bochud F. and Froidevaux P. (2016) Probing the Kinetic Parameters of Plutonium–Naturally Occurring Organic Matter Interactions in Freshwaters Using the Diffusive Gradients in Thin Films Technique. *Environ. Sci. Technol.* **50**, 5103–5110.

Cusnir R., Steinmann P., Bochud F. and Froidevaux P. (2014) A DGT Technique for Plutonium Bioavailability Measurements. *Environ. Sci. Technol.* **48**, 10829–10834.

Cusnir R., Steinmann P., Christl M., Bochud F. and Froidevaux P. (2015) Speciation and Bioavailability Measurements of Environmental Plutonium Using Diffusion in Thin Films. *J. Vis. Exp. JoVE*, e53188.

Warnken K. W., Davison W., Zhang H., Galceran J. and Puy J. (2007) In situ measurements of metal complex exchange kinetics in freshwater. *Environ. Sci. Technol.* **41**, 3179–3185.



## **Appendix 5 : Curriculum vitae**

**Ruslan Cusnir**

### **Informations personnelles**

Etat civil : célibataire

Date de naissance : 23.08.1987

Origine : Rîșcani, République de Moldavie

### **Formation**

- |                  |  |
|------------------|--|
| <b>2006-2010</b> | Bachelor en Chimie, spécialisation en chimie inorganique et chimie de coordination, à l'Université d'Etat de Moldavie                  |
| <b>2010-2012</b> | Master en Chimie, spécialisation en électrochimie, photochimie et chimie pharmacologique, à l'Ecole Polytechnique Fédérale de Lausanne |
| <b>2013-2016</b> | Thèse de doctorat ès Sciences de la vie, spécialisation en radioécologie, à l'Institut de Radiophysique à l'Université de Lausanne     |

## Appendix 6 : List of publications resulted from the thesis

### Original Articles in Peer-Reviewed Journals

**Cusnir R.**, Jaccard M., Bailat C., Christl M., Steinmann P., Haldimann M., Bochud F. and Froidevaux P. "Probing the kinetic Parameters of Pu-NOM interactions using the DGT technique". *Environmental Science and Technology* 2016, **50**, 5103-5110, DOI: 10.1021/acs.est.5b05435

**Cusnir R.**, Steinmann P., Christl M., Bochud F. and Froidevaux P. "Speciation and bioavailability measurements of environmental plutonium using diffusion in thin films". *Journal of Visualized Experiments* 2015, **105**, e53188, DOI: 10.3791/53188

**Cusnir R.**, Steinmann P., Bochud F. and Froidevaux P. "A DGT technique for plutonium bioavailability measurements". *Environmental Science and Technology* 2014, **48**, 10829-10834, DOI: 10.1021/es501149v

### Unpublished Articles

**Cusnir R.**, Christl M., Steinmann P., Bochud F. and Froidevaux P. „Plutonium is bioavailable in karstic freshwater environments“. Article **in preparation** for *Geochimica et Cosmochimica Acta*

### Conference Proceedings

**Cusnir R.**, P. Steinmann, F. Bochud and P. Froidevaux "Development of the DGT technique for *in-situ* Pu speciation measurements". Oral Presentation, 3<sup>rd</sup> International Conference on Radioecology and Environmental Radioactivity, Barcelona, Spain (September 2014)

**Cusnir R.**, P. Steinmann, F. Bochud and P. Froidevaux "Development of the DGT technique for Pu speciation measurements". Poster Presentation, Conference on DGT and the Environment, Lancaster, UK (July 2013)